1-1-2018

Network Wide Signal Control Strategy Base on Connected Vehicle Technology

Lei Zhang

Network wide signal control strategy base on connected vehicle technology

By

Lei Zhang

A Dissertation
Submitted to the Faculty of
Mississippi State University
in Partial Fulfillment of the Requirements
for the Degree of Doctor of Philosophy
in Civil Engineering
in the Department of Civil and Environmental Engineering

Mississippi State, Mississippi

August 2018

Network wide signal control strategy base on connected vehicle technology

By

Lei Zhang

Approved:

_____

Li Zhang
(Major Professor)

_____

Pengfei Li
(Co-Major Professor)

_____

Veera Gnaneswar Gude
(Committee Member)

_____

Linkan Bian
(Committee Member)

_____

Farshid Vahedifard
(Graduate Coordinator)

_____

Jason Keith
Dean
Bagley College of Engineering

Name: Lei Zhang

Date of Degree: August 10, 2018

Institution: Mississippi State University

Major Field: Civil Engineering

Major Professor: Li Zhang

Title of Study: Network Wide Signal Control Strategy Base on Connected Vehicle Technology

Pages in Study 172

Candidate for Degree of Doctor of Philosophy

This dissertation discusses network wide signal control strategies base on connected vehicle technology. Traffic congestion on arterials has become one of the largest threats to economic competitiveness, livability, safety, and long-term environmental sustainability in the United States. Arterials usually experience severe blockage, specifically at intersections. There is no doubt that emerging technologies provide unequaled opportunities to revolutionize "retiming" and mitigate traffic congestion at intersections. Connected vehicle technology provides unparalleled safety benefits and holds promise in terms of alleviating both traffic congestion and the environmental impacts of future transportation systems.

The objective of this research is to improve the mobility, safety and environmental effects at signalized arterials with connected vehicles. The solution proposed in this dissertation is to formulate traffic signal control models for signalized arterials based on connected vehicle technology. The models optimize offset, split, and cycle length to minimize total queue delay in all directions of coordinated intersections. Then, the models are implemented in a centralized system—including closed-loop systems—first, before expanding the results to distributed systems. The benefits of the models are realized at the infant stage of connected vehicle

deployment when the penetration rate of connected vehicles is around 10%. Furthermore, the benefits incentivize the growth of the penetration rate for drivers. In addition, this dissertation contains a performance evaluation in traffic delay, volume throughput, fuel consumption, emission, and safety by providing a case study of coordinated signalized intersections. The case study results show the solution of this dissertation could adapt early deployment of connected vehicle technology and apply to future connected vehicle technology development.

Keywords: Connected Vehicle, Traffic Signal Coordination, Signal Optimization, Fuel Consumption and Emission, Safety

DEDICATION

To my family

ACKNOWLEDGEMENTS

I would like to express my deepest gratitude to my advisor, Dr. Li Zhang. Dr. Zhang not only provided invaluable guidance during my PhD, but also gave me insightful suggestions when I faced difficulties. Thanks also to Dr. Zhang for providing opportunities to work on US DOT projects that have laid the foundations of this desertion. During the rest of my PhD studies, I also worked as research assistant under the supervision of Dr. Li Zhang on a variety of US DOT and Mississippi State DOT projects.

I also want to convey thanks to all of my committee members: Dr. Pengfei Li, Dr. Linkai Bian, and Dr. Gnaneswar Gude. Thanks for your constructive suggestions and for reviewing my dissertation with your helpful comments and suggestions.

I am grateful to the staff and faculty members within the Department of Civil and Environmental Engineering at Mississippi State University. I also want to thank my friends and colleagues at MSU: Dr. Jizhan Gou, Dr. Yi Wen, Dr. Zhitong Huang, and Mr. William Case Fulcher, among others.

I am further grateful for the support from Connected Inc. and New Global System for Intelligent Transportation Management (NGS) Corp for my dissertation research. Connected Inc. and NGS provided the intern opportunities for my dissertation. I also want to thank colleagues at Connected Inc and NGS: Ms. Xiang Li and Mr. Tom Simmerman on ETFOMM simulation software technical support. And I want to thank the support provided by the Turner Fairbank Highway Research Center of Federal Highway

Administration. And I must thank the Connected Inc. and NGS provided open source (ALPTOM), connected vehicle application development platform and microscopic traffic simulation software, as well as the intellectual properties associated with those software, models and algorithms in my dissertation research.

TABLE OF CONTENTS

LIST OF TABLES

LIST OF FIGURES

CHAPTER I

INTRODUCTION

This dissertation details multiple tasks of a case study performed to prove the benefits of connected vehicles at signalized intersections, and describes the different programs and methods employed in this project.

As a United Stated Department of Transportation (US DOT) major research initiative, connected vehicle technology is an emerging technology. Vehicle-to-vehicle (V2V) and vehicle-to-infrastructure (V2I) are two of the major initiatives of connected vehicle technology. V2V technology is the use of wireless devices to achieve communication between vehicles. The vehicles could share location, speed, brake status, and other information to achieve mobility and safety targets. In V2I technology, V2I can wirelessly exchange key safety and operating data between vehicles and highway infrastructure including traffic signals, traffic status monitors, and other devices [1]. The infrastructure of connected vehicles must be deployed by state DOTs and local agencies; however, budgetary, institutional, technological, and training constraints have caused uncertainty in terms of deployment timelines. This is particularly true for rural areas, where the local economy often lags that of urban areas, making it challenging to synchronize connected vehicle deployment across states and regions. It is also of the utmost importance to encourage early deployment of this technology for agencies and state DOTs.

Synchronized early deployment brings the benefits of connected vehicles, particularly increased safety and mobility, to millions of drivers. For example, an important component of the connected vehicle infrastructure is the Signal Phasing and Timing (SPaT) system [2]. The SPaT system offers the benefit of red light prevention: the ability for vehicles to adjust their speeds to avoid the need to stop at a signalized intersection during its red phase.

Traffic signal systems on arterials are the weakest points in a bottleneck. The basic requirement of signal control strategies are models and algorithms using real-world data and suggested minor upgrades to the existing system to demonstrate the benefits of the signal control strategy deployment of connected vehicle infrastructure at signalized intersections.

This research targets the closed loop traffic signal control system that have dominant percentage of installations in US. The software developed could be installed on a central computer or distributed traffic signal system in order to allow adjustment of traffic signal timing plans by program and software.

The objective of this dissertation is to demonstrate the relationship of benefits of signal control strategy and penetration rate (a system in which some vehicles are connected vehicles, while others are common vehicles) of connected vehicle at signalized intersections. To accomplish this objective, this dissertation first establishes the framework of traffic signal control incorporating connected vehicle operations. Based on this framework and the basic safety message (BSM) simulation functions Enhanced Transportation Flow Open-source Microscopic Model) (ETFOMM) provides, this

dissertation has created an platform to develop, debug, test and evaluate traffic signal control systems/algorithms with connected vehicle operations.

In this dissertation, I develop a traffic control system using a queue propagation model, delay model and optimization algorithm based on prior queue model in FHWA report. The splits are dynamically adjusted to clear queues on non-coordinated phases or optimized to minimize the delays; cycle length and offset are optimized to minimize total queue delay. This dissertation also explored the critical cycle length method in manual timing plan development in conjunction with offset optimization and split adjustment.

Calculations of safety in case study are based on VDOT performance report and ETFOMM simulation. The smooth traffic operations resulting from the proposed optimization model could reduce total conflicts by 50 percent overall, with 51 percent and 76 reductions in rear end conflicts and severer crossing conflicts, according to the FHWA's Surrogate Safety Assessment Model (SSAM). SSAM also indicates an 11 percent increase in lane changing conflicts due to better mobility.

The network wide fuel consumption and emission is calculated based on EPA's PERE model in the case study. Using the recommended control strategy produces 12-19 percent total fuel savings and 8-18 percent emission reductions. A 10 percent fuel and emission reduction can be easily achieved.

The conclusions about mobility benefits are based on centralized traffic signal control strategies in which BSMs from each connected vehicle is re-routed to a central server. For the distributed algorithms in which BSMs do not need to be transmitted from each intersection to the server to host the algorithm, the case study indicated the mobility

benefits of up to 44 percent delay reduction on major and improved delays on minor are still significant (about 16%).

One critical finding of this study is that the state DOT/local agencies do not need to wait for a high penetration rate connected vehicles. At the 10 percent penetration rate, control delays are reduced by at least 10 percent on major streets in the congested Virginia network, while control delays on minor are reduced simultaneously with 40 percent control delay reduction. In addition, the model could easily reduce fuel consumption by 10 percent, according to EPA's PERE model. These savings for highway users justify the cost for DSRC and communication upgrades at intersections. Even a 10 percent penetration rate results in more than 25 percent fuel savings.

CHAPTER II

LITERATURE REVIEW

This literature review reviews related previous studies, organized under four subcategories: 1) optimization for traffic signal coordination; 2) adaptive traffic control systems; 3) connected vehicle and basic safety message (BSM); (4) connected vehicle technology in traffic signal control; (5) distributed system in traffic signal control.

2.1 Optimization for Traffic Signal Coordination

Traffic signal coordination has proven effective in reducing delays and alleviating congestion. It has been widely used in urban areas. Popular optimization models for traffic signal coordination include MAXBAND, MULTIBAND, PROS, etc.

Little, Kelson, et al. [10], introduced the MAXBAND, which is a software package to set up signal timings for arterials and triangular networks to achieve maximum coordination bandwidths. MAXBAND can generate cycle length and speed within a given range. It can also produce optimal directional bandwidths based on user-defined weights. This model's development was based on the previous model presented by Little [11]. The branch and bound algorithm was also used for solving the model presented.

Gartner, Assmann, et al. [12] presented the MULTIBAND, which optimizes directional bandwidth for each section of arterials. The authors selected NETSIM as the

simulator used in the case study. Two computer programs, MAXBAND and MULTIBAND, were used to optimize signal settings for an arterial. When compared to MAXBAND, MULTIBAND showed significant enhancements with respect to delays (16% for major streets; 11% for all traffic) and number of stops (25% of major streets; 15% of all traffic).

Wallace and Courage [13] expanded a progression opportunity (PROS) to optimize fixed-time traffic signal coordination. Based on the results of a case study, Wallace and Courage showed that the expanded PROS method could significantly outperform the maximum bandwidth method, especially for study arterials. The maximum improvements for bandwidth and delays for study arterials were 30.4% and 21.4%, respectively.

Lieberman, Chang, et al. [14] designed a real-time traffic signal control policy with special attention to oversaturated arterials. This method was named a Real-Time/Internal Metering Policy to Optimize Signal Timing (RT/IMPOST). The key concept of this reference was to optimally control and stabilize queue length dynamics. According to the results of a case study, when compared with the results of PASSER, TRANSYT and SYNCHRO, RT/IMPOST significantly improved mean travel speed and decreased total delays. This study was based on the fixed-time control mode and was a responsive traffic signal control strategy.

Cesme and Furth [15] described “self-organizing” approaches using several rules widely accepted for traffic demand and fine-tuning traffic signal timing. The essence of “self-organizing” is the dynamic cycle length, which includes green truncation in cases of intersection spillback, early green and double realization for left turn phases prone to

pocket spillback, and dynamic coordination for groups of signals spaced too closely together. Simulation tests based on a benchmark network invented by Liberman show 45% delay reductions compared to the coordinated control plan calculated by SYNCHRO, TRANST-7F and PASSER, with 8-35% reduction in real network. The authors did not address how transition logic would affect the frequently changed cycle length.

Messer, Whitson, et al. [16] developed a program for multiple phases of arterial progression optimization, and considered four general phase options. The program generated phase sequences and movement green time durations for maximum progression with respect to a specific selected cycle length. The Brooks' interference algorithm was used for generating the maximum bandwidth. This program was tested in the field at a study site and generated optimal results as expected.

2.2 Adaptive Traffic Control System

Adaptive traffic signal control systems were based on different advanced traffic surveillance systems designed to actively and proactively control traffic according to real-time and predicted traffic data. RHODES, ACS-lite, SCOOT, SCATS, OPAC, and InSync were major adaptive traffic signal control systems implemented in the U.S. and internationally. These systems and their core algorithms are reviewed in this sub-section.

Mirchandani and Head [17] presented an introduction, methodology, architecture and prototype called RHODES: a traffic adaptive signal control system with a hierarchical structure comprised of three control levels: network load control, network flow control, and intersection control. RHODES had several algorithms to predict platoon arrivals and individual vehicle arrivals for network flow control (REALBAND) and intersection control

(COP). A simulation study was conducted to evaluate the performance of RHODES; when compared with the semi-actuated control system, RHODES reduced average vehicle delay for both low and high loads. RHODES has been field tested and installed at a few U.S. locations.

Luyanda F., et al. [18], introduced the major algorithmic architecture of the ACS-lite system, which includes three key algorithmic components: a time-of-day (TOD) tuner, a run-time refiner, and a transition manager. The TOD tuner was used to update a used phase plan (cycle, splits, and offsets) offline according to traffic volumes and phase plan performance. The run-time refiner was used to optimize the current phase plan by implementing incremental adjustments which slightly modified the parameters of the current phase plan. This component also determined the most suitable time to switch to a scheduled or unscheduled phase plan. The transition manager decided to use the built-in transition method of controllers in order to impact traffic as little as possible.

Robertson and Bretherton [19] introduced the SCOOT traffic responsive control system based on TRANSYT. Three major principles of SCOOT were: 1) assess real-time cyclical flow profiles; 2) produce a continuously updating online queue model; and 3) adjust signal settings in an incremental mode. Bandwidth, average queues, and vehicle stops were three major optimization criteria for the system. According to the results of conducted studies, the scholars suggested that SCOOT could save 12% for delay on average, when paired with good fixed-time plans. SCOOT was the mostly widely installed ACS system in the world.

The Roads and Traffic Authority (RTA) of New South Wales, Australia developed the Sydney Co-ordinated Adaptive Traffic System (SCATS) software [20]. Wilson and Millar, et al. [20] assess the benefits of SCATS's coordinated signal control by micro-simulation. Three control modes were evaluated in the simulation: fixed-time coordinated control, isolated actuated control (each intersection independently controlled by vehicle actuation mode) and coordinated control. Delay and number of stops were the selected performance indices. Based on the simulation results, the performances of the three modes were similar under light traffic. SCATS's isolated actuated control and coordinated control performed better than fixed-time control when traffic increased. For the heavy traffic, SCATS's coordinated control had the best results since it can best adapt to traffic variations.

Gartner, Pooran, and Andrew's research on Optimized Policies for Adaptive Control (OPAC) considered green split, offset, and cycle length. One framework of adaptive control strategy had been implemented and tested in test bed. Observations indicated that the strategy was instrumental in reducing delays and stops when compared with a well-tuned, fixed-time system that maintained progression along the arterial. They also [21] presented field implementation procedures for traffic signal control system in Northern Virginia. For OPAC, the upstream detectors of each link in intersections were needed for collecting real-time vehicle counts and occupancy. The performances of fixed traffic signal timing plans were optimized by TRANSYT and used as the benchmark. Due to the frequent communication disruptions of several intersections as a result of system upgrades by a phone company and the simultaneous construction activities of OPAC

deployment, the OPAC system was not as fine-tuned as it needed to be for the study. However, based on results from the field, OPAC outperformed the fixed traffic signal timing optimized by TRANSYT with an average 5-6% decrease for delays and stops.

Chandra and Gregory [22] described the functions and benefits of InSync, which was developed by Rhythm Engineering in 2008 as a new adaptive traffic signal control system that had been installed in some U.S. cities. InSync has global and local optimization devices and adjusted signal timing with second-by-second adjustments responding to real-time traffic. The local and global optimizers aimed to improve individual intersections and corridors. The authors indicated that implementing InSync had significant benefits with respect to travel time, number of stops, fuel consumption and emission, and reduced accidents.

Park, Messer and Urbanik [23] presented a traffic signal optimization program for oversaturated conditions. The program used a genetic algorithm approach to optimize four control parameters: cycle length, green split, offset, and phase sequence. The green split parameter did not show an important influence in their program. In addition, compared with TRANSYF-7F signal optimization software, the program had few benefits on control delay and throughput.

Lertworawanich [24] used a time-space diagram to optimize green split. The author provided a model to solve the queue extend detector problem. This model used density, time-space diagram, and critical time points to optimize green split for minimizing total control delay.

The VTRC report [25], contained different traffic timing optimization methods. The authors displayed research on several different stochastic and microscopic simulation programs. Green split was one control variable in most optimization models but is only affected by offset and cycle length.

In a University of Virginia research paper [27], the authors mentioned that time-of-day (TOD) could affect the coordinated actuated signals system. Green split was an important variable in TOD breakpoints that could decrease delay and improve traffic operation.

Xia et al. [28] presented an approach of traffic signal coordination based on travel speed variations. The authors proposed a green split and offset optimization procedure. The model used a common cycle length and two basic strategies to allocate green splits. Both strategies considered minimizing coordinated green time and non-coordinated green time to optimize timing parameters. The authors used link-based travel speed to calculate optimized green split. After green split calculation, the proposed methodology could calculate offsets for signal timing plan.

In summary, field evaluation and simulation evaluation about adaptive traffic control systems were reported to have a 10-15 percent delay reduction [21, 22, 24, 25].

2.3 Connected Vehicle Technology

Connected vehicle technology could work with state and local transportation agencies, vehicle and device makers, and the public to test and evaluate technology. The connected vehicle technology also enables cars, buses, trucks, trains, roads and other infrastructure, and smartphones and other devices to “talk” to one another. Several types

of connected vehicle technology contain Vehicle-to-Vehicle (V2V) and Vehicle-to-Infrastructure (V2I). The focus of this research is optimization of coordinated signal control using V2I technology.

Basic safety message (BSM) is firstly used for vehicle safety application [29]. Currently, BSM is one kind of connected vehicle data could be used on other operation managements and applications. BSM is used in a variety of applications to exchange safety data. This message is broadcast frequently to surrounding vehicles with a variety of data required by safety and other applications. Transmission rates are beyond the scope of BSM standard, but a rate 10 times per second is typical.

BSM data contains vehicle location data (latitude, longitude, and elevation data) and motion data (speed, heading, acceleration rate, and so on). BSM is designed for safety purposes and connected vehicle safety applications could dramatically reduce the number of fatalities and serious injuries caused by accidents on roads and highways. The vehicle status data could be used in traffic operation management.

2.4 Connected Vehicle Technology in Traffic Signal Control

Goodall [9] presented a traffic signal control algorithm, the predictive microscopic simulation algorithm (PMSA), based on the connected vehicle environment which implements rolling horizon concept. The proposed algorithm collected the speed, location and heading of connected vehicles within DSRC communication distance, i.e. 300 meters (which translates to 15 seconds' travel time based on speed of the study corridor). Next, microscopic simulation predicted cumulative delays of the upcoming 15 seconds for possible phasing configurations. Then, the phase with the minimum delay was chosen as

the optimal phase for the next time period. An operation constraint was added so no phase would experience red time for more than 120 seconds. Based on the results of the simulation study, the proposed algorithm was found to be more effective when the penetration rate of connected vehicles was at least 25% and traffic conditions were under-saturated.

Joyoung Lee [30] presented a cumulative travel time responsive (CTR) control algorithm for real-time intersection traffic signal control based on IntelliDrive (now known as connected vehicle technology). The cumulative travel time (CTT) of all vehicles traversing an intersection was estimated by adaptive Kalman filter. CTTs were grouped by NEMA possible phase combinations to determine the highest CTT phase combinations. A switch to the phase combination with the highest CTT was made if that phase was not the current phase. The phase timing plan was considered the optimized timing plan. The simulation study indicated that the proposed model could improve 92% congestion condition compared with the actuated control when the penetration rate of connected vehicle was over 30%.

He et al. [31] proposed PAMSCOD, which is a multi-modal online traffic signal control model based on vehicle to infrastructure (V2I) communication (25). There were two major components in this model: first, a platoon identification algorithm which uses critical headway to identify moving platoons; second, a mixed integer linear programming model to generate signal timing based on platoons. The objective function of the mixed integer linear programming model was minimizing total delays of the entire network. PAMSCOD provided dynamic progression, and no common cycle length exists. VISSIM

was used as the simulator to evaluate the effectiveness of PAMSCOD. Signal timing plans optimized by Synchro were used as benchmark cases. According to the results, when the penetration rate of connected vehicle was over 40%, the performance of PAMSCOD was better than signal timings generated by Synchro. Compared with coordinated signal timing generated by Synchro, average vehicle delay decreased by 8% and average bus delay decreased by 25-30% after implementing PAMSCOD. PAMSCOD reduced average vehicle delay 20-30% and increased average bus delay by 3% when compared with transit priority output by Synchro.

He, Head et al. [32] proposed a mixed integer linear program model for multi-modal traffic signal control optimization. The presented model considered priority, actuated controller features, and signal coordination simultaneously. The scholars utilized priority to materialize signal coordination. Passenger vehicles, buses, and pedestrians were the three traffic modes considered. The model of this reference was decentralized and designed to optimize arterial coordination by decomposing the problem to optimize each intersection within the arterial separately. The authors conducted a simulation case study using strategies of actuated coordination, actuated coordination with transit signal priority, and the model. The model outperformed the actuated coordination with a transit signal priority strategy and proved to work well within the high-volume scenario. Compared with the actuated coordination with transit signal priority strategy, the proposed model decreased bus delays by 24.9%, pedestrian delays by 14%, and showed comparable passenger vehicle delay.

Priemer and Friedrich [33] presented an adaptive signal control algorithm based on vehicle to infrastructure (V2I) data. Based on vehicle arrival data from V2I and stop bar detectors, the algorithm optimized phase sequences for 20 seconds in order to minimize queue lengths while implementing the algorithm every 5 seconds. In this study, the V2I communication zone was 280 meters from the stop bar. The algorithm of this reference was decentralized and did not have cycle length or offset. The authors conducted a simulation study to evaluate the algorithm, and the pre-time signal timing plan optimized by TRANSYT-7F was utilized as the benchmark scenario. The authors concluded that, when compared to the benchmark scenario, a maximum of 24% mean delay decrease and 5% mean speed increase was achieved. The significant improvements required the minimum penetration rate of connected vehicles to be around 25%.

Feng, Khoshmagham et al. [34] proposed an online adaptive traffic signal control algorithm in the connected vehicle environment that optimizes phase sequences and phase duration. This algorithm was solved on two levels. For the first level, the duration of a barrier group (i.e. duration of major or minor streets' phases) was determined, and for the second the duration and sequence of each phase in the barrier group was optimized. A simulation study evaluated the proposed algorithm. The performances of a fine-tuned actuated controller were referred to as the benchmark. The results showed that in certain traffic conditions (V/C = 0.8), the proposed algorithm can decrease delays by 6% and 16.6%, respectively, in low and high penetration rates. However, the medium traffic condition performances of the presented algorithm could not compete with those of the actuated controller, except in the case of 100% penetration rate.

2.5 Distributed System in Traffic Signal Control

In the report of the Florida Department of Transportation (FDOT) 2016 [35], the research group summarized different adaptive signal control technology (ASCT) systems. Five ASCT systems were distributed systems, including ACS Lite, InSync, Kadence, OPAC, and RHODES. All ASCT systems require communications infrastructure to share data in real time between signal controllers or ASCT processors in a distributed system architecture. The local controllers first process traffic data then communicate with a centralized server for coordination adjustment.

ACS Lite is a distributed system; however, the system's master controller is replaced with an ACS Lite field processor, which communicates with local controllers. InSync has a distributed system architecture that places a processor in each cabinet that is compatible with nearly all signal controllers in use. While the additional cabinet space requirements are minimal, some agencies reported that they had to upgrade their cabinets in order to accommodate the added equipment. Kadence uses a distributed offset adjustment method [36]. This method makes offset adjustments for each controller independently, but with consideration of the effects of each independent decision on adjacent signals. Each controller considers a range of offset settings: no change, adjust up to Δ seconds earlier, or adjust up to Δ seconds later. OPAC is an ASCT system with a distributed system architecture. The system requires an OPAC box in each signal cabinet that controls the ASCT system. One agency refers to the OPAC box as a "black box," noting that it is difficult to understand how the system functions in order to address citizen questions. The OPAC interface is integrated into the MIST ATM software, which is a

commonly-cited reason for selecting the system over another ASCT. RHODES contains distributed effective system parts and processes traffic network to platoon flow first, then sends data to a centralized computer for network logic.

Wongpiromsarn et al. [37] presented a backpressure-based traffic signal control system, which considered the phase to be activated at each junction as determined independently from other junctions, using only local information, namely the queue length on each of the links associated with this junction and the current traffic status around this junction. The optimization model showed that backpressure routing leads to maximum network throughput. The optimization model only estimates queue length in local and no master computer to control total network. The study found that a backpressure-based traffic signal control system could decrease overall queue length more than SCATS in a MITSIMLab simulation environment. The system only deploys and measures in the simulation.

Chow and Sha [38] introduced centralized and distributed systems for urban traffic control. The research contained descriptions of centralized, semi-distributed, and distributed systems. The semi-distributed system contained green split (centralized linear quadratic regulator), distributed offset controller, and distributed cycle-time controller, all of which are separately optimized. The local controller is to optimize offset and one central computer is to estimate cycle length. The distributed system used the max pressure (MP) algorithm. The major difference between MP and semi-distributed rules is that TUC would allocate the green according to the predefined nominal green split if there is low or even zero queue detected, while the MP controller simply allocate the green uniformly in a low

(or zero) queue circumstance. The optimization algorithm only tests and evaluates in the simulation.

Ahmed and Easa [39] addressed a real time distributed signal control system. The system included a new purely distributed control logic with a person-based hypothesis aiming to enhance area-wide control without any centralized infrastructure. The research set up control decision check points to determine congestion in intersections. In addition, the system considered the transit signal priority module and incident status. The control logic model was applied to a large network of 49 intersections under various demand patterns in a simulation environment. The local controller is to set up each phase green time with queue length. And master computer which has the area-wide control strategy is to coordinate all intersections on offset, split and cycle length. The final results is summarized in mathematic simulation.

Timotheou, Panayiotou, and Polycarpou [40] presented a distributed system using the cell transmission model. The researchers used the cell transmission model to define traffic signal network and network traffic signal control (NTSC) to distributed system formulation and solution. The alternating direction method of multipliers (ADMM) was the algorithm used to solve NTSC distributed system formulation. In the simulation, the total travel time of the network could be reduced by more than 10 percent with a congestion level of 50% (total travel time on free flow speed/total travel time on traffic). The following year, the authors presented a new version of the distributed system [41] that involved multiple intersection traffic signal controls. With the same ADMM algorithm and additional constraints of distributed routing, the simulation results showed 20 percent total

travel time reduction in the best scenario: 50% congestion level. The distributed system is to estimate departure rate on local.

Yuan, Knoop and Hoogendoorn [42] researched a different system of distributed traffic signal control, using a backpressure algorithm for a basic distributed signal control method. However, the authors modified the algorithm to a dynamic optimal slot time method. The simulation results indicate that the dynamic slot time method saves approximately 6.5% compared to the best performance of fixed timing plan strategy.

Zaidi, Kulcsar, and Wymeersch [43] implemented the decentralized back-pressure method of traffic signal control optimization. The authors considered traffic signal timing plan and vehicle routing together. The signal control algorithm for each junction was decentralized and adaptive route control algorithm computed for each junction. The simulation results included fixed time, single-commodity back-pressure, and proposed adaptive routing back-pressure. VISSIM simulation results showed proposed adaptive routing back-pressure could improve on 40% number of trips completed, 70% average travel time, and 70% average speed of vehicles in best case. The local computer is to calculate signal control timing plan. And maximum total throughput is the objective of central computer task.

CHAPTER III

TRAFFIC MODELLING

3.1 Overall Framework

The signal modelling strategy of this dissertation is based on an eight-phase, dual-ring NEMA controller model. Figure 3.1 shows the typical traffic signal dual-ring diagram of the NEMA controller.

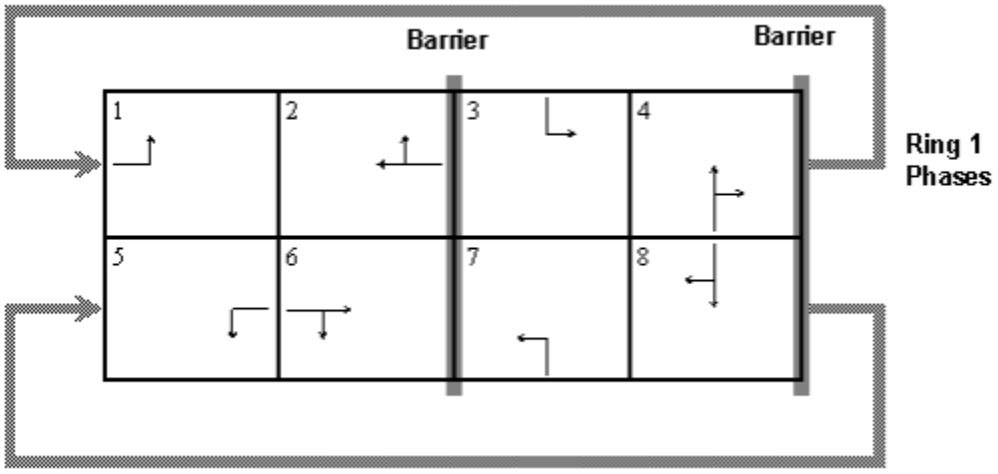

Figure 3.1 Typical Traffic Signal Dual-ring Diagram of NEMA Controller.

Figure 3.2 shows the entire framework of the system. The first step is to collect and process real-time traffic data. In addition to the BSMs from the RSUs at all coordinated intersections, one or more upstream detectors are expected to be installed on all lanes of each approach. The upstream detector(s) is (are) used to collect upstream arrival vehicle

profiles for each approach, including speed and time stamps. Traffic data of all approaches are predicted based on the collection of real-time traffic data and the signal timing plan. The predicted data for a coordinated intersection includes pending traffic demands, vehicle queue length of all phases, average approach travel time, etc. In terms of practical approaches for traffic engineers to re-time the signals in the field, splits and/or cycle length are adjusted to clear the queues on all approaches based on predicted data. With the predicated queue lengths at all approaches and all signalized intersections, green split, cycle length and offset can be optimized to minimize total queue delays in all approaches. There are also mixed-the state of practice and optimization strategies: for example, to adjust splits and optimize cycle length and offset. Different strategies are used to consider different, modified methods of split, offset, and cycle length. One method is adjusted splits, optimized offsets, and cycle length implemented for all coordinated intersections. Optimized splits, offsets, and cycle length is another all optimization strategy.

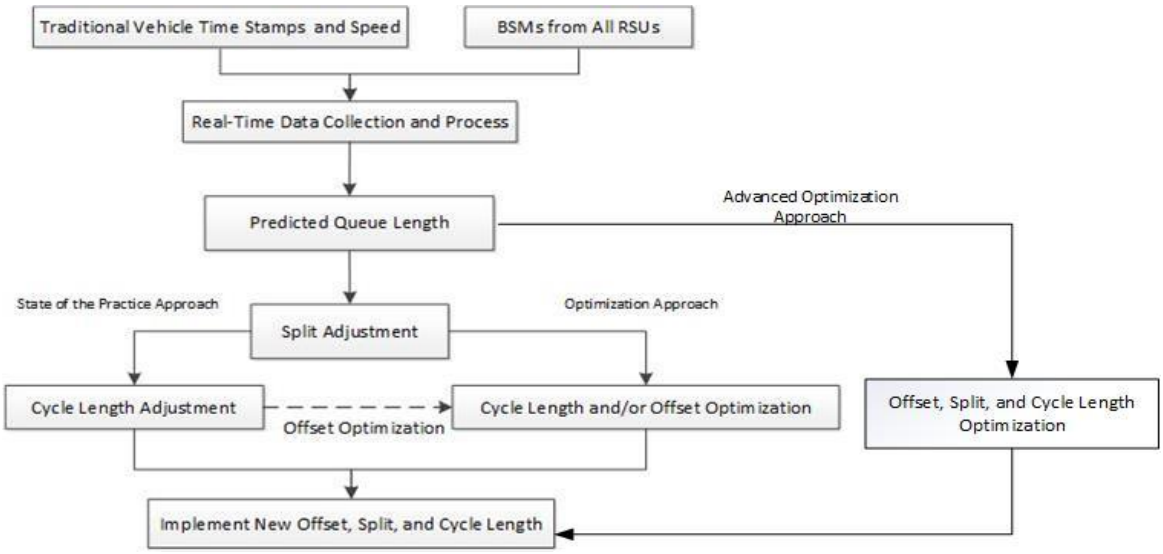

Figure 3.2 Flow Chart of Optimization Model Framework

3.2 Queue Length Forecast

Split, offset, and cycle length adjustment/optimization are based on predicated queue length. Methods to predict queue length are addressed in this section. Since each approach has an additional upstream detector and conventional stop bar detectors for actuated controllers, the time stamps of vehicles arriving and departing the approaches are used in queue length prediction. The additional information is connected vehicle data (BSMs) that contains speed and vehicle trajectories, which is useful for increasing accuracy of queue length prediction. The connected vehicle data has different penetration rates at different stages (an early stage may have a lower penetration rate, while a later stage may have a higher penetration rate). Therefore, the queue length prediction method should consider the penetration rate in the forecast.

The initial queue length at the beginning of each projection horizon—one phase from current green start time to next green start time, usually a cycle length or the residual queue length of the last projection horizon—is determined by traffic signal splits and remaining green time. If signal indication is red, all vehicles currently traveling on an approach could arrive the intersection, stop, and become the initial queue length for the next projection horizon. On the other hand, if traffic signal indication is green, a prediction needs to be made on how many vehicles currently traveling on the link could traverse the intersection within the remaining green time. Based on arrival times of vehicles indented by the upstream detector, a scheduled departure time at stop bar could be estimated. The connected vehicle data not only provide the connected vehicle arrive time based on speed

and trajectory, but also could support determination of trajectories for regular vehicles near the connected vehicle.

Based on vehicle scheduled departure time, an approach could be divided into four possible regions: 1) queuing region, which usually contains resident queue from the previous projection horizon; 2) queue formulation region, in which the vehicles at the upstream of the approach or a upstream link join the last vehicle in the queue; queue length in this region is calculated by vehicle speed, existing queue length, and departing vehicle headways at the stop bar; 3) progression region 1, in which vehicles are traveling from upstream of the approach and could be released during the remaining green time; and 4) progression region 2, in which vehicles are traveling from upstream of the approach, but cannot pass the intersection during the remaining green time and stop before a stop bar. Progression region 1 considers a favorable speed to travel to the intersection. However, this system includes the assumption of slow moving vehicles ahead and does not consider lane changes. Some vehicles in progression region 1 have the opportunity to join the predicted resident queue; The vehicles in progression region 2 are considered when resident queue length for the next cycle is predicted. Figure 3.3 shows the basic concept and range of four-region queue length prediction. The queuing region is close to the intersection. The queue formulation region is next to the queuing region. Progression regions 1 and 2 are further from the intersection. The ranges of these four regions are not fixed values and would instead be determined by vehicle trajectory data and signal timing plan.

Figure 3.3 Queue Length Prediction Regions (QR: Queuing Region; QFR: Queuing Formulation Region; PR1: Progression Region 1; PR2: Progression Region 2)

Figure 3.4 shows the space-time diagram of four regions of vehicles on the upstream link of an intersection. Queue region vehicles wait at the intersection stop bar until the signal changes to green. Queue formulation region vehicles arrive at the intersection during the green time and join the queue. Progression region 1 vehicles arrive at the intersection on green and may go through the intersection. Progression region 2 vehicles arrive the intersection on red and wait for the next projection horizon. The red lines in Figure 3.4 are connected vehicle trajectory and the blue lines are regular vehicle data. Figure 3.4 shows several connected vehicles in the vehicle platoon. This situation makes using the connected vehicle data to forecast or validate all vehicle trajectory possible.

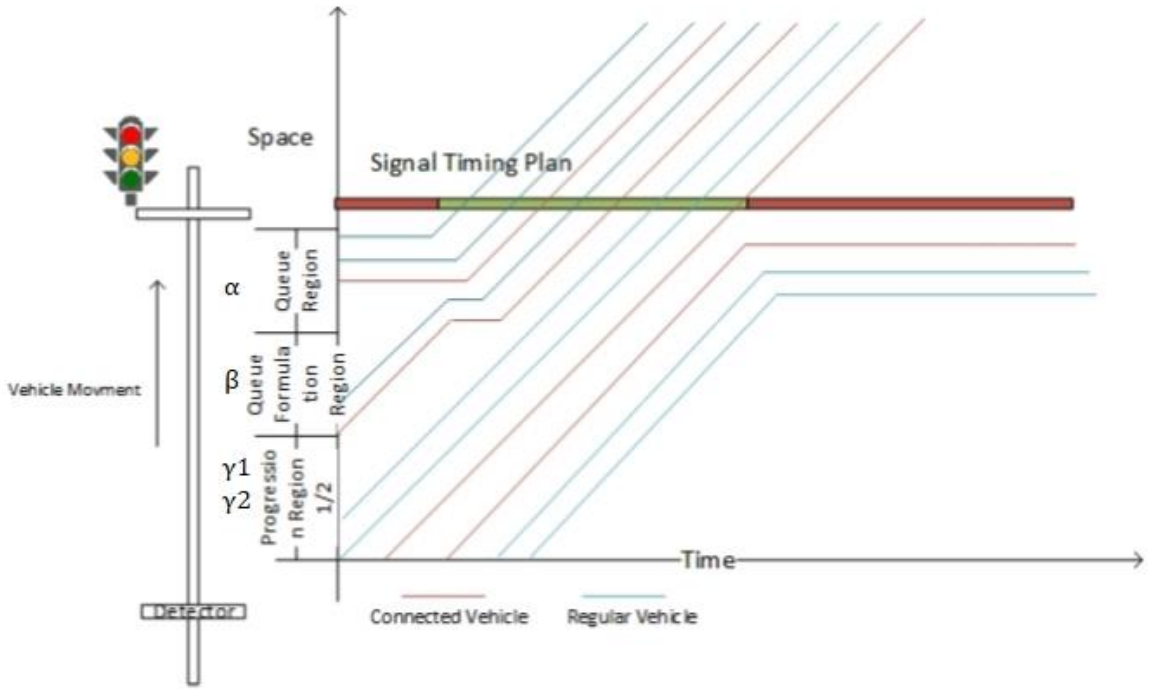

Figure 3.4 Space-Time Diagram of Queue Length Prediction

The following equation shows that the predicted queue region vehicle should be the same as the last cycle prediction residual queue.

$$\alpha_{m,d,t} = q_{m,d,0} - \eta_{m,d,t} \geq 0 \text{ (E3.2.1)}$$

$\alpha_{m,d,t}$: Number of vehicles in initial queue region at intersection m that remain in the queue at time interval t (vehs, in a none coordination phase).

$q_{m,d,0}$: the number of vehicles in queue on approach d of one intersection m at time interval 0.

$\eta_{m,d,t}$: the number of discharge vehicles in approach d at intersection m at projection horizon t (vehs).

In the queue formulation region, all vehicles may join the existing queue and may leave the approach if the existing queue length is not too large. Vehicle departing time is calculated by remaining green time and discharge profile from the stop bar detector.

The following equation shows one constraint of queue formulation region prediction. If the queuing region has a long queue, the queue formulation region may disappear, and no vehicles remain in the queue formulation region. The equation finds the maximum vehicle between zero and the number of discharge vehicles; the queuing region vehicle could determine the number of vehicle in queue formulation region.

$$\beta_{m,d,t} = max(0, \eta_{m,d,t} - (\alpha_{m,d,t} + n\{ where \ \sum_{i=0}^{t} H_{m,d,t,i} < \lambda_t \ and \ \sum_{i=0}^{t+1} H_{m,d,t,i} \geq \lambda_t \})$$

(E3.2.2)

$\beta_{m,d,t}$: the number of vehicles in queue formulation region at intersection m at time interval t (vehs, in a non-coordination phase).

$\alpha_{m,d,t}$: the number of vehicles in initial queue region at intersection m that remain in the queue at time interval t (vehs, in a non-coordination phase).

$\eta_{m,d,t}$: the number of discharge vehicles in approach d at intersection m at projection horizon t (vehs).

In progression region 1, vehicles may not join the queue. The vehicles may depart at the stop bar of the intersection in the remaining green time. Some vehicles in this region could go through the intersection; some of them stop and join the predicted queue for the next cycle. The number of departing vehicles minus queuing region vehicles and queue

formulation region vehicles is the number of vehicles that could go through the intersection in this region. The remaining vehicles join the predicted queue length.

Vehicles in the queue formulation region and progression region 1 are dynamic. When the resident queue length is too large, the queue formulation region has more vehicles. On the other hand, if total discharging vehicles with remaining green time is greater than or equal to the number of vehicles in the queue region and the queue formulation region, progression region 1 hasn't any vehicles. In progression region 2, vehicles stop before the intersection and do not depart the stop bar before the next green phase. The vehicles' departure time depends on red time and vehicles' travel time. The equations below show the basic concept of determination of progression of vehicles in regions 1 and 2.

$$\gamma_{1,m,d(n),t} = ar_{m,d,\tau} \times g_{m,d,\tau} - dc_{m,d,\tau} \quad \text{(E3.2.3)}$$

$$\gamma_{2,m,d(n),t} = ar_{m,d,\tau} \times c_{m,\tau} - dc_{m,d,\tau} - vp1_{m,d,\tau} \quad \text{(E3.2.4)}$$

$$\gamma_{1,m,d,t} + \gamma_{2,m,d,t} = n\{ where \ \sum_{i=0}^{t} H_{m,d,i} < c_m \ and \ \sum_{i=0}^{t+1} H_{m,d,i} \geq c_m \} - \eta_{m,d,t} \quad \text{(E3.2.5)}$$

$\gamma_{1,m,d(n),t}$: the number of vehicles in progression region 1 on approach d of one intersection m at projection horizon τ.

$\gamma_{2,m,d(n),t}$: the number of vehicles in progression region 2 on approach d of one intersection m at projection horizon τ.

$\eta_{m,d,t}$: the number of vehicles that could discharge on approach d of one intersection m at projection horizon τ.

$H_{m,d,i}$: the arrival rate at which a vehicle could arrive at the intersection or stop bar on approach d of one intersection m at projection horizon τ.

c_m : the cycle length of one intersection m at projection horizon τ.

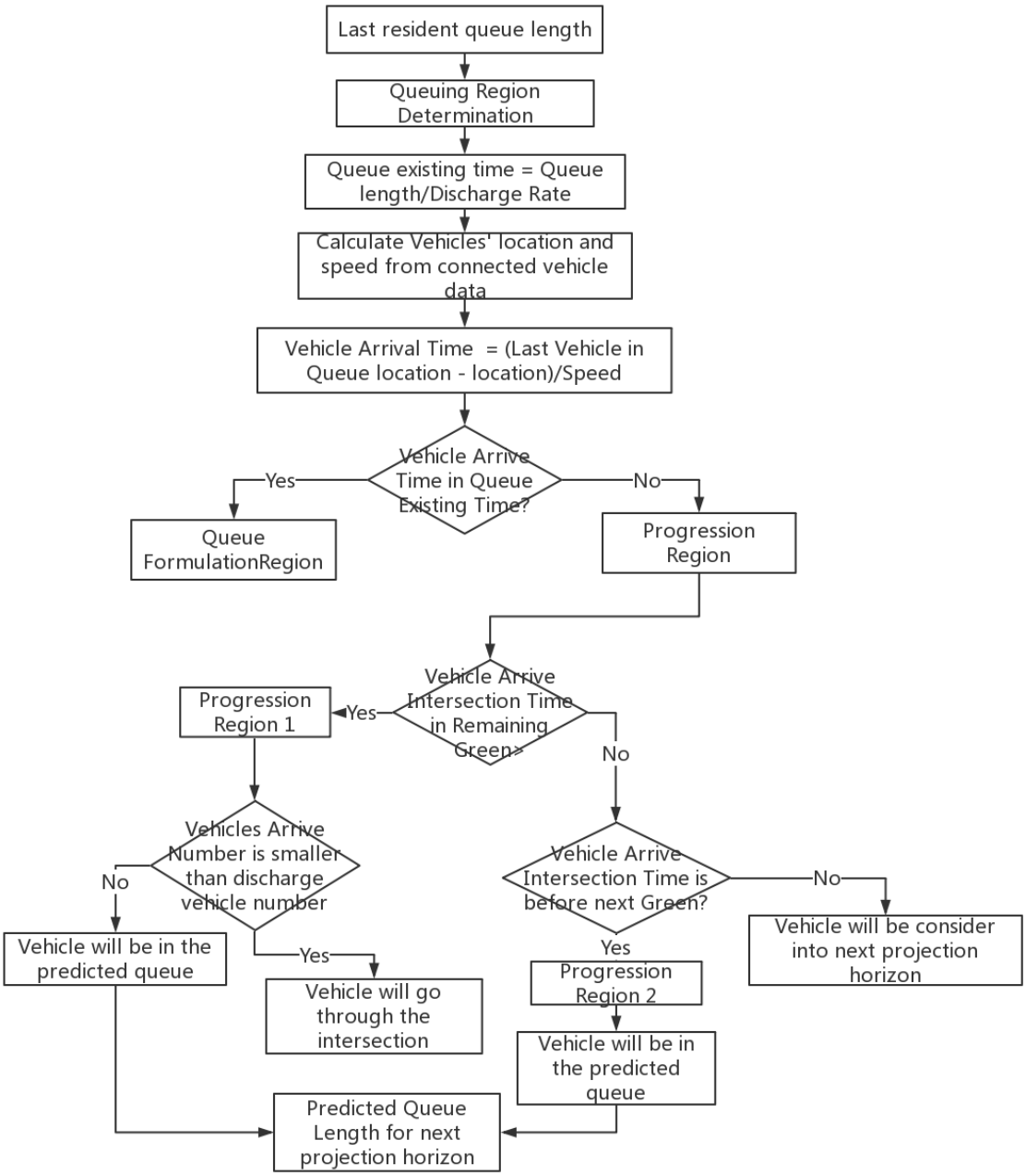

Figure 3.5 Flow Chart of Predicted Queue Length Logic

The queue length logic determines each vehicle region from intersection to upstream link second by second. The arrival time of vehicles is used in determination of the four regions. Then, the queue length could be predicted and calculated by the summation of the numbers of four vehicle regions.

3.3 Queue Length and Connected Vehicles

The focus of this dissertation is the effect of connected vehicle technology on queue length forecast. The connected vehicle could provide BSMs to a signal operation system. The BSMs contain vehicle speed and location and matching the BSM vehicle IDs from loop detectors provide the vehicle arrival sequence.

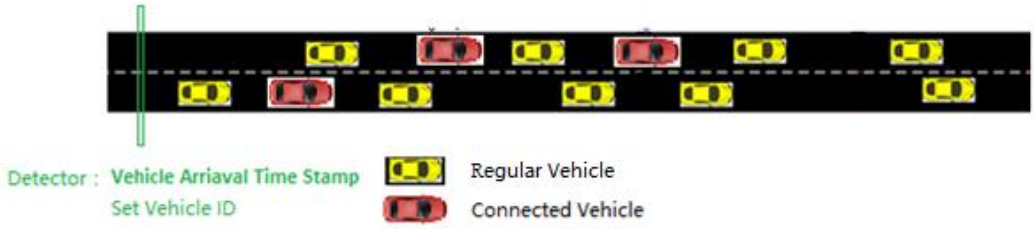

Figure 3.6 Connected Vehicle and Detector Data for Queue Length Prediction

As described previously, the length of the remaining green time determines each vehicle's region and how many vehicles are in each region. Vehicles' positions are estimated one by one from the arrival time on the approach. Figure 3.6 shows the detector and connected vehicle status in queue length prediction. Penetration rate affects the accuracy of the queue length estimation and forecast.

First, the vehicles in the queue region are validated and adjusted through connected vehicle location and speed. If connected vehicles are in the queue (determined by queue

length and connected vehicle ID), other vehicles' speed is adjusted against the speed from the connected vehicles' BSMs (which should be close to zero). The second adjustment is the vehicle's location, which should be near the stop bar of the intersection. Figure 3.7 shows how connected vehicle data adjust the queuing region. If the check of speed of a vehicle is not zero, the logic would find the last connected vehicle for which the speed is close to zero. Then, that vehicle would be recognized as the last vehicle in the queue. The queue length is determined from that connected vehicle to the first vehicle stopped at the intersection stop bar.

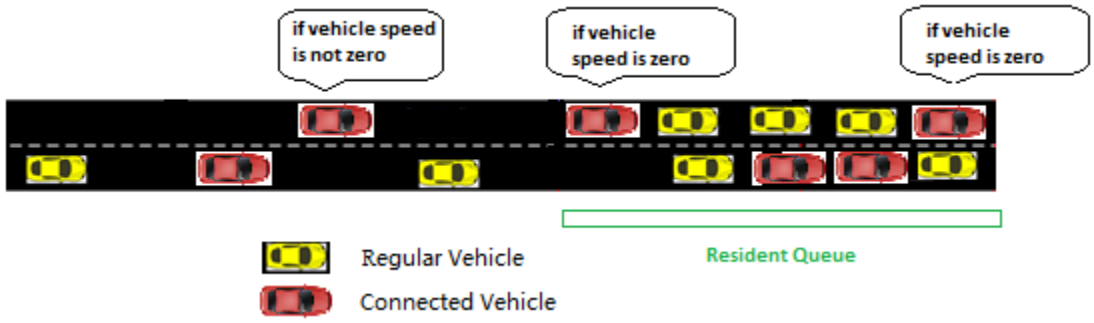

Figure 3.7 Connected Vehicle and Adjustment of Queuing Region

Another use of connected vehicle data is to determine the vehicle speed and departure headways. The upstream detector could determine vehicle arrival profile and create the vehicle ID to both connected vehicles and regular vehicles. Assuming that the vehicle does not overtake other vehicles, the connected vehicles are in the same position of vehicle arrival sequence. The connected vehicle speed could adjust regular vehicle speed near the connected vehicles. BSMs from connected vehicles could help to determine vehicles' speed and departure headways. Figure 3.8 displays the connected vehicles' speeds, which are used to adjust other vehicles' speeds. The nearby vehicle speed could be

adjusted by connected vehicle speed ahead and connected vehicle speed behind. The estimated nearby vehicle speed could be used in other regular vehicles has no connected vehicle nearby (ahead or behind)

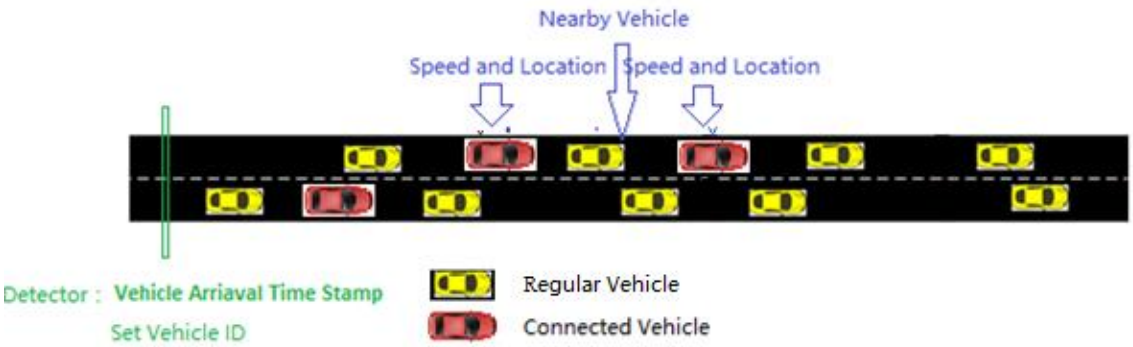

Figure 3.8 Connected Vehicles' Speed Use to Determine Nearby Non-Connected Vehicle Speed Assumption

CHAPTER IV

SIGNAL CONTROL STRATEGIES

4.1 Strategy Design

In real world, DOTs and local agencies may not need the complicated system and prefer simply system. The strategies optimize or adjust all offset, split, and cycle length may be not necessary. So, this dissertation includes the use of six strategies for different requirements of DOTs and local agencies:

S1: Offset optimization

S2: Offset optimization and Split Adjustment

S3: Split Adjustment and Cycle Length Adjustment

S4: Offset optimization, Split Adjustment, and Cycle Length Adjustment

S5: Offset optimization, Split Adjustment, and Cycle Length Optimization

S6: Offset optimization, Split Optimization, and Cycle Length Optimization

4.1.1 Strategy 1 Offset Optimization

The first strategy is to optimize two approaches of coordinated direction offsets. The offset optimization retains use of green split and cycle length already in the field. The coordinated direction offset is the only decision variable in the optimization model. The strategy's focus shift to optimize offsets of all intersections in the entire arterial

simultaneously, in order to provide smooth progression for the whole arterial. When offset of a signal controller is changed, a transition period may be desirable; traffic flow is disrupted during this transition period, which may cause an unnecessary extra delay. To mitigate this disruption, attention is given to restraining the value change of the offset within a small interval to facilitate the direct transition. To that end, this dissertation optimizes offsets of a coordinated intersection within a predefined interval. There are three major steps in the proposed offset optimization module: 1) predict upcoming vehicle trajectories based on a traffic propagation model; 2) forecast the number of vehicles in the queue at stop bar after all queues are cleared and predict discharging profiles of the target intersection; 3) offset optimization for the entire arterial. Steps 1 and 2 are repeated for all coordinated intersections from the first intersection to the last according to traffic flow propagation sequences. Figure 4.1 displays the basic logic of offset optimization.

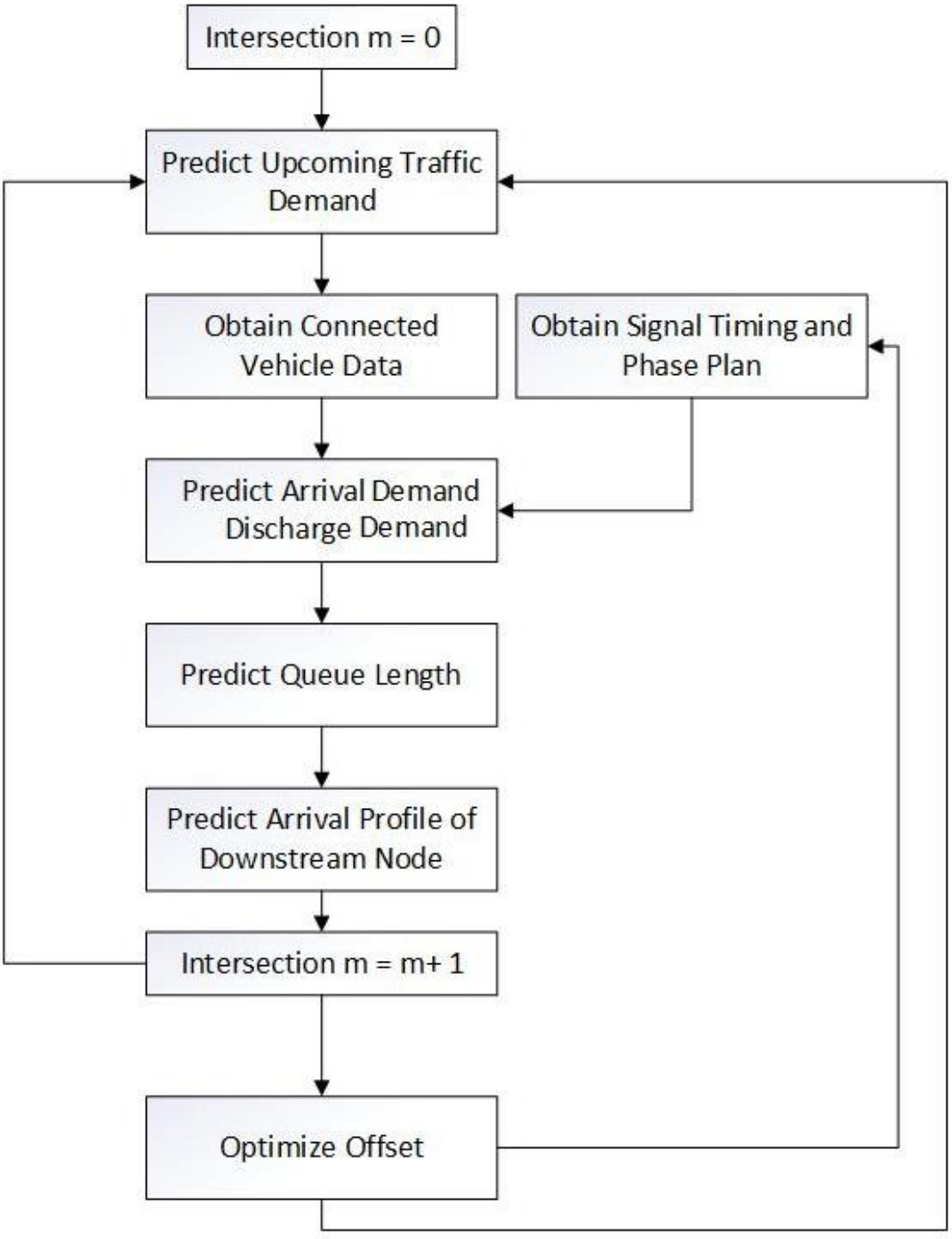

Figure 4.1 Logic of Offset Optimization

4.1.2 Strategy 2 Offset Optimization and Split Adjustment

The second strategy is to optimize offsets and split adjustment. The difference between strategy 2 and strategy 1 is split adjustment, which is added in Strategy 2. The green split adjustment is based on the arrival profile of upstream link of the coordinated intersection. Three data sets are needed to collect, measure, and predict for split adjustment. The first is the signal phasing plan and timing interval data of phases, such as minimum and maximum green time, yellow time, all red time, etc. The second data set is upcoming traffic demands (i.e. number of arrivals) within the next projection horizon for each phase. The final data set is the field data which determines discharge/departure characteristics of corresponding lane groups of a phase, such as lane configuration, discharge headway, startup lost time, etc.

Signal phase and timing data are easier to obtain and compare with the other two data sets. They can be obtained from DOTs, local transportation agencies, or field traffic signal controllers.

With respect to predicting real-time upcoming traffic demand within the next projection horizon for each phase, this study employs a simple procedure. Since upstream detectors are deployed for each approach of a coordinated intersection, the upstream arrival profiles of an approach during the last projection horizon may be obtained. In general, traffic propagates from upstream intersections to downstream intersections. This dissertation directly extracts upstream arrival profiles of the last projection horizon from the installed upstream detector, and those extracted arrival profiles are referred to as the upcoming upstream arrival profiles for the next projection horizon. Then, the forthcoming total number of vehicles for an approach in the next projection horizon could be generated by summarizing the collected upstream arrival profiles. After the upcoming total demand of an approach is obtained, it is

necessary to estimate traffic demands of each movement by evaluating real-time turning percentages for an approach.

4.1.3 Strategy 3 Split Adjustment and Cycle Length Adjustment

The third strategy is to develop a method of finding split and cycle length to mimic the state of practice in fine-tuning a traffic signal timing plan. Traffic volume and queue length were monitored at each phase at the intersections. If there are queues in one phase and the green is at a maximum, it is necessary to increase the split and then check whether the queue clears up in the next cycle. On the other hand, if there is unused green time in one phase but no queue at the end of the green time, the split of the phase is reduced. The above strategy is applied to all phases of an intersection. For example, in a network that contains five intersections, the strategy monitors actual green time and queue length at each phase and each intersection. Figure 4.1 displays a flow chart of the strategy to adjust green split and cycle lengths.

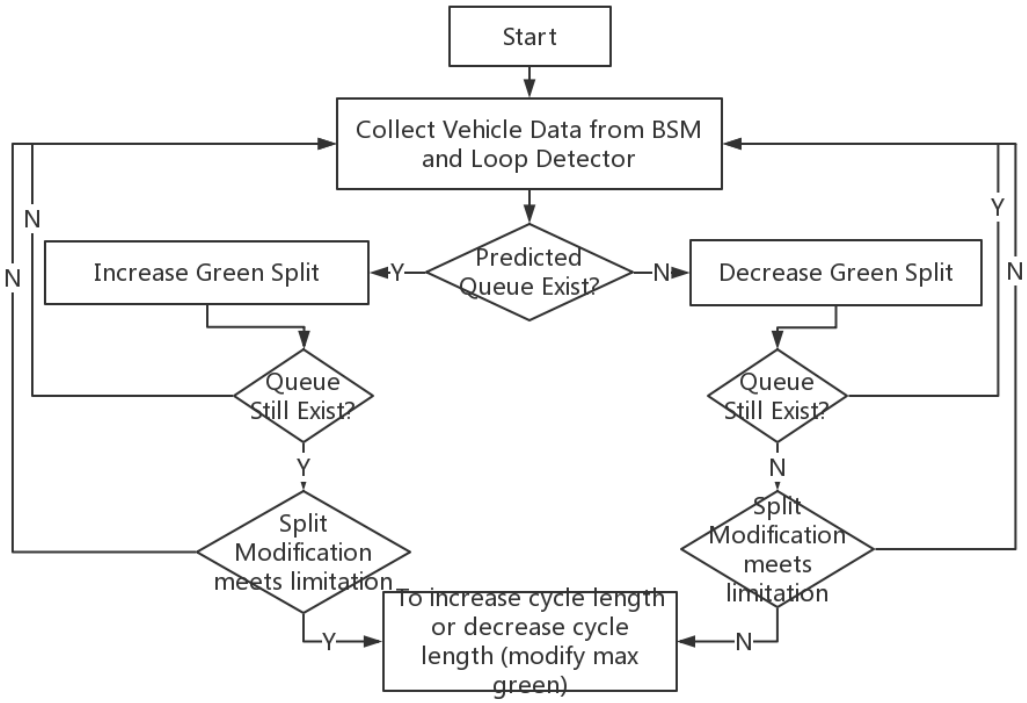

Figure 4.2 Flow Chart of Split Adjustment and Cycle Length Adjustment Strategy

The spilt adjustment has imposed a limitation of +/- 5 seconds in each cycle length to avoid the interruption of traffic progressions in transition phases. Due to limited changes in split, this dissertation implements direct transitions.

The cycle length adjustment method involves modifying cycle length when green split adjustments are not effective in reducing queue length. Summations of green, yellow, and red time intervals in all phases are added to the cycle length. When one intersection's cycle length increases, all other intersections' cycle length is increased to maintain the common cycle length in coordination. When the traffic is relatively stable, green splits within a cycle are adjusted to balance the fluctuations among different phases. When there are more vehicles in consecutive cycles that the cycle can handle, split adjustments have

little positive effect on queue length reduction (the existing queue length still increase or do not decrease). Therefore, cycle length should be adjusted and increased to accommodate competing traffic in all phases. When cycle length needs to be adjusted three times, it does not improve total queue length on all approaches, and cycle length increases by 5 seconds. Cycle length reduction is performed in the same way when there is unused green time within a cycle. When all intersections request cycle length reduction, cycle length is reduced by 5 seconds.

Split and/or cycle length adjustment is only implemented into several strategies in this dissertation. After split adjustment, offset and cycle length still needs to be optimized by the model (strategy 4). Another strategy is that, after split and cycle length adjustment, offset still needs to be optimized by the model (strategy 5).

4.1.4 Strategy 4 Offset Optimization, Split Adjustment, and Cycle Length Adjustment

Strategy 4 is the combination of strategy 1 and strategy 3. After strategy 3 adjusts green split and cycle length, strategy 4 employs the strategy 1 to optimize offsets of coordinated intersections. Firstly, strategy 4 adjusts split and cycle length. Then, to use new values of split and cycle length into offset optimization.

4.1.5 Strategy 5 Offset Optimization, Split Adjustment, and Cycle Length Optimization

Strategy 5 is to adjust split and optimize offset and cycle length. After split adjustment, strategy 5 uses the optimization model to generate optimal offset and cycle length for the new signal timing plan.

Cycle length optimization is different from cycle length adjustment; cycle length adjustment is to increase or decrease a fixed amount (5s) of cycle lengths when green split adjustments meet the previously described limitations and the queue length still doesn't decrease. It mimics critical intersection concepts in state-of-the-practice traffic signal retiming.

There are possible combinations of adjustment and optimization for the three parameters (offset, cycle length, and splits). For example, after split adjustments are completed locally, the purpose of cycle length optimization is to minimize the sum of queue delay in all phases and all signalized intersections; the common cycle length for all intersections and offsets for each coordinated intersection may be decision variables. The object function is non-linear and has multiple decision variables.

4.1.6 Strategy 6 Offset optimization, Split Optimization, and Cycle Length Optimization

Strategy 6 is to use the optimization algorithm to optimize offset, split, and cycle length. The cycle length, split, and offset optimization would use same objective function as the strategy 5 model. The only difference is to involve split into optimization instead of split adjustment. Split adjustment is finished during vehicle data collection. In cycle length, split, and offset optimization, the split adjustment is in the optimized algorithm as cycle length and split. In this methodology, split adjustment limitation (-/+5 seconds maximum) no longer affects split change. The optimal solution of objective function is deployed in the next project horizon.

4.2 Distributed System

This dissertation also considers distributed system design for real-world field deployment. In terms of real-world field deployment, it is necessary to address communication issues and computing power /time consumption of a centralized computer. To this end, two types of distributed system strategies are designed and implemented in this study.

4.2.1 The Framework of a Distributed System

4.2.1.1 Framework of the Distributed System

Figure 4.3 shows the proposed system which is deployed at client computers at all intersections and a master computer, for example, at the Traffic Management Center. In the client's computer, cycle length and splits can be obtained at the intersection level, as described in the state-of-the-practice method. The cycle length information is sent back to the server computer for approval. One distinct character of the distributed system is that the queue length is forecasted at the local client computer then sent to the server for optimization. That is, when the master computer sends out the offset, cycle length, and splits, the client computers estimate the queue lengths for all phases by taking the BSMs and traditional detector data stored locally. Queue length and other information is returned to the server. In this scenario, the offset, cycle length, and splits is placed in a virtual controller container and isn't implemented at the local controller.

The server provides the same objective function as a centralized model; however, the queue lengths are generated by the client computer. The same optimization algorithm is used. In each iteration, the optimization algorithm updates offset and cycle length. The

updated values are sent back to each computer at all intersections for the estimation of new queue lengths. The iterations end once there is little room to improve the delays or offset, cycle length and split changes are too small between consecutive iterations.

The optimization and local adjustment may work together for different decision variables. For example, optimization of the offset may be processed while cycle length and splits may be decided by state-of-the-practice methods. Details concerning these strategies are addressed in the sections that follow.

The physical layer architecture of distributed systems is shown in Figure 4.4; in this system, a master computer is placed at a centralized location as a server that could communicate with client computers. Client computers are installed into signal controller cabinet and connected controller box at each intersection in the field. The client computer interfaces with signal controller, BSM RSU and detectors. It receives "raw" traffic information data, processes the data, and generates aggregated data that can be used in the optimization model and algorithms in the server computer, in which cycle length and offset are generated.

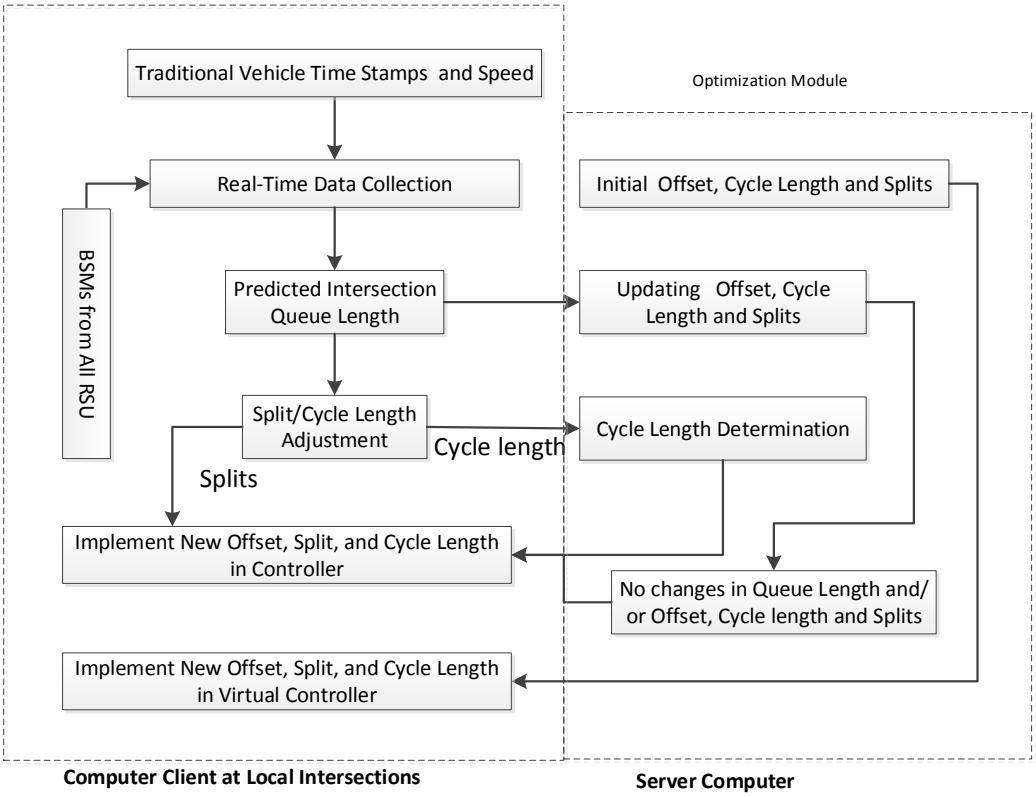

Figure 4.3 The Proposed Distributed System

The distributed architecture makes the system scalable. In this method, performance evaluations are distributed at computers in local intersections directly networked with RSU. It overcomes the centralized method issue in which BSM and raw detector information need to be sent through the network, processed by a centralized server, and evaluated by the server.

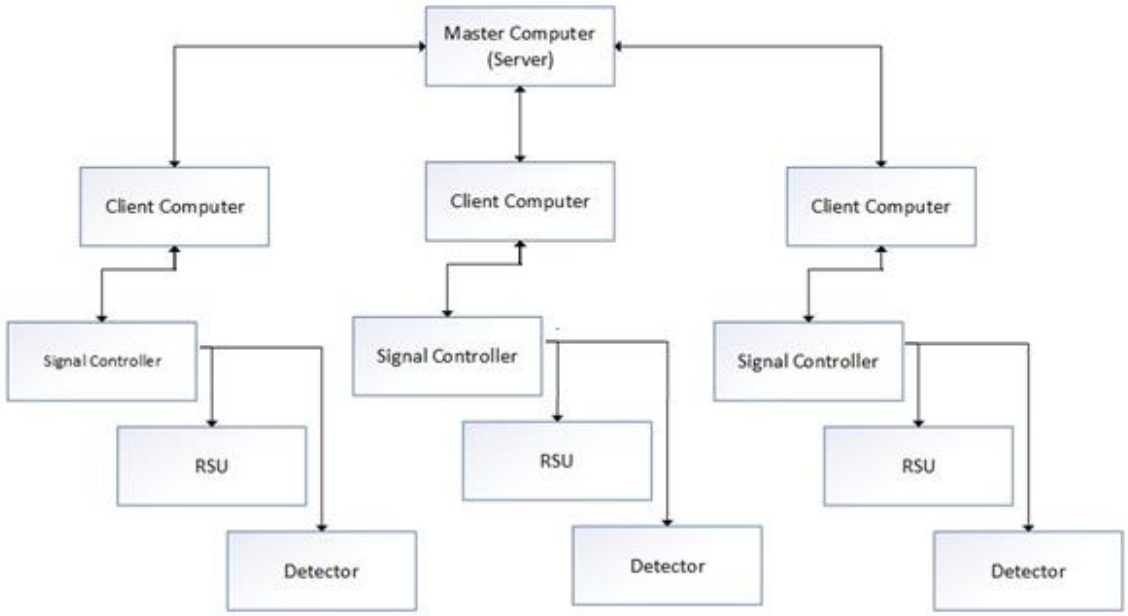

Figure 4.4 Physical Layer Distributed System Architecture

4.2.1.2 Common Cycle Length Estimation

In the distributed architectures, a centralized computer (server) is networked with computers (clients) deployed at each intersection. The server receives traffic and signal status information from clients and controls the cycle length and offsets of each client. Two options are considered. In both options, the splits can be adjusted in the same way as they were in the centralized method. That is, the BSM information around intersections is used to estimate queue length on the client side and send this information to the sever. The splits are dynamically adjusted on the client side, using the same principle to clear the queues as in the centralized system. This adjustment ensures that queues are dispersed within a cycle. However, the offset and common cycle length are adjusted differently.

In the distributed system, splits are dynamically adjusted in each cycle to balance queue length. If summation of the split is more than 105 percent of common cycle length

for three consecutive cycles, a 5 percent increase of common cycle length can be requested by a client. The server approves the new common cycle length, which is sent to all intersections (clients) to be executed. If the summation of split for one client is less than 95 percent for three consecutive cycles, a 5 percent decrease of common cycle length is registered. A Boolean array of common cycle length statuses are designed in the server. If elements in the array are all marked, the server grants a common cycle length reduction and broadcasts the new common cycle length to all intersections.

For the common cycle length adjustment in the first strategy, this dissertation employs one "no" veto for all rules. That is, the new common cycle length isn't granted unless all clients request it. The experiment could contain a supermajority rule (if 66 percent of intersections requested common cycle length reduction), majority rules (50 percent or more intersections make the request), or a minority rule (33 percent make the request). Similarly, for a common cycle length increase, the case study could change to the majority, supermajority, and minority rules to vote on common cycle length increase. This dissertation tested the majority rule in its case studies.

When the methodology only adjusts or optimizes split and cycle length, offset is a fixed value in the objective function. It should then be decided by another method (for example, manual travel time calibration). For example, in S3, offset is assigned as constant, and the program only adjusts split and cycle length, then chooses common cycle length.

4.2.1.3 Offset Estimation

The experiments indicated that the performance of the above strategies is somewhat not as good as those in the centralized methods in the case study for Dolly Madison Blvd.

(VA-123) in Mclean VA: Therefore, only strategies 3-6 (offset, green split and common cycle length optimization) with 5 different penetration rates (10 percent, 25 percent, 50 percent, 60 percent, 70 percent) are discussed.

The optimization program produces offset length plans for performance evaluation for clients, who pass performance index (PI) data back to the server. The performance evaluation program and traffic models are decentralized and deployed in client computers at intersections. The PIs include queue length and length of green after queue is cleared at all intersections. Once the server receives PIs from all clients, new common cycle lengths and offsets for all intersections are generated and sent back to traffic models in client computers at local intersections for PI reevaluation. With PIs from each intersection, objective functions corresponding to a specific set of offsets and one common cycle length are generated by the server. With the new common cycle length and splits, clients in turn send new PIs back to server without implementation in signal controller. The processes are repeated until there is no performance index gain or little change in offset/common cycle length or time out.

4.2.2 Two Stages Optimization in Distributed System

Another distributed system strategy is to optimize offset, split, and cycle length of major and minor directions of intersections individually. The green phases on major and minor streets are called sequentially at different times in a cycle. If the traffic model estimates queue length on major and minor only once in a cycle, the forecast time horizon is long (at least a cycle). To increase accuracy of vehicle profile and queue length estimation, the prediction of queue length of major/minor is considered twice a cycles.

When major or minor are shorter links or RSU's communication range could not cover entire length of a link, the prediction of queue length may not contain all of vehicles need to be count. For example, the cycle length of intersections is 150-200 seconds in case study, when the vehicle travel in free flow speed of 30mph could travel a substantial distance of over one mile. In this case, random nature of traffic progression makes queue length forecast unpredictable. The solution to improve queue length accuracy is to divide time stamp of estimating queue length into two stages.

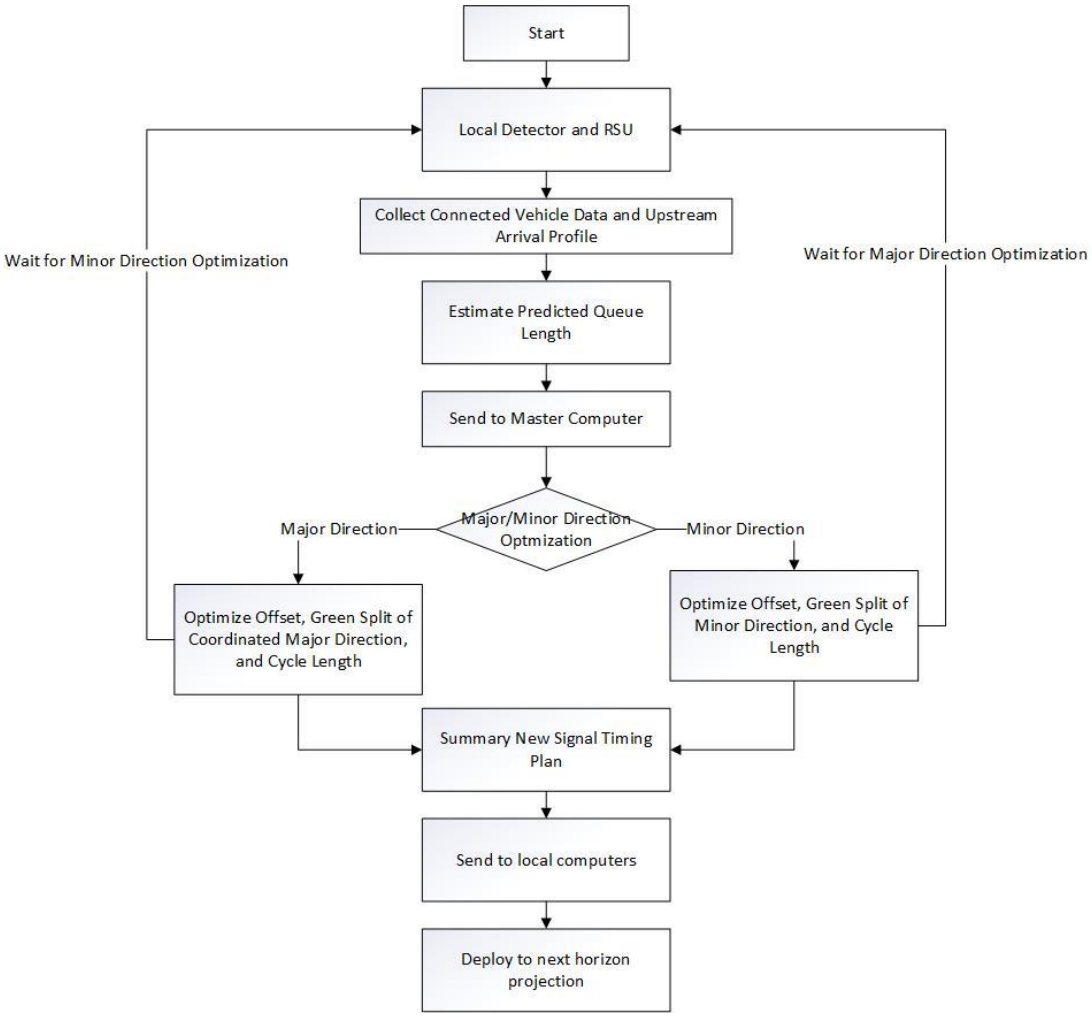

Figure 4.5 Flow Chart of Distributed System

In the meantime, the optimization of signal control key variables, green split and cycle length could be divided to two groups according to the forecast stages: major street/coordination and minor street. The distributed system therefore optimizes major/minor variables in each of two stages alternately. At major direction green indication start time, the control variables are minor direction signal timing plan. At the minor direction green indication start time, the control variables are major direction signal timing plan. Figure 4.5 displays the procedure of the distributed system optimization strategy. As shown in Figure 4.5, the predicted queue length is estimated in the local client computer based on connected vehicle data and detectors in the upstream. Then, queue lengths are transmitted to a master centralized computer. In the centralized computer, the optimization model generates new offset, split, or cycle length. Then new offset, split, or cycle length are sent back to local signal controllers and deployed for the next horizon projection.

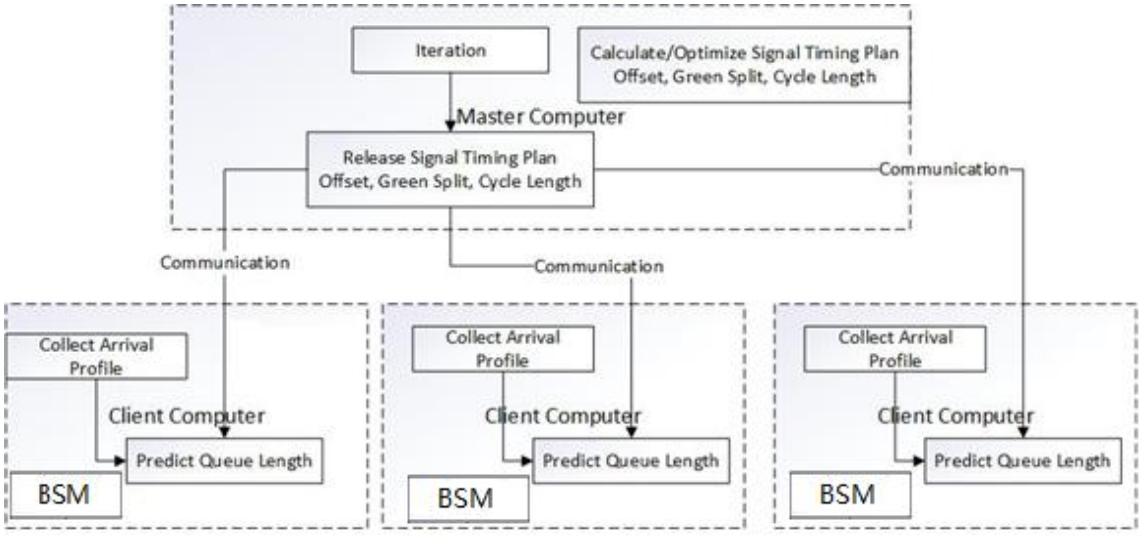

Figure 4.6 Functional Chart of Distributed System in Functional Level

In addition, Figure 4.6 displays the functional chart of the distributed system. In this system, the master computer is responsible for generating and optimizing the signal timing plan. The communication link connects the master computer and client computers. Each client computer only receives the signal timing plan of its controller. The queue length forecast of all approaches of this intersection is based on connected vehicle BSM data, upstream link detector vehicle arrival profile data, and coordinated direction discharge vehicle data of the previous cycle. The client computer predicts the queue lengths with this cycle. Finally, the results of the queue length forecast are sent back to the master computer. The master computer uses all client computers' queue length forecasts to optimize the new signal timing plan.

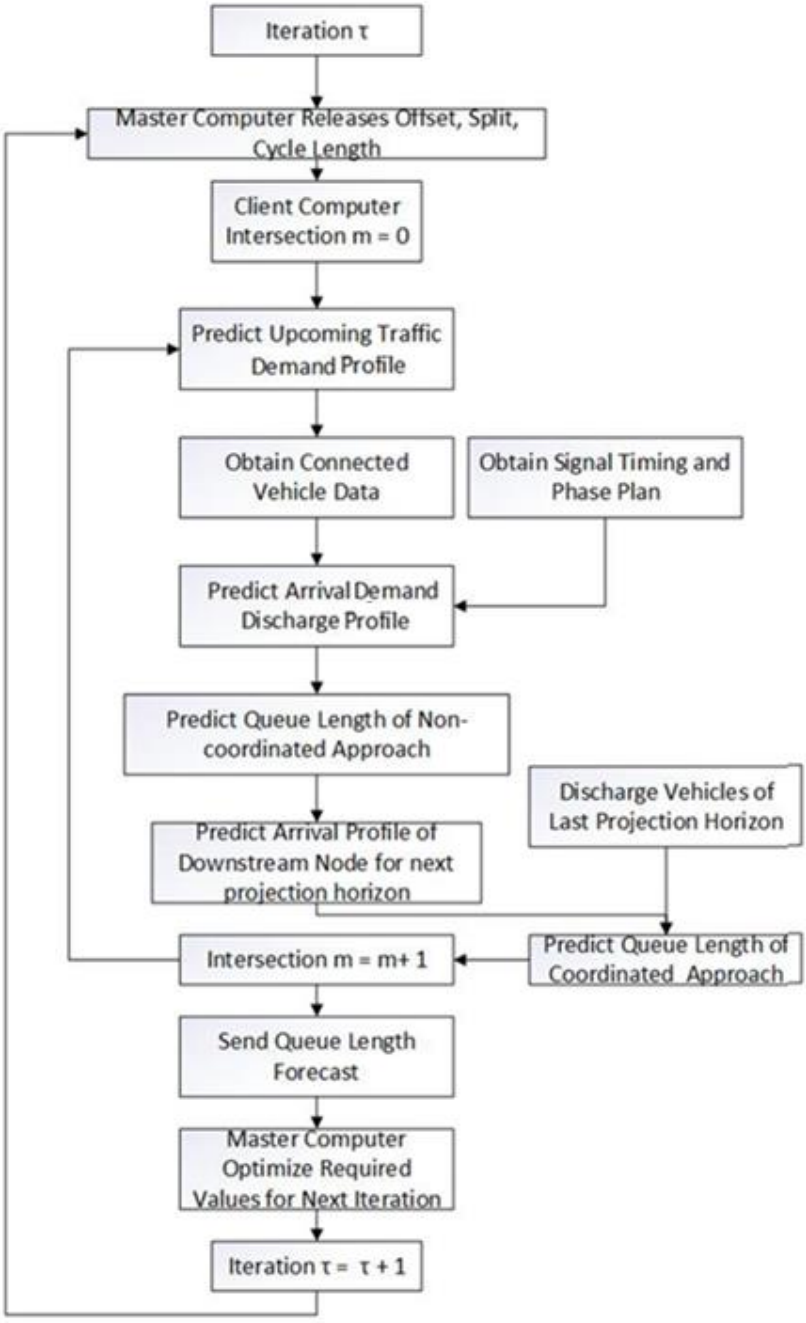

Figure 4.7 Algorithm Logic of Distributed System in Iteration

Figure 4.7 shows the algorithm of the distributed system. In each iteration, the distributed system could assign different tasks to the master computer and client computers.

The client computer parallelly forecast the queue length and compute objective functions; in this way, small amount of data is communicated between the master computer and client computers. These features could improve system performance in terms of time consumption and reliability.

There are two strategies of this new signal timing plan choice. The first is weighted calculation. After major and minor optimizations finish, the new signal timing plan is calculated by different weight of major and minor directions. The following equation shows the new signal timing plan calculation.

$$o_m = \frac{v_{major}}{v_{total}} * o_{m,major} + \frac{v_{minor}}{v_{total}} * o_{m,minor} \quad \text{(E4.2.1)}$$

$$g_{m,p} = \frac{v_{major}}{v_{total}} * g_{m,p,major} + \frac{v_{minor}}{v_{total}} * g_{m,p,minor} \quad \text{(E4.2.2)}$$

$$c_m = \frac{v_{major}}{v_{total}} * c_{m,major} + \frac{v_{minor}}{v_{total}} * c_{m,minor} \quad \text{(E4.2.3)}$$

v_{major}: The traffic volume of major direction (coordinated direction) of one intersection *m*.

v_{minor}: The traffic volume of minor direction (non-coordinated direction) of one intersection *m*.

Anther strategy is to use two stage optimizations for major and minor direction separately. The different key variables in major and minor direction are optimized in different stages. In the major direction optimization, optimized variables contain offset, green split of major direction, and part of cycle length. In the minor direction optimization, optimized variables contain green split of minor direction and part of cycle length. When

the optimization runs, the cycle length is calculated by old green split and green split variables. After the two stage optimizations finish, the new signal timing plan is the summary of major and minor direction optimizations. The equations below are major and minor direction optimization objective functions.

$$\text{Major Direction: } \min \sum_{m \in M} \sum_{p_{(c)} \in P_{(c)}} s_{m,p}(o_m, g_{m,p(c)}) \quad \text{(E4.2.4)}$$

$$\text{Minor Direction: } \min \sum_{m \in M} \sum_{p_{(n)} \in P_{(n)}} s_{m,p}(g_{m,p(n)}) \quad \text{(E4.2.5)}$$

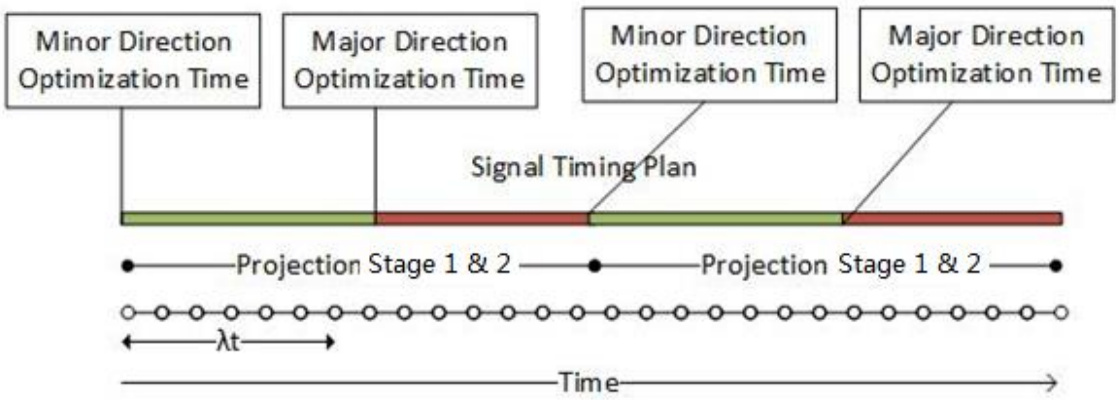

Figure 4.8 Optimal Time Step of Two Stages Optimization Distributed System

As indicated in Figure 4.8, the major and minor direction optimization stage occurs at different times. The start time of green indication of major direction optimizes the minor direction signal timing plan. When green indication ends, the minor direction starts green indication and optimize the major direction signal timing plan. Each cycle includes two stages for optimizations.

The strength of two stages optimization distributed system strategy is to increase the accuracy of queue length forecast. The method of optimization at two stages times can mitigate the issue of vehicles failing to be counted in the upstream detector.

One of the limitations for the distributed system strategy is time limitation. Compared to the centralized system, the distributed system has shorter computing time of optimization. Whereas the centralized system has the whole cycle (150-200 seconds), the distributed system only has half of the cycle. The major direction optimization may occur in only 30-40 seconds or less. In the two stages-optimization distributed system, it is necessary to consider computing time consumption. The result of the signal timing plan may not be the optimal solution and may affect the performance of optimal model. Another limitation is two stages optimization. The major and minor directions only optimize the specific signal timing plan. The other key variables in a centralized system would use the previous optimal solution, which would decrease the performance of signal timing plan in terms of mobility. Chapter VIII provides discussion and analysis of performance measurement of the distributed system.

CHAPTER V

OBJECTIVE FUNCTION

5.1 Parameters and Variables of Objective Function

Table 5.1 Set subscripts parameters and variables used in formulation.

m	The index of coordinated intersections (m= 1, 2, 3, ···, M)
M	Total number of coordinated intersections in a signalized arterial
k	Turning movement (left =1, through =2, and right=3)
d	Approach of each intersection (d= 1, 2, 3, …, and D)
D	Total number of approaches for an intersection
p	The index of phases for an intersection (p =1, 2, 3, … and P)
P	Total number of phases for an intersection
Δ	Time interval to calculate s (1 second is used)
t	The t'th time interval in the projection horizon (t =1, 2, 3, … and T)
T	Total number of time interval in the projection horizon
λ_t	Time since the beginning of projection horizon $\lambda_t = \Delta \times t$
$F(s_{m,p})$	The queue delay function in phase p at intersection m within the projection horizon (one cycle)
$s_{m,p}$	The total stop-delay of phase p at intersection m within the projection horizon (one cycle)
$q_{m,d,t}$	The queue length of approach d at intersection m at time interval t
o_m	Offset of intersection m
$R_{m,p}$	The duration of red indications before green phase p at intersection m (seconds)
$g_{m,p}$	The duration of green time of phase p at intersection m (seconds)
c_m	The cycle length of coordinated intersections
l_m	The total lost time of intersection m due to all red and startup loss time (seconds)
$\omega_{m,p}$	Vehicle movement of phase p at intersection m within projection horizon (%)
$v_{m,d,t}$	Number of arrival vehicles at intersection m at projection horizon t (vehs)

Table 5.1 Set subscripts parameters and variables used in formulation. (Continued)

$\alpha_{m,d(n),t}$	Number of vehicles in initial queue region at intersection m that is still remains in queue at time interval t (vehs, in a none coordination phase)
$\beta_{m,d(n),t}$	Number of vehicles in queue formulation region at intersection m at time interval t (vehs, in a none coordination phase)
$\gamma_{1,m,d(n),t}$	Number of vehicles in progression formulation region 1 at intersection m at time interval t (vehs, in a none coordination phase)
$\gamma_{2,m,d(n),t}$	Number of vehicles in progression formulation region 2 at intersection m at time interval t (vehs, in a none coordination phase)
$\gamma_{m,d(n),t}$	Total number of vehicles in progression formulation region 1 and 2 at intersection m at time interval t (vehs, in a none coordination phase)
$\rho_{m,p}$	Number of connected vehicle in the queue at the beginning of a projection horizon associated with phase p at intersection m (vehs)
$\sigma_{\mathrm{m,p}}$	Number of connected vehicles discharged during phase p at coordinated intersection m within a projection horizon (vehs)
$\theta_{m,d(c),t}$	Number of vehicles couldn't arrive at coordinated approach d at coordinated intersection m in the projection horizon t (vehs)
$\tau_{m,d(c),t}$	The travel time of vehicle could arrive to coordinated intersection from an approach d of a coordinated intersection m at projection horizon t (seconds)
$L_{m,d(c)}$	The length of link of an approach d at coordinated intersection m (ft.)
$\varphi_{m,d(c),t}$	The distance of last vehicle in the queue to stop bar of an approach d at coordinated intersection m at projection horizon t (ft.)
$\mu_{m,d(c)}$	The free flow speed of link of an approach d at coordinated intersection m (ft./sec)
$\eta_{m,p,t}$	Number of discharge vehicles in phase p at intersection m at projection horizon t (vehs)
$V_{m-1,p}$	Number of vehicles entering the coordinate phase from all phases of previous cycle at the upstream intersection
$\eta_{m,d,t}$	Number of discharge vehicles in approach d at intersection m at projection horizon t (vehs)
$h_{m,p,t}$	Discharge headway of vehicle in phase p at intersection m at projection horizon t (vehs/sec)
$H_{m,d,t}$	Arrival headway of vehicle in approach d at intersection m at projection horizon t (vehs/sec)
$H_{m,p,t}$	Arrival headway of vehicle in phase p at intersection m at projection horizon t (vehs/sec)
$u_{\mathrm{m,p}}$	The number of connected vehicles associated with phase p at intersection m within project horizon
U_{m}	The number of connected vehicles in all critical movements at intersection m within project horizon
r	r'th iteration in seeking optimal offset and cycle length

5.2 Strategy 5 Offset and Cycle Length Optimization

As described in the queue length forecast section, when traffic propagates from one intersection to the next intersection, queue length within the projected time can be estimated. The total queue delay of all phases at all intersections is summarized as:

$$min \sum_{m\in M} \sum_{p\in P} s_{m,p,t} = \sum_{m\in M} \sum_{p\in d} \int_0^{c_{m,t}} q_{m,d,t} d\lambda_t \quad \text{(E5.2.1)}$$

$$s_{m,p} = \int_0^{R_{m,p}} (\omega_{m,p,t} \times v_{m,d,t}) d\lambda_t + \int_{R_{m,p}}^{R_{m,p}+g_{m,p}} (\omega_{m,p,t} \times v_{m,d,t} - \eta_{m,p,t}) d\lambda_t + \int_{R_{m,p}+g_{m,pt}}^{c_m} (\omega_{m,p,t} \times v_{m,d,t}) d\lambda_t \quad \text{(E5.2.2)}$$

$$s_{m,p} = \int_0^{c_m} (\omega_{m,p,t} \times v_{m,d,t}) d\lambda_t - \int_{R_{m,p}}^{R_{m,p}+g_{m,p}} \eta_{m,p,t} \, d\lambda_t \quad \text{(E5.2.3)}$$

The purpose of the cycle length and offset optimization method is to consider all directions' queue length and minimize total queue length. Cycle length and offset optimization is one of part of cycle length, green split, and offset optimization. The following section introduces more details of the optimization model. The objective function in this section is same as the next section; the only difference is decision variables.

$$min \sum_{m\in M} \sum_{p\in P} s_{m,p,t} = \sum_{m\in M} \sum_{p\in P} \int_0^{c_{m,t}} q_{m,p,t} d\lambda_t \quad \text{(E5.2.4)}$$

The queue length is determined by the arrival vehicle and discharge vehicle. The number of arrival vehicles of each phase is used to determine vehicle movement and number of approaching vehicles. The number of discharge headway $h_{m,p,\tau,i}$ is determined by stop bar detectors and connected vehicle data. Then, queue length may be used in queue delay estimation in one cycle.

$$s_{m,p} = \int_0^{R_{m,p}} (\omega_{m,p} \times v_{m,d,t}) d\lambda_t + \int_{R_{m,p}}^{R_{m,p}+g_{m,p}} (\omega_{m,p} \times v_{m,d,t} - \eta_{m,p,t}) d\lambda_t +$$

$$\int_{R_{m,p}+g_{m,pt}}^{c_m} (\omega_{m,pt} \times v_{m,d,t}) d\lambda_t \quad \text{(E5.2.5)}$$

$$s_{m,p} = \int_0^{c_m} (\omega_{m,p,t} \times v_{m,d,t}) d\lambda_t - \int_{R_{m,p}}^{R_{m,p}+g_{m,p}} \eta_{m,p,t}\, d\lambda_t \quad \text{(E5.2.6)}$$

$$\eta_{m,p,t} = n\{ where \sum_{i=R_{m,p}}^{t} h_{m,p,i} < (\lambda_t - R_{m,p}) \le g_{m,p} and \sum_{i=R_{m,p}}^{t+1} h_{m,p,i} <$$

$$(\lambda_t - R_{m,p}) \le g_{m,p}\} \quad \text{(E5.2.7)}$$

$$\eta_{m,d,t} = \sum_{p \in d} \eta_{m,p,t} \quad \text{(E5.2.8)}$$

In this algorithm, green split is not optimized; rather, it is distributed by online traffic.

$$g_{m,p} = \frac{u_{m,p}}{U_m} (c_m - l_m) \quad \text{(E5.2.9)}$$

Therefore,

$$\frac{\partial (s_{m,p})}{\partial c_m} = (\omega_{m,p,t} \times v_{m,d,t}) - \eta_{m,p,t} \frac{\partial \left(R_{m,p} + \frac{u_{m,p}}{U_m} (c_m - l_m) \right)}{\partial c_m} = (\omega_{m,p,t} \times v_{m,d,T}) -$$

$$\eta_{m,p,T} \frac{u_{m,p}}{U_m} \text{ (when } \lambda_t = C_m, t = T) \quad \text{(E5.2.10)}$$

$$\frac{\partial (s_{m,p})}{\partial o_m} = \omega_{m,p} \times \int_0^{c_m} \frac{\partial (v_{m,d,t})}{\partial o_m} d\lambda_t \quad \text{(E5.2.11)}$$

The number of vehicles in queue length forecast is summarized by vehicles in four regions, with two different conditions: the coordinated approach and non-coordinated approach to intersection. The assumption of minor direction vehicle arrival rate is unique.

$$v_{m,d(n),t} - \eta_{m,d(n),t} = \alpha_{m,d(n),t} + \beta_{m,d(n),t} + \gamma_{2,m,d(n),t} + \gamma_{1,m,d(n),t} \quad \text{(E5.2.12)}$$

$$v_{m,d(c),t} = \sum_{p \in P(m-1)} \eta_{m,d(c),0} - \theta_{m,d(c),t} \quad \text{(E5.2.13)}$$

The formula (E5.2.14 to E5.2.20) addresses how to get E5.2.12 and E5.2.13. Vehicle movement in one phase at an intersection is estimated online. It is calculated by summary of connected vehicles in the queue within a projection horizon for vehicle movement p and the number of connected vehicles discharged within a project horizon. Then, the percentage of one type vehicle movement associated with phase p is divided by sum of all movements in approach d.

The number of vehicles in the residual queue region is the same as previous queue length in the last projection horizon. The number of vehicles in the queue formulation region is the maximum number between zero and the potential number of vehicles discharged in the remaining green time. The number of vehicles in progression region 1 is calculated by the number of vehicles that arrive in the remaining green time and discharge capacity. The number of vehicles in progression region 2 is calculated by number of vehicles that could arrive in this projection horizon (arrive on red) and discharge capacity.

$$\omega_{m,p} = \frac{\rho_{m,p} + \sigma_{\mathrm{m,p}}}{\sum_{p \in d} \rho_{m,p} + \sum_{p \in d} \sigma_{\mathrm{m,p}}} \times 100\% \quad \text{(E5.2.14)}$$

$$\alpha_{m,d,t} = q_{m,d,0} - \eta_{m,d,t} \quad \text{(E5.2.15)}$$

$$\beta_{m,d,t} = \eta_{m,d,t} - (\alpha_{m,d,t} + n\{ where \ \sum_{i=0}^{t} H_{m,d,i} < \lambda_t \ and \ \sum_{i=0}^{t+1} H_{m,d,i} \geq \lambda_t \}) \quad \text{(E5.2.16)}$$

The number of vehicles in the queue progression region is determined by the arrival headway of upstream link vehicles and green time or cycle length. Green time and cycle length can be used to estimate the range of the vehicle determination.

$$\gamma_{m,d,t} = \gamma_{1,m,d,t} + \gamma_{2,m,d,t} = n\{ where \ \sum_{i=0}^{t} H_{m,d,i} < c_m \ and \ \sum_{i=0}^{t+1} H_{m,d,i} \geq c_m \} - \eta_{m,d,t} \quad \text{(E5.2.17)}$$

Therefore, $v_{m,d(n),t}$ can be obtained from E5.2.15-E5.2.17. It is also important to note that (E5.2.14), (E5.2.15), (E5.2.16), and (E5.2.17) are not the function of offset (o_m). (E5.2.14), (E5.2.15), and (E5.2.16) are not the function of cycle length (c_m). $\gamma_{m,d,t}$ *or* (E5.2.17) does change with the change of cycle length c_m .

In E5.2.12, the number of vehicles that could not arrive in the current projection horizon is determined by arrival time and offset of next coordinated intersection. The duration of vehicle arrival at a coordinated intersection from a coordinated intersection is calculated by length of link and free flow speed on the link. E5.2.20 is obtained to replace E5.2.13

$$\theta_{m,d(c),t} = \left\{n \ where \ \sum_{i=0}^{\tau_{m,d(c),t}} H_{m,d,i} < \lambda_t \ and \ \sum_{i=0}^{\tau_{m,d(c),t}+1} H_{m,d,i} \geq \lambda_t\right\} - \left\{n \ where \ \sum_{i=0}^{\tau_{m,d(c),t}} H_{m,p,i} < o_m \ and \ \sum_{i=0}^{\tau_{m,d(c),t}+1} H_{m,d,i} \geq o_m\right\} = \bar{H}_{m,d,t} \times (\tau_{m,d(c),t} - o_m) \quad \text{(E5.2.18)}$$

$$\tau_{m,d(c),t} = (L_{m,d(c)} - \varphi_{m,d(c),t})/\mu_{m,d(c)} \quad \text{(E5.2.19)}$$

$$v_{m,d(c),t} = \sum_{d \in P(m-1)} V_{m-1,d} - \bar{H}_{m,d,t} \times (\tau_{m,d(c),t} - o_m) \quad \text{(E5.2.20)}$$

$$F(O_m, C_m) = \sum_{m \in M} \sum_{p \in P} s_{m,p} = \sum_{m \in M} \sum_{p \in P} \left[\int_0^{c_m} (\omega_{m,p} \times v_{m,d,t}) d\lambda_t - \int_{R_{m,p}}^{R_{m,p}+g_{m,p}} \eta_{m,p,t} \, d\lambda_t\right] \quad \text{(E5.2.21)}$$

$$\frac{\partial F}{\partial C_m} = \sum_{p \in P} (\omega_{m,p,t} \times v_{m,d,\mathrm{T}}) - \eta_{m,p,T} \frac{u_{\mathrm{m,p}}}{U_m} \quad \text{(E5.2.22)}$$

As indicated before, for all non-coordinated phases, $\frac{\partial s_{m,p(n)}}{\partial o_m} = 0$.

Therefore,

$$\frac{\partial F}{\partial o_m} = \frac{\partial s_{m,p(c)}}{\partial o_m} = \omega_{m,p(c)} \int_0^{c_m} \frac{\partial (v_{m,d,t})}{\partial o_m} d\lambda_t = \omega_{m,p(c)} \sum_{t=1}^{T} \bar{H}_{m,d,t} \quad \text{(E5.2.23)}$$

S.T.

$$c_1 = c_2 = c_3 \ \ldots = c_m \quad \text{(E5.2.24)}$$

$$\alpha_{m,d(n),t} \geq 0 \quad \text{(E5.2.25)}$$

$$\beta_{m,d(n),t} \geq 0 \quad \text{(E5.2.26)}$$

$$\gamma_{1,m,d(n),t} \geq 0 \quad \text{(E5.2.27)}$$

$$o_m < c_m \quad \text{(E5.2.28)}$$

$$o_m < \tau_{m,d(c),t} \quad \text{(E5.2.29)}$$

The object function is non-linear, in this case, because Newton's iteration method is advantageous when compared to rapid local convergence, (L. Grippo, F. Lampariello, and S. Lucidi, 1986) it is chosen as the algorithm to find the minimum point of the function F(Offset, Cycle Length).

$$(O_m, C_m)^{r+1} = (O_m, C_m)^r - F(O_m, C_m)/F'(O_m, C_m) \quad \text{(E5.2.30)}$$

5.3 Strategy 6 Offset, Split, and Cycle Length Optimization

As described in the predicted queue length section, when traffic propagates from one intersection to the next intersection, the queue length during the projected time can be estimated. The total queue delay of all phases at all intersections is summarized as:

$$min \sum_{m\in M} \sum_{p\in P} s_{m,p,t} = \sum_{m\in M} \sum_{p\in P} \int_0^{c_{m,t}} q_{m,p,t} d\lambda_t \quad \text{(E5.3.1)}$$

The queue length is determined by arrival vehicle and discharge vehicle. The number of arrival vehicle of each phase is used as the vehicle movement and number of arrival vehicles of one approach. Discharge headway $h_{m,p,\tau,i}$ is determined by stop bar detectors and connected vehicle data. Then, queue length can be used in queue delay estimation for one cycle.

$$s_{m,p} = \int_0^{R_{m,p}} (\omega_{m,p} \times v_{m,d,t}) d\lambda_t + \int_{R_{m,p}}^{R_{m,p}+g_{m,p}} (\omega_{m,p} \times v_{m,d,t} - \eta_{m,p,t}) d\lambda_t + \int_{R_{m,p}+g_{m,pt}}^{c_m} (\omega_{m,pt} \times v_{m,d,t}) d\lambda_t \quad \text{(E5.3.2)}$$

$$s_{m,p} = \int_0^{c_m} (\omega_{m,p,t} \times v_{m,d,t}) d\lambda_t - \int_{R_{m,p}}^{R_{m,p}+g_{m,p}} \eta_{m,p,t} \, d\lambda_t \quad \text{(E5.3.3)}$$

$$\eta_{m,p,t} = n \{ where \ \sum_{i=R_{m,p}}^{t} h_{m,p,i} < (\lambda_t - R_{m,p}) \le g_{m,p} and \ \sum_{i=R_{m,p}}^{t+1} h_{m,p,i} < (\lambda_t - R_{m,p}) \le g_{m,p} \} \quad \text{(E5.3.4)}$$

$$\eta_{m,d,t} = \sum_{p\in d} \eta_{m,p,t} \quad \text{(E5.3.5)}$$

Therefore,

$$\frac{\partial(s_{m,p})}{\partial c_m} = (\omega_{m,p,t} \times v_{m,d,t}) \quad \text{(E5.3.6)}$$

$$\frac{\partial(s_{m,p})}{\partial O_m} = \omega_{m,p} \times \int_0^{c_m} \frac{\partial(v_{m,d,t})}{\partial o_m} d\lambda_t \quad \text{(E5.3.7)}$$

$$\frac{\partial(s_{m,p})}{\partial g_{m,p}} = -\eta_{m,p,T} \quad \text{(E5.3.8)}$$

The number of vehicles in queue length forecast is summarized by vehicles in four regions. There are two different conditions: coordinated approach to intersection and non-coordinated approach. There is an assumption that minor direction vehicle arrival rate is unique.

$$v_{m,d(n),t} - \eta_{m,d(n),t} = \alpha_{m,d(n),t} + \beta_{m,d(n),t} + \gamma_{2,m,d(n),t} + \gamma_{1,m,d(n),t} \quad \text{(E5.3.9)}$$

$$v_{m,d(c),t} = \sum_{p\in P(m-1)} \eta_{m,d(c),0} - \theta_{m,d(c),t} \quad \text{(E5.3.10)}$$

The vehicle movement in one phase at an intersection is estimated online. It is calculated by summary of connected vehicles in the queue within a projection horizon for a vehicle movement p and the number of connected vehicles discharged within a project horizon. Then percentage of one type of vehicle movement associated with phase p is divided by sum of all movements in approach d.

$$\omega_{m,p} = \frac{\rho_{m,p} + \sigma_{\mathrm{m,p}}}{\sum_{p \in d} \rho_{m,p} + \sum_{p \in d} \sigma_{\mathrm{m,p}}} \times 100\% \quad \text{(E5.3.11)}$$

The number of vehicles in the residual queue region is the same as previous queue length of the last projection horizon. The number of vehicles in the queue formulation region is the max number between zero and the number of vehicles that could be discharge in the remaining green time. The number of vehicles in progression region 1 is calculated by number of vehicles that could arrive in the remaining green time and discharge capacity. The number of vehicles in progression region 2 is calculated by the number of vehicles that could arrive in this projection horizon (arrive on red) and discharge capacity.

$$\alpha_{m,d,t} = q_{m,d,0} - \eta_{m,d,t} \quad \text{(E5.3.12)}$$

$$\beta_{m,d,t} = \eta_{m,d,t} - (\alpha_{m,d,t} + n\{ where \ \sum_{i=0}^{t} H_{m,d,i} < \lambda_t \ and \ \sum_{i=0}^{t+1} H_{m,d,i} \geq \lambda_t \}) \quad \text{(E5.3.13)}$$

The vehicles in the queue progression region are determined by the arrival headway of upstream link vehicles and green time or cycle length. Green time and cycle length can be used to estimate the range of the vehicle determination.

$$\gamma_{m,d,t} = \gamma_{1,m,d,t} + \gamma_{2,m,d,t} = n\{ where \ \sum_{i=0}^{t} H_{m,d,i} < c_m \ and \ \sum_{i=0}^{t+1} H_{m,d,i} \geq c_m \} - \eta_{m,d,t} \quad \text{(E5.3.14)}$$

In E5.3.15, the number of vehicles that could not arrive in the current projection horizon is determined by arrival time and offset at the next coordinated intersection. Duration between vehicle arrival time at a coordinated intersection and departure from the previous coordinated intersection is calculated by length of link and free flow speed on the link. E5.3.17 is obtained to replace E5.3.10

$$\theta_{m,d(c),t} = \left\{n \; where \; \sum_{i=0}^{\tau_{m,d(c),t}} H_{m,d,i} < \lambda_t \; and \; \sum_{i=0}^{\tau_{m,d(c),t}+1} H_{m,d,i} \geq \lambda_t\right\} - \left\{n \; where \; \sum_{i=0}^{\tau_{m,d(c),t}} H_{m,p,i} < o_m \; and \; \sum_{i=0}^{\tau_{m,d(c),t}+1} H_{m,d,i} \geq o_m\right\} = \bar{H}_{m,d,t} \times (\tau_{m,d(c),t} - o_m) \quad \text{(E5.3.15)}$$

$$\tau_{m,d(c),t} = (L_{m,d(c)} - \varphi_{m,d(c),t})/\mu_{m,d(c)} \quad \text{(E5.3.16)}$$

$$v_{m,d(c),t} = \sum_{d \in P(m-1)} V_{m-1,d} - \bar{H}_{m,d,t} \times (\tau_{m,d(c),t} - o_m) \quad \text{(E5.3.17)}$$

$$F(O_m, C_m) = \sum_{m \in M} \sum_{p \in P} s_{m,p} = \sum_{m \in M} \sum_{p \in P} \left[\int_0^{c_m} (\omega_{m,p} \times v_{m,d,t}) d\lambda_t - \int_{R_{m,p}}^{R_{m,p}+g_{m,p}} \eta_{m,p,t} \, d\lambda_t\right] \quad \text{(E5.3.18)}$$

$$\frac{\partial F}{\partial C_m} = \sum_{p \in P} (\omega_{m,p,t} \times v_{m,d,\mathrm{T}}) - \eta_{m,p,T} \frac{u_{\mathrm{m,p}}}{U_m} \quad \text{(E5.3.19)}$$

$$\frac{\partial F}{\partial g_{m,p}} = \eta_{m,p,T} \frac{u_{\mathrm{m,p}}}{U_m} \quad \text{(E5.3.20)}$$

S.T.

$$c_1 = c_2 = c_3 \ldots = c_m \quad \text{(E5.3.21)}$$

$$\begin{cases} g_{m,1} + g_{\mathrm{m},2} = g_{\mathrm{m},5} + g_{\mathrm{m},6} \\ g_{\mathrm{m},3} + g_{\mathrm{m},4} = g_{\mathrm{m},7} + g_{\mathrm{m},8} \end{cases} \quad \text{(E5.3.22)}$$

$$g_{m,1} + g_{\mathrm{m},5} + g_{\mathrm{m},3} + g_{\mathrm{m},7} + l_m = c_m \quad \text{(E5.3.23)}$$

$$\alpha_{m,d(n),t} \geq 0 \quad \text{(E5.3.24)}$$

$$\beta_{m,d(n),t} \geq 0 \quad \text{(E5.3.26)}$$

$$\gamma_{1,m,d(n),t} \geq 0 \quad \text{(E5.3.27)}$$

$$o_m < c_m \quad \text{(E5.3.28)}$$

$$o_m < \tau_{m,d(c),t} \quad \text{(E5.3.29)}$$

As indicated before, for all non-coordinated phases $\frac{\partial s_{m,p(n)}}{\partial o_m} = 0$. Therefore,

$$\frac{\partial F}{\partial o_m} = \frac{\partial s_{m,p(c)}}{\partial o_m} = \omega_{m,p(c)} \int_0^{c_m} \frac{\partial (v_{m,d,t})}{\partial o_m} d\lambda_t = \omega_{m,p(c)} \sum_{t=1}^{T} \bar{H}_{m,d,t} \quad \text{(E5.3.30)}$$

The object function is non-linear, in this case, because Newton's iteration method is advantageous when compared to rapid local convergence, which is chosen as the algorithm to find the minimum point of the function F(Offset, Cycle Length).

$$(O_m,\ G_m, C_m)^{r+1} = (O_m,\ G_m, C_m)^r - F(O_m,\ G_m, C_m)/F'(O_m,\ G_m, C_m) \quad \text{(E5.3.31)}$$

The cycle length optimization is different from cycle length adjustment. The cycle length adjustment increases or decreases a fixed amount (5s) of cycle lengths when the green split adjustments are not effective; that is, adjusting green split cannot decrease queue length or unused green split when splits are adjusted. The above process mimics critical intersection concepts that are a part of state-of-the-practice traffic signal retiming.

The offset, green split, and cycle length optimization functions are, at a minimum, the summation of queue lengths in all coordinated intersections and approaches.

CHAPTER VI

OPTIMIZATION ALGORITHM

6.1 Development and Test Platform

For the purposes of this study, the microscopic traffic simulator, ETFOMM, functions as the simulator. ETFOMM was developed based on CORSIM algorithms and concepts with updated traffic flow models, advanced technology, and computing features, such as the connected vehicle simulation feature.

Trajectory Conversion Algorithm (TCA) software produced by Noblis, Inc. can simulate DSRC communication between connected vehicles and RSUs according to data sets such as vehicle trajectory, RSUs' location information, strategy information, etc. Based on TCA, in addition to transmitting Basic Safety Messages (BSMs), equipped vehicles can also generate ITS SPaT messages and/or European Cooperative messages by DSRC and/or cellular. This software can also consider communication latency and loss rate according to users' settings.

New Global Systems for Intelligent Transportation Management Inc. (NGS) is the developer of ETFOMM. As NGS has integrated TCA with ETFOMM, the system can now provide an ideal connected vehicle simulation environment, which is used to develop, debug, and evaluate ALTPOM within variable penetration rates of connected vehicle

conditions. ETFOMM also provides functions to reverse BSMs to vehicle trajectories. All performance measures addressed in this section are based on 10 simulation runs.

ETFOMM provided a cross platform and cross-language application programming interface (ETAPI). ETAPI is based on Microsoft's most recent Windows Communications Foundation (WCF) which facilitates mobile computing and distributed computing. All control strategies developed in this research are implemented in C++ and interface with ETFOMM through ETAPI.

6.2 Optimize Algorithm

6.2.1 MATLAB Solver Optimized Framework

The objective function is one non-linear programming problem. The algorithm of solving this optimized function must use a non-linear programming algorithm. The gradient projection method of Rosen projects the negative gradient in such a way that improves the objective function and meanwhile maintains feasibility. The gradient projection method for solving a problem of the form to minimize objective function, which is subject to linear constraints.

The main method is to use MATLAB solver script to solve the optimization function. MATLAB could solve minimization with linear quality constraints. It provides several functions to support solving linear and non-linear equations and systems. The MATLAB Engine API for C++ provides connections and enables the use of MATLAB functions and methods.

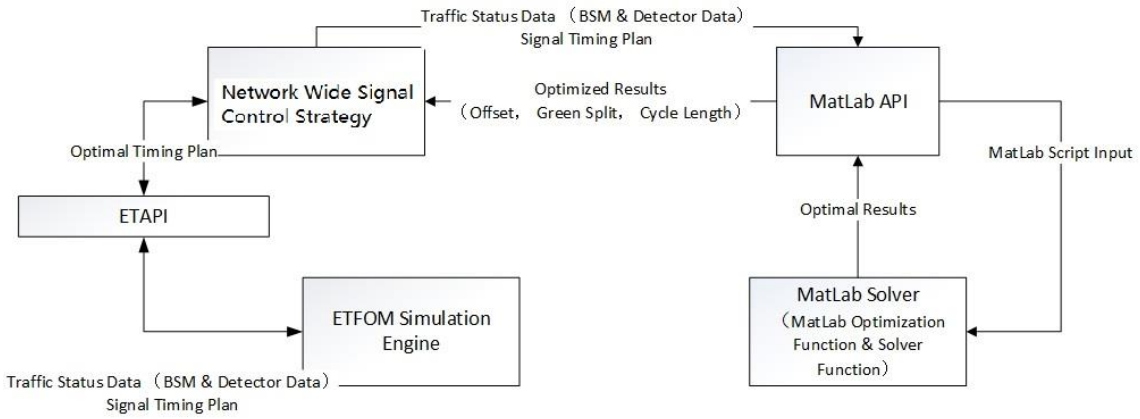

Figure 6.1 ETFOMM and MATLAB Optimization Solver Flow Chart

Figure 6.1 displays the flow chart of using MATLAB Optimization Solver to optimize objective function. The optimization program is connected to the ETFOMM simulation engine and MATLAB program. The ETFOMM simulation engine provides vehicle status data containing BSM data and detector data. BSM data is simulated data assuming some of the vehicles in the network are connected vehicles. The SPaT system on the signal controller could receive vehicle speed and vehicle location. Vehicle detector data is set up using the loop detector in the upstream link of each approach at each intersection. It is used to simulate penetration rates of connected vehicles. Then, the ETFOMM simulation program keeps the current signal timing plan for each intersection. When the program starts and needs to modify the signal timing plan, the ETFOMM simulation program packages traffic status data and the signal timing plan and sends this data to MATLAB Solver through MATLAB API. MATLAB API contains several functions in its system library and users can define their own functions and save these into the program script. For example, the function for estimating predicted queue length could be saved as a script. MATLAB API integrates input data and required functions to generate suitable

format script that is sent into the MATLAB solver. MATLAB solver contains different methodologies for solving the non-linear programming problem.

After MATLAB Solver calculates the optimized results, these results are sent back to MATLAB API. The three decision variables—offset, split, and cycle length—are received by the ETFOMM simulation program and deployed for the next cycle into the simulation engine. In addition, MATLAB solver time consumption is recorded into an individual file and used for data analysis of different solving methodologies in the next chapter.

6.2.2 Newton's Non-linear Programming Method

The object function is non-linear programming problem. Newton's Method is a good method as above descripted. The below formula is Newton's Method details for this optimization model.

F(Offset, Green Split, Cycle Length).

$$(O_m,\ G_m, C_m)^{r+1} = (O_m,\ G_m, C_m)^r - F(O_m,\ G_m, C_m)/F'(O_m,\ G_m, C_m)$$

In this iteration, the objective function and first degree of derivative of function could be presented as:

$$F'^{(O_m,\ G_m, C_m)} = [\omega_{m,p} \times \int_0^{C_m} \frac{\partial(v_{m,d,t})}{\partial o_m} d\lambda_t\ , \eta_{m,p,T}\ \frac{u_{\mathrm{m,p}}}{U_m},\ \ \sum_{p\in P}(\omega_{m,p,t} \times v_{m,d,\mathrm{T}}) - \eta_{m,p,T}\ \frac{u_{\mathrm{m,p}}}{U_m}]$$

The function is to estimate queue delay of all phases of all intersection in one projection horizon. The green time queue length needs to consider arrival vehicles and discharge vehicles. However, the red time queue length needs to consider arrival vehicles.

The coordinated directions are different with non-coordinated directions. The arrival rates of vehicles are different forecast method in the objective function. The queue length forecast needs different arrival and discharge rates of each second. The objective function is discrete, so, the first degree of derivative of function should be presented in the value to run Newton's method.

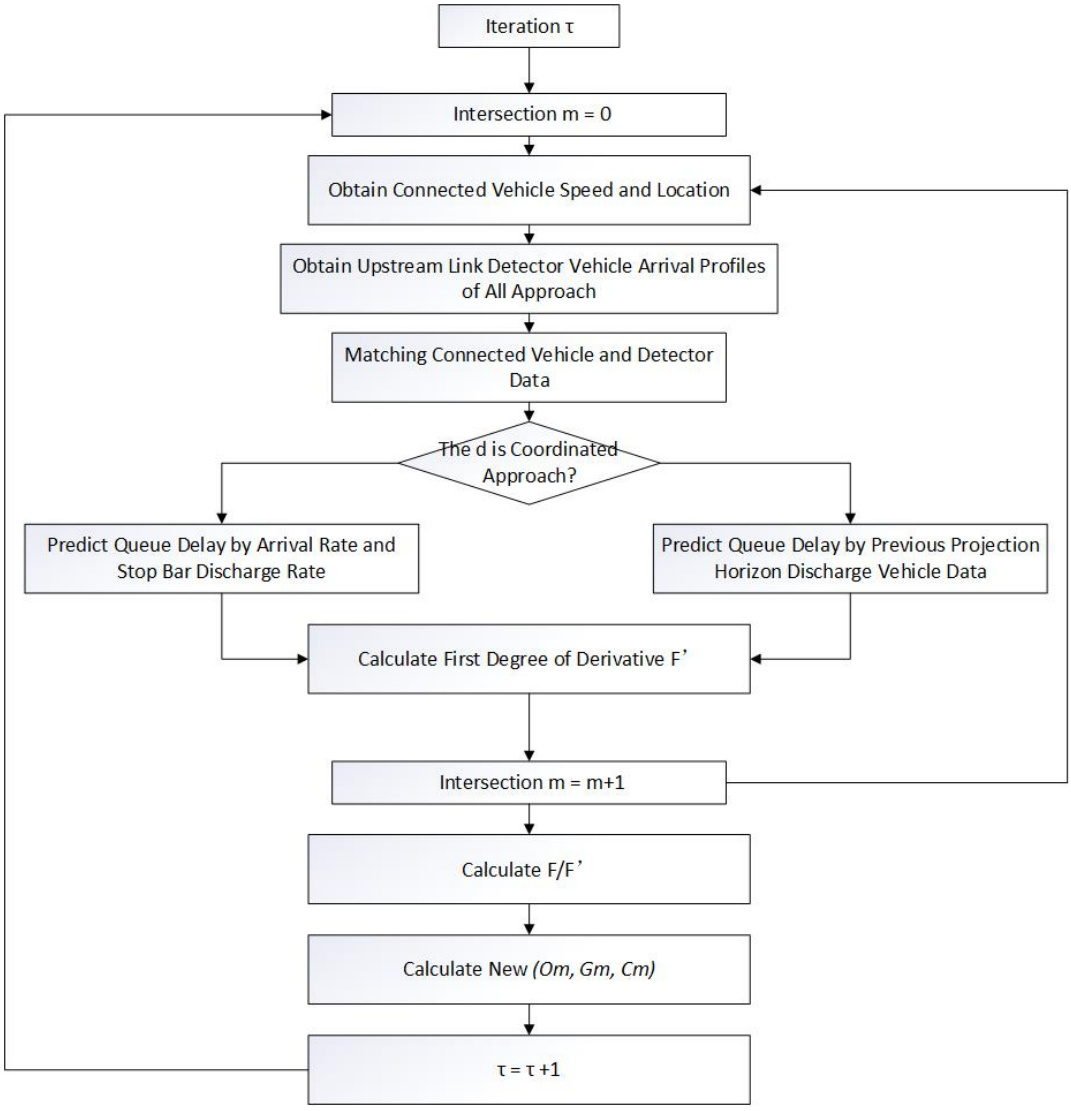

Figure 6.2 Newton Method Optimization Flow Chart

Figure 6.2 shows the flow logic of the Newton method. The basic objective function shows in previous section in Chapter V. The details of each step in Figure 6.2 are discussed in section 5.3.

6.2.3 Steepest Descent Non-linear Programming Method

Another non-linear programming method is the steepest descent method. The steepest descent method is a first-order iterative optimization algorithm for finding the minimum of a function. To find a local minimum of a function using gradient descent, one takes steps proportional to the negative of the gradient (or approximate gradient) of the function at the current point. If instead one takes steps proportional to the positive of the gradient, one approaches a local maximum of that function; the procedure is then known as gradient ascent.

$$(O_m,\ G_m, C_m)^{r+1} = (O_m,\ G_m, C_m)^r - \gamma_\tau \times \nabla F(O_m,\ G_m, C_m)^r$$

$$\gamma_\tau = \frac{[(O_m, G_m, C_m)^r - (O_m, G_m, C_m)^{r-1}]^{\mathrm{T}} \times [\nabla F(O_m, G_m, C_m)^r - \nabla F(O_m, G_m, C_m)^{r-1}]}{[\nabla F(O_m, G_m, C_m)^r - \nabla F(O_m, G_m, C_m)^{r-1}]^2}$$

$\gamma_\tau \times \nabla F$: is subtracted from $O_m,\ G_m, C_m$

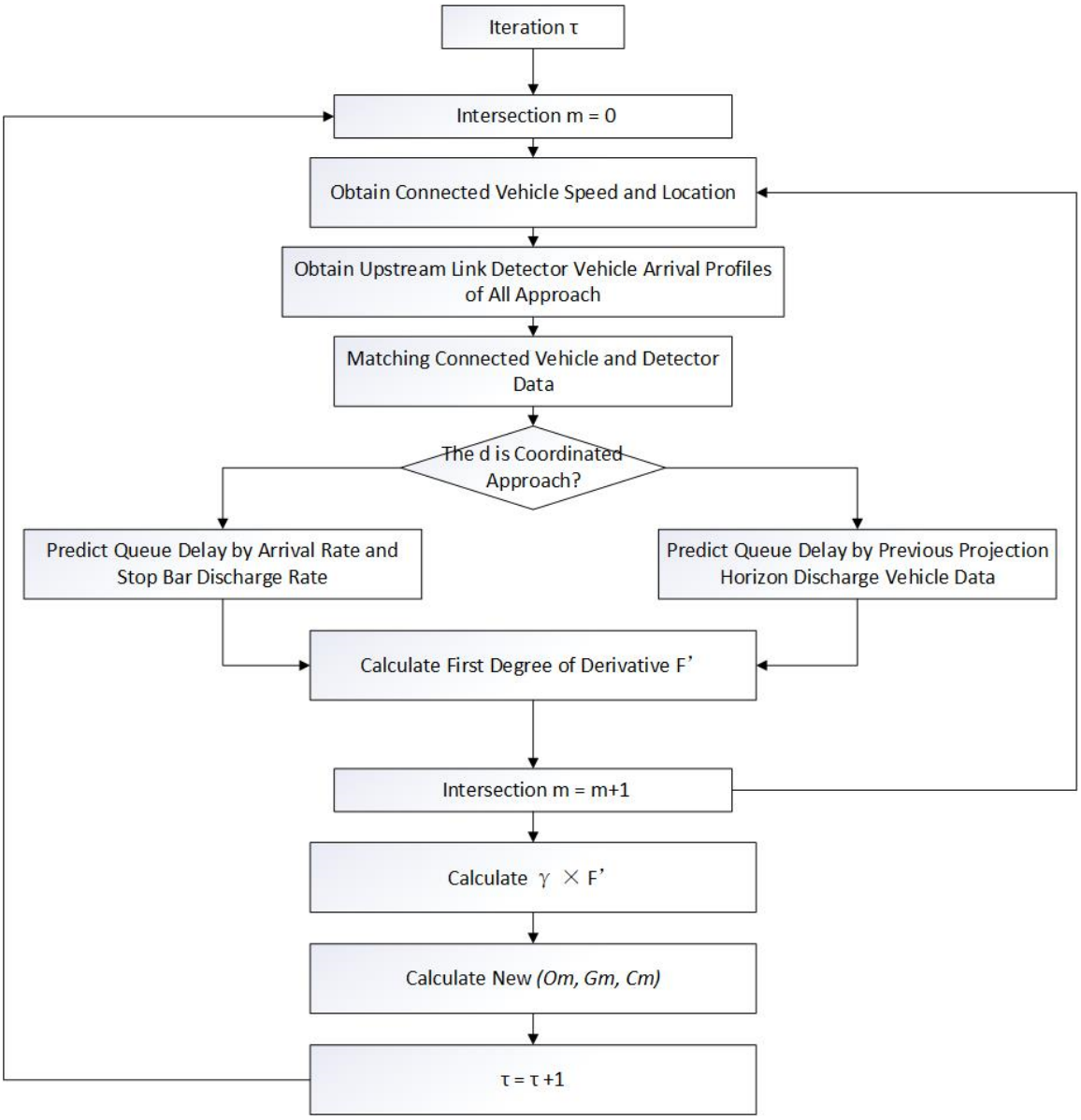

Figure 6.3 Steepest Descent Method Optimization Flow Chart

The steepest descent method is similar to Newton's method. The only difference is that the steepest descent method uses a fixed value γ instead of $F(O_m, G_m, C_m)/F'(O_m, G_m, C_m)$. The main steepest descent method is still to calculate the first order of derivative of function. Figure 6.3 displays the flow chart of steepest descent method. The

only difference of flow chart is in the final step of each iteration for calculating new result of timing plan.

6.2.4 Nelder-Mead Non-linear Programming Method

The Nelder–Mead method is a commonly applied numerical method used to find the minimum or maximum of an objective function in a multidimensional space. It is applied to nonlinear optimization problems for which derivatives may not be known. However, the Nelder–Mead technique is a heuristic search method that can converge into non-stationary points on problems that can be solved by alternative methods. The MATLAB supports Nelder-Mead method directly. The Fminsearch uses the Nelder-Mead simplex algorithm. This algorithm uses a simplex of $n + 1$ points for n-dimensional vectors x. The algorithm first makes a simplex around the initial guess $x0$ by adding 5% of each component $x0(i)$ to $x0$. The algorithm uses these n vectors as elements of the simplex in addition to $x0$ (the algorithm uses 0.00025 as component i if $x0(i) = 0$). Then, the algorithm modifies the simplex repeatedly according to the following procedure.

1. Let $x(i)$ denote the list of points in the current simplex, $i = 1,...,n+1$.
2. Order the points in the simplex from lowest function value $f(x(1))$ to highest $f(x(n+1))$. At each step in the iteration, the algorithm discards the current worst point $x(n+1)$, and accepts another point into the simplex. [Or, in the case of step 7 below, it changes all n points with values larger than $f(x(1))$].
3. Generate the *reflected* point

   $r = 2m - x(n+1)$,

   where

   $m = \Sigma x(i)/n$, $i = 1...n$,

   and calculate $f(r)$.
4. If $f(x(1)) \leq f(r) < f(x(n))$, accept r and terminate this iteration. **Reflect**
5. If $f(r) < f(x(1))$, calculate the expansion point s

$$s = m + 2(m - x(n+1)),$$

and calculate $f(s)$.

a. If $f(s) < f(r)$, accept s and terminate the iteration. **Expand**

b. Otherwise, accept r and terminate the iteration. **Reflect**

6. If $f(r) \geq f(x(n))$, perform a *contraction* between m and the better of $x(n+1)$ and r:

   a. If $f(r) < f(x(n+1))$ (that is, r is better than $x(n+1)$), calculate

   $$c = m + (r - m)/2$$

   and calculate $f(c)$. If $f(c) < f(r)$, accept c and terminate the iteration. **Contract outside** Otherwise, continue with Step 7 (Shrink).

   b. If $f(r) \geq f(x(n+1))$, calculate

   $$cc = m + (x(n+1) - m)/2$$

   and calculate $f(cc)$. If $f(cc) < f(x(n+1))$, accept cc and terminate the iteration. **Contract inside** Otherwise, continue with Step 7 (Shrink).

7. Calculate the n points

$$v(i) = x(1) + (x(i) - x(1))/2$$

and calculate $f(v(i))$, $i = 2,...,n+1$. The simplex at the next iteration is $x(1)$, $v(2),...,v(n+1)$. **Shrink**

CHAPTER VII

CASE STUDY

7.1 Case Study Network

The case study network selected for this study was Dolly Madison Blvd. (VA-123) in McLean, VA. Four intersections at Dolly Madison Blvd. are coordinated. Scenarios are designed under different traffic control strategies with different penetration rates of connected vehicles (Figure 7.1 is from Google Map38.940993, -77.1732995). The number marks are the coordinated intersection ID in case study.

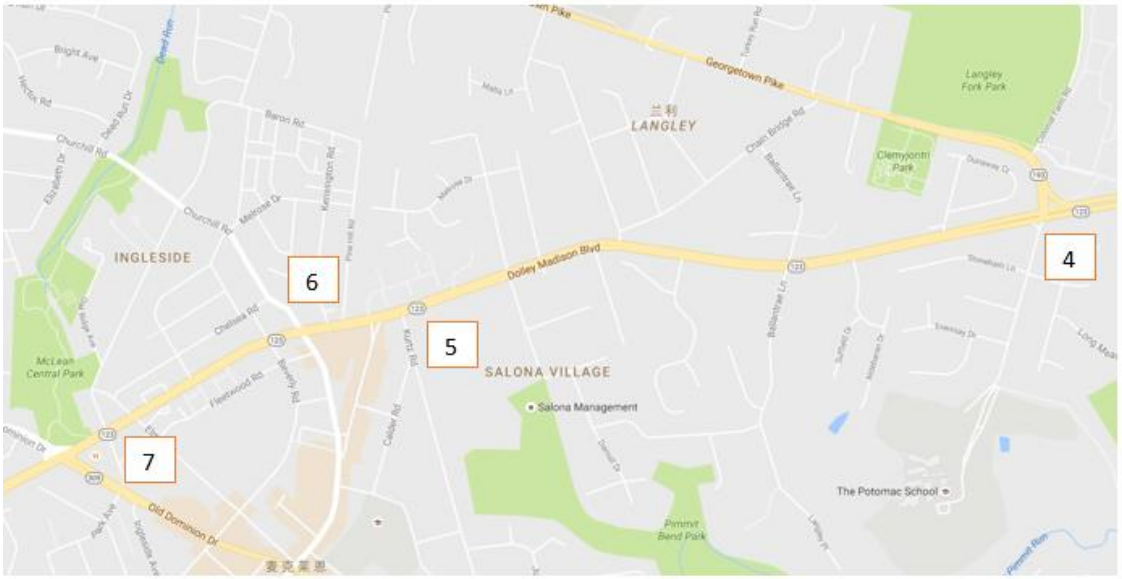

Figure 7.1 Case Study Location in VA-123 Mclean, VA

To warm up the network studied, the proposed models are not called with 900 seconds of the simulation. The proposed models are rolled forward in every cycle to optimize traffic progressions of all study intersections. The penetration rates of connected vehicles are considered at 10%, 25%, 50%, 60%, and 70%.

Base Case: Since the four intersections are coordinated in the field, the field signal timing plan provided by the Virginia Department of Transportation is utilized. These plans are produced by Synchro to generate an optimized traffic signal coordination plan. The performance measures of this case are used as the benchmark to evaluate the effectiveness of the proposed models. The base case has been calibrated according to the VDOT performance report, which was generated by Synchro, as discussed in the simulation calibration section. Each strategy and volume scenarios are run 10 times with different random seed to collect simulation results.

Six control strategies are discussed in relation to this case study:

S1: Offset optimization

S2: Offset optimization and Split Adjustment

S3: Split Adjustment and Cycle Length Adjustment

S4: Offset optimization, Split Adjustment, and Cycle Length Adjustment

S5: Offset optimization, Split Adjustment, and Cycle Length Optimization

S6: Offset optimization, Split Optimization, and Cycle Length Optimization

7.2 Simulation Calibration

7.2.1 Control Delay Calibration

The Virginia Department of Transportation provided the Synchro file; the traffic signal timing plan has been optimized. The performance report is generated by Synchro. The comparison of control delay between the VDOT performance report and the ETFOMM simulation results need to be the same. The calibration is to modify car following parameters and start up time in the intersection to close the VDOT performance report and ETFOMM simulation basic case result.

The calibration part of the case study includes running the basic case network in ETFOMM. The Virginia Department of Transportation (VDOT) provided the Synchro file; the traffic signal timing plan has been optimized. The performance report is generated by Synchro. The comparison of control delay between the VDOT performance report and ETFOMM simulation results are shown in Tables 7.1, 7.2, 7.3, and 7.4.

Table 7.1 Intersection 4 VDOT Control Delays and ETFOMM Control Delays (no calibrations)

4	Potomac School Rd/Georgetown Pike & Dolley Madison Blvd.									
Control Delay	EBL	EBT	EBR	WBL	WBT	WBR	NBL	NBT	SBL	SBT
VDOT	101	143	1	159	49	0	103	82	96	170
ETFOMM	210.9	173.25	12.4	95.74	30.13	0.75	78	78.6	71.2	181

Table 7.2 Intersection 5 VDOT Control Delays and ETFOMM Control Delays (no calibrations)

5	Chain Bridge Road/Madison Mclean Drive & Dolley Madison Blvd.								
Control Delay	EBL	EBT	WBL	WBT	WBR	NBT	NBR	SBT	SBR
VDOT	2	15	70	10	0	79	180	69	0
ETFOMM	7.21	17.03	12.02	4.23	1.19	84.15	65.3	82.3	0

Table 7.3 Intersection 6 VDOT Control Delays and ETFOMM Control Delays (no calibrations)

6	Old Chain Bridge Road/Churchill Road & Dolley Madison Blvd.							
Control Delay	EBL	EBT	WBL	WBT	NBL	NBT	NBR	SBT
VDOT	3	21	48	30	77	108	2	86
ETFOMM	3.27	4.72	11.78	17.33	76.66	83.84	0.53	69.9

Table 7.4 Intersection 7 VDOT Control Delays and ETFOMM Control Delays (no calibrations).

7	Old Dominion Drive & Dolley Madison Blvd.									
Control Delay	EBL	EBT	EBR	WBL	WBT	NBL	NBT	SBL	SBT	SBR
VDOT	26	60	14	48	50	91	68	87	139	5
ETFOMM	36.54	35.58	9.63	52.45	40.88	70.64	52.3	80.9	97.3	0.85

To bridge the gaps between control delays in VDOT performance reports and those of the ETFOMM simulation results, the calibration needs to modify the link between startup time and car following parameters on links between intersections. Figure 7.2 displays the calibration process.

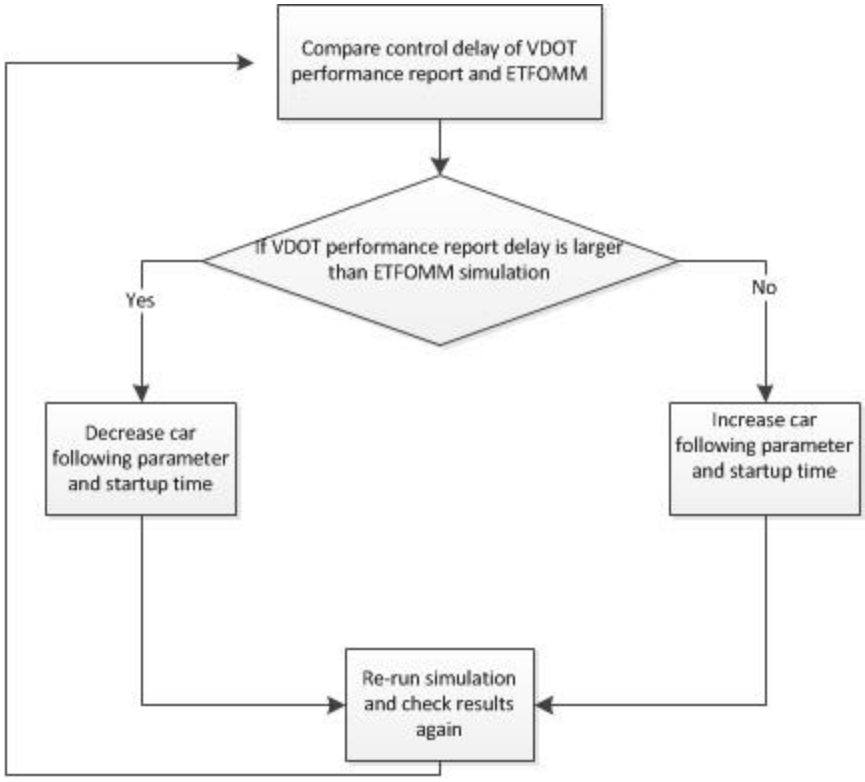

Figure 7.2 Calibration Logic of ETFOMM Simulation

The final calibration parameter adjustment shows in Table 7.5. The NB, SB, EB, and WB columns display the car following sensitive parameter in ETFOMM link. The start-up time column displays the vehicle discharge start up duration in intersections.

Table 7.5 Calibration Adjustment Results (Car-Following Sensitive %; Startup Time Seconds)

	NB	SB	EB	WB	Startup Time
4	116%	109%	75%	162%	2.8
5	114%	85%	76%	175%	3.0
6	111%	114%	169%	148%	3.2
7	117%	120%	116%	105%	2.5

After the calibration, new simulation results are shown in Table 7.6 – Table 7.9. The adjusted result of calibration is much smaller than original ETFOMM simulation results.

Table 7.6 Intersection 4 Control Delays after the Calibration

4	Potomac School Rd/Georgetown Pike & Dolley Madison Blvd.									
Control Delay	EBL	EBT	EBR	WBL	WBT	WBR	NBL	NBT	SBL	SBT
VDOT	101	143	1	159	49	0	103	82	96	170
ETFOMM	210.9	173.2	12.4	95.7	30.1	0.75	78.0	78.6	71.2	181
Difference	109.9	30.2	11.4	-63.3	-18.9	0.75	-24.9	-3.3	-24.7	11
Adjusted	121.4	148.	1.74	162	48.8	0	100.9	81.1	92.3	172.4
Difference	20.45	5.5	0.74	3.4	-0.19	0	-2.09	-0.83	-3.7	2.4

Table 7.7 Intersection 5 Control Delays after the Calibration

5	Chain Bridge Road/Madison McLean Drive & Dolley Madison Blvd.								
Control Delay	EBL	EBT	WBL	WBT	WBR	NBT	NBR	SBT	SBR
VDOT	2	15	70	10	0	79	180	69	0
ETFOMM	7.21	17.03	12.02	4.23	1.19	84.15	65.3	82.38	0
Difference	5.21	2.03	-57.98	-5.77	1.19	5.15	-114.7	13.38	0
Adjusted	2.88	15.54	21.09	9.03	0.43	80.94	88.9	70	0
Difference	0.88	0.54	-48.91	-0.97	0.43	1.94	-91.1	1	0

Table 7.8 Intersection 6 Control Delays after the Calibration

6	Old Chain Bridge Road/Churchill Road & Dolley Madison Blvd.							
Control Delay	EBL	EBT	WBL	WBT	NBL	NBT	NBR	SBT
VDOT	3	21	48	30	77	108	2	86
ETFOMM	3.27	4.72	11.78	17.33	76.66	83.84	0.53	69.95
Difference	0.27	-16.28	-36.22	-12.67	-0.34	-24.16	-1.47	-16.1
Adjusted	3.18	15.89	31.71	25.85	76.9	100.43	1.77	79.41
Difference	0.18	-5.11	-16.29	-4.15	-0.1	-7.57	-0.23	-6.59

Table 7.9 Intersection 7 Control Delays after the Calibration

7	Old Dominion Drive & Dolley Madison Blvd.									
Control Delay	EBL	EBT	EBR	WBL	WBT	NBL	NBT	SBL	SBT	SBR
VDOT	26	60	14	48	50	91	68	87	139	5
ETFOMM	36.54	35.58	9.63	52.45	40.88	70.64	52.39	80.72	97.39	0.85
Difference	10.54	-24.42	-4.37	4.45	-9.12	-20.4	-15.61	-6.28	-41.61	-4.15
Adjusted	27.45	54.87	12.53	49.74	47.98	80.71	63.22	84.51	127.56	3.45
Difference	1.45	-5.13	-1.47	1.74	-2.02	-10.29	-4.78	-2.49	-11.44	-1.55

Table 7.10 Traffic Volume after the Calibration

Node 4	EB	WB	NB	SB
VDOT	2572	1864	272	651
ETFOMM	2567	1861	272	650
DIFFERENCE	5	3	0	1
Node 5	EB	WB	NB	SB
VDOT	2111	1602	570	16
ETFOMM	2111	1601	569	16
DIFFERENCE	0	1	1	0
Node 6	EB	WB	NB	SB
VDOT	1990	1405	216	384
ETFOMM	1990	1403	216	383
DIFFERENCE	0	2	0	1
Node 7	EB	WB	NB	SB
VDOT	2248	1469	913	1018
ETFOMM	2246	1465	913	1017
DIFFERENCE	2	4	0	1

The number of discharged vehicle of VDOT report display the unserved vehicles are 673 vehs. The calibration results show the unserved vehicles are 641 vehs. The difference between VDOT report and ETFOMM simulation is only 4.75% on throughput.

7.2.2 Accuracy of Queue Length Forecast and Examples of Cycle Length and Splits

The algorithm is based on queue length forecast at intersections. The queue length forecast algorithm is described in section 3.2: queue length forecast. The accuracy of queue length forecast directly affects the accuracy of the objective function. The cases discussed in this section are based on 50% penetration rate.

Figure 7.3, Figure 7.4, Figure 7.5, and Figure 7.6 display examples of actual queue length, predicted queue length, split optimization, and cycle length adjustment of two scenarios (volume 4000 vehicles and volume 6000 vehicles) in test network, which is northbound (the non-coordinated direction) phase (phase 6) at node 4 (first coordinated intersection). At the beginning, the approach suffers a long queue. Green split on phase 6 and cycle length were adjusted to balance the queue length. With green split and cycle length increase, queue length decreases and almost disappears. As a result, control delay, stop delay, and travel time are also reduced.

In the distributed system model, the cycle length is adjusted four times and six times, or 20 seconds and 30 seconds higher than the initial cycle length, at the low volume (4000 vehicles) and high volume (6000 vehicles) scenarios. The cycle length became stable after about 60 cycles. The control strategy works itself in increasing green split and cycle length, when green splits allowed by the cycle length could not clear queues in the network. Split changes more frequently than offset and cycle length. This starts to grow until cycle length becomes stabilized. After that, it becomes oscillated. As expected, the results of this dissertation indicate that, similar to cycle length, green split is smaller at the low volume (4000 vehicles) than at high volume (6000 vehicles).

In addition, Figure 7.3 Figure 7.4, Figure 7.5, and Figure 7.6 demonstrate the queue length model and successfully predict the queue length at the specific approach.

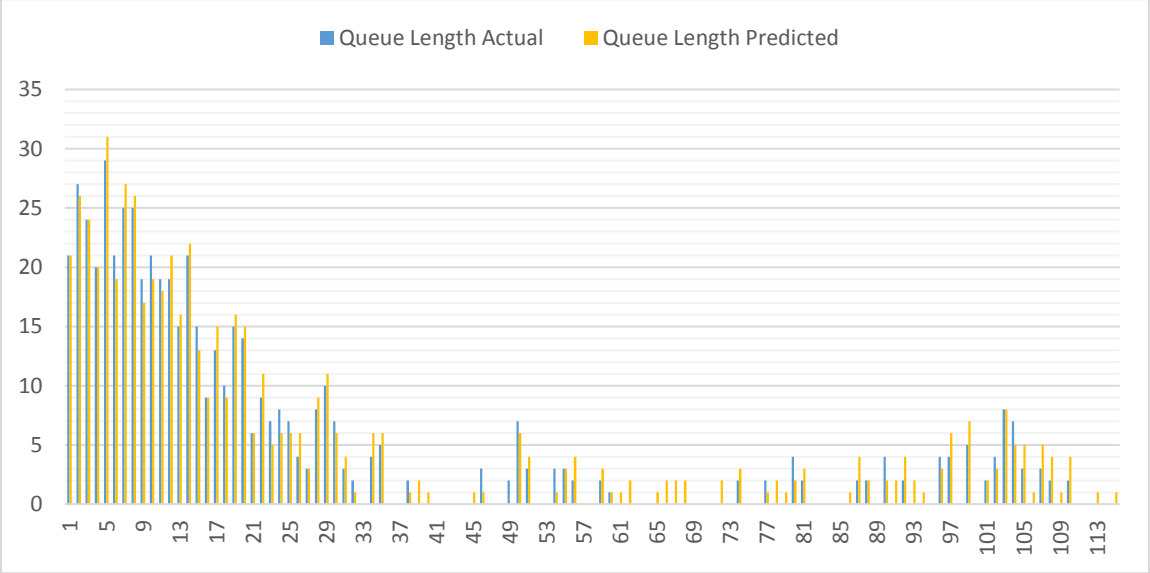

Figure 7.3 Queue Length in Coordinated Node 4 Northbound

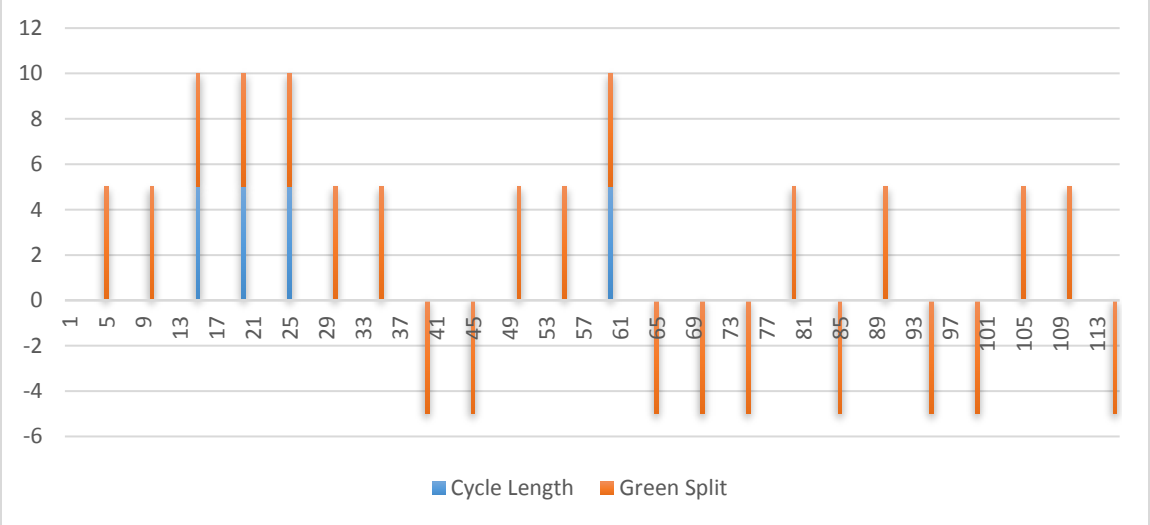

Figure 7.4 Split and Cycle Length in Coordinated Node 4 Northbound

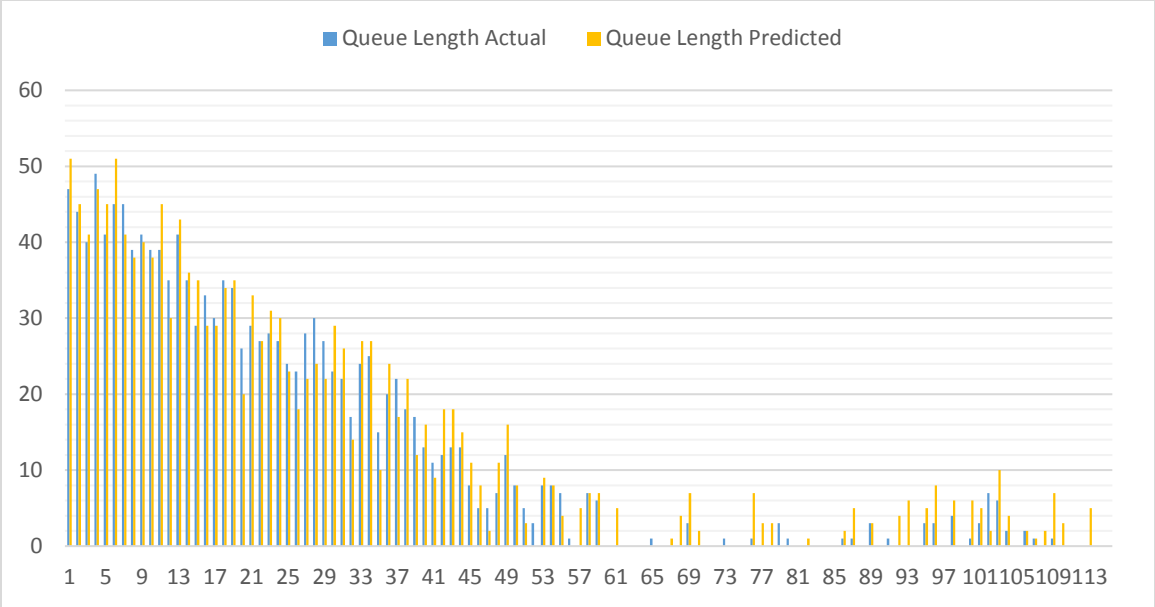

Figure 7.5 Queue Length in Coordinated Node 4 Northbound

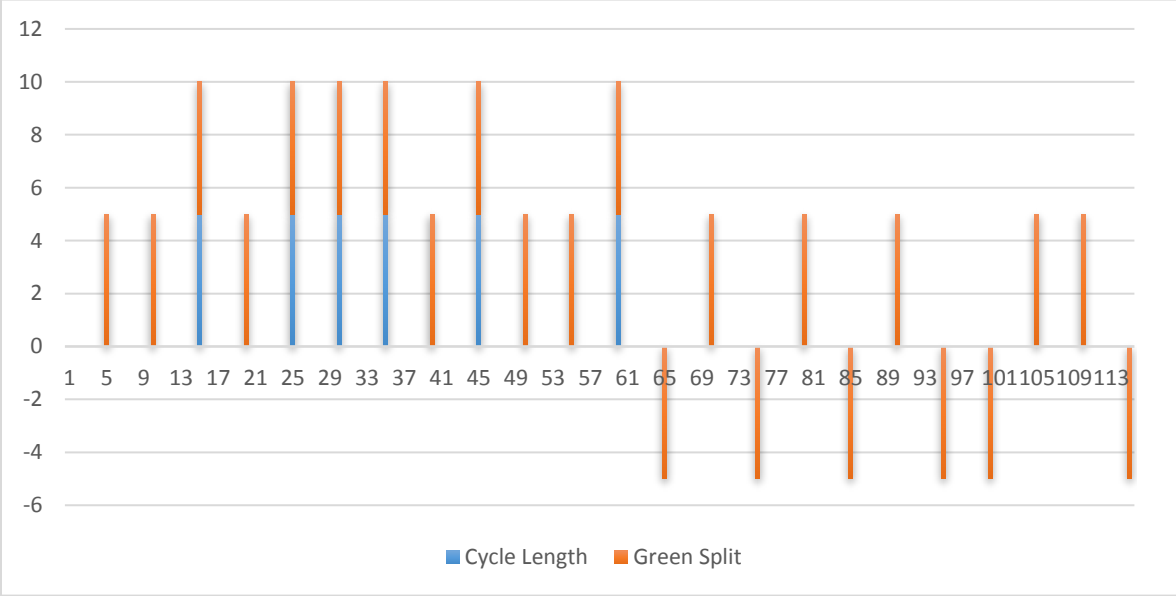

Figure 7.6 Split and Cycle Length in Coordinated Node 4 Northbound

Figure 7.7 and Figure 7.8 show queue length prediction, green split adjustment, and cycle length optimization. They additionally prove queue length model and successfully predict the queue length at the specific approach.

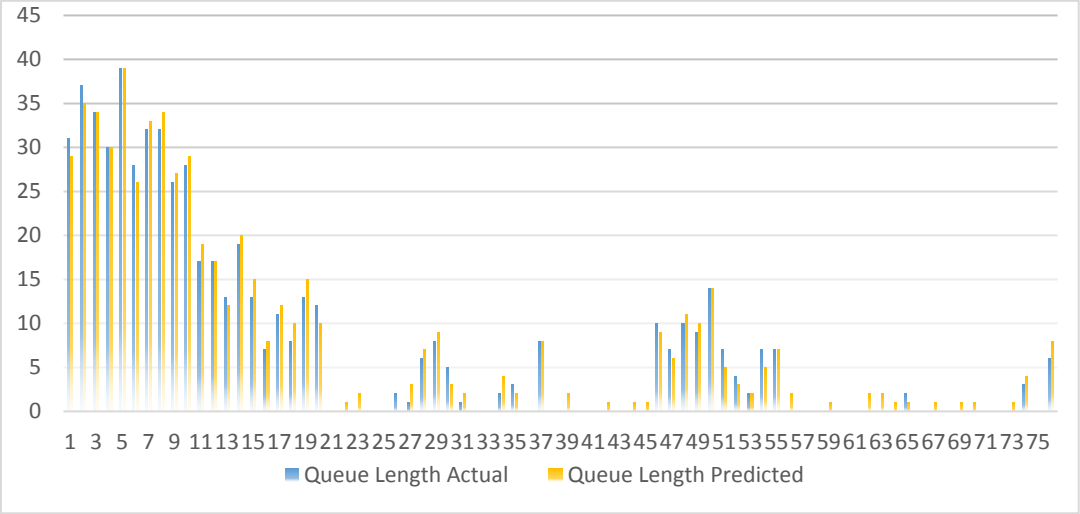

Figure 7.7 Predicted Queue Length and Actual Queue Length in Coordinated Node 4 Eastbound

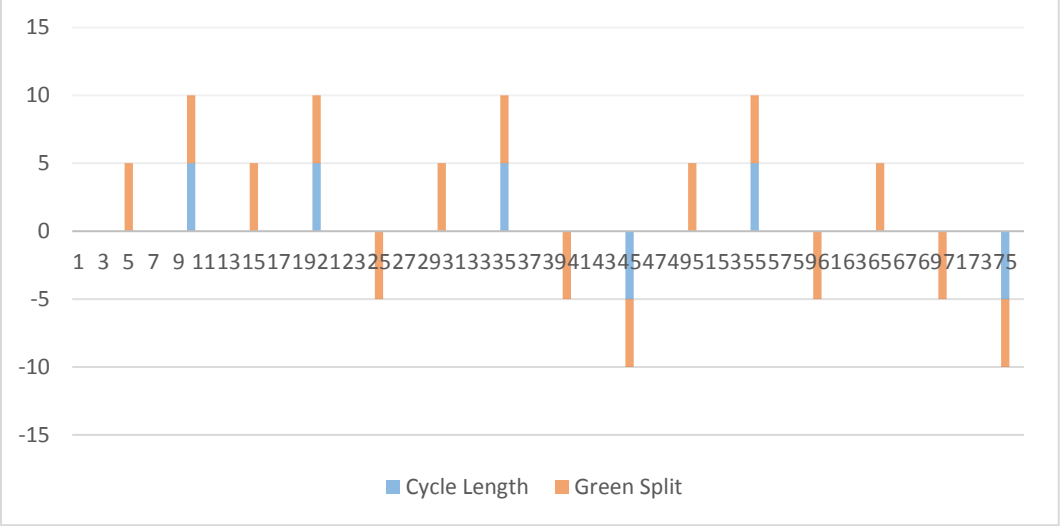

Figure 7.8 Split Adjustment and Cycle Length Optimization in Coordinated Node 4 Eastbound

CHAPTER VIII

SENSITIVE ANALYSIS

8.1 Data Analysis

8.1.1 Volume Scenarios

This case study contains sensitive analysis with different traffic volume in the VA-123 case. Table 8.1 displays the five different traffic volume scenarios in VA-123.

Table 8.1 Scenario design with different traffic volume (vehs/hour)

Scenario (Volume Ratio)	1.0 (Base)	0.8	0.9	1.1	1.2
Intersection 4					
WB	2248	1799	2024	2473	2698
NB	1048	839	944	1153	1258
SB	913	731	822	1005	1096
Intersection 5					
NB	384	308	346	423	461
SB	216	173	195	238	260
Intersection 6					
NB	16	13	15	18	20
SB	570	456	513	627	684
Intersection 7					
EB	1864	1492	1678	2051	2237
NB	651	521	586	717	782
SB	272	218	245	300	327

Table 8.1 shows all traffic input of VA-123 network. All six strategies are simulated in each traffic volume network.

Table 8.2 Control Delay Per Vehicle (seconds) of Four Coordinated Intersections of Five Volume Ratio Scenarios (EB: East Bound; WB: West Bound; NB: North Bound; SB: South Bound)

Volume Ratio1.0				
Node 4	Control Delay Per Vehicle (sec/v)			
	EB	WB	NB	SB
Base Case	114.7	62.1	89.6	126.5
Node 5	Control Delay Per Vehicle (sec/v)			
	EB	WB	NB	SB
Base Case	11.8	13.6	90.6	32.5
Node 6	Control Delay Per Vehicle (sec/v)			
	EB	WB	NB	SB
Base Case	14.4	25.7	67.1	78.9
Node 7	Control Delay Per Vehicle (sec/v)			
	EB	WB	NB	SB
Base Case	37.7	49.3	75.7	83.4
Volume Rati o0.8				
Node 4	Control Delay Per Vehicle (sec/v)			
	EB	WB	NB	SB
Base Case	92.9	49.0	72.6	101.2
Node 5	Control Delay Per Vehicle (sec/v)			
	EB	WB	NB	SB
Base Case	9.4	11.0	73.4	26.3
Node 6	Control Delay Per Vehicle (sec/v)			
	EB	WB	NB	SB
Base Case	11.4	20.8	53.7	63.9
Node 7	Control Delay Per Vehicle (sec/v)			
	EB	WB	NB	SB
Base Case	30.6	39.9	59.8	65.9
Volume Ratio0.9				
Node 4	Control Delay Per Vehicle (sec/v)			
	EB	WB	NB	SB
Base Case	104.4	55.9	80.6	112.6
Node 5	Control Delay Per Vehicle (sec/v)			

Table 8.2 Control Delay Per Vehicle (seconds) of Four Coordinated Intersections of Five Volume Ratio Scenarios (EB: East Bound; WB: West Bound; NB: North Bound; SB: South Bound) (Continued)

	EB	WB	NB	SB
Base Case	10.5	12.1	80.6	29.2
Node 6	Control Delay Per Vehicle (sec/v)			
	EB	WB	NB	SB
Base Case	13.1	22.8	59.7	71.0
Node 7	Control Delay Per Vehicle (sec/v)			
	EB	WB	NB	SB
Base Case	33.6	44.9	67.4	74.2
Volume Ratio1.1				
Node 4	Control Delay Per Vehicle (sec/v)			
	EB	WB	NB	SB
Base Case	125.1	68.9	98.6	140.5
Node 5	Control Delay Per Vehicle (sec/v)			
	EB	WB	NB	SB
Base Case	13.2	15.1	101.4	36.4
Node 6	Control Delay Per Vehicle (sec/v)			
	EB	WB	NB	SB
Base Case	15.6	28.8	74.5	85.2
Node 7	Control Delay Per Vehicle (sec/v)			
	EB	WB	NB	SB
Base Case	41.9	53.8	83.3	91.7
Volume Ratio 1.2				
Node 4	Control Delay Per Vehicle (sec/v)			
	EB	WB	NB	SB
Base Case	137.7	73.3	109.3	151.9
Node 5	Control Delay Per Vehicle (sec/v)			
	EB	WB	NB	SB
Base Case	14.3	16.3	107.8	39.3
Node 6	Control Delay Per Vehicle (sec/v)			
	EB	WB	NB	SB
Base Case	17.2	31.1	79.2	96.2
Node 7	Control Delay Per Vehicle (sec/v)			
	EB	WB	NB	SB
Base Case	44.5	58.7	90.9	101.7

8.1.2 Simulation Results on Mobility

8.1.2.1 Centralized System

The entire simulation time for the six scenarios is at least 3600 seconds (60 min), which approximates the local peak hour time. In this case, the effective communication range between an RSU and an OBE is 1,500 ft. The outcomes or performance report for different strategies with different penetration rates are shown in this chapter. This section aims to compare different scenarios and base case on delay and throughput. The basic data analysis is in this section to find out how to best optimize or adjust on traffic signal timing. In multiple optimization scenarios, data analysis could determine contributions of offset, split, and cycle length on traffic improvement. Tables A.1 to A.30 display the control delay reduction of different scenarios S1-S6 in four coordinated intersections in the volume ratio 1.0 scenario.

Table 8.3 shows the delays and throughput (capacity) at the critical intersection and network level. Intersection level throughput is summations of vehicles passing stop bars from all approaches. The network throughput are summations of throughput for all four intersections. Network delays are total control delays on all approaches of all four intersections in multiplication of control delays in second per vehicle and total vehicles.

Figure 8.1, Figure 8.2, and Figure 8.3 show a detailed performance report by different control strategies.

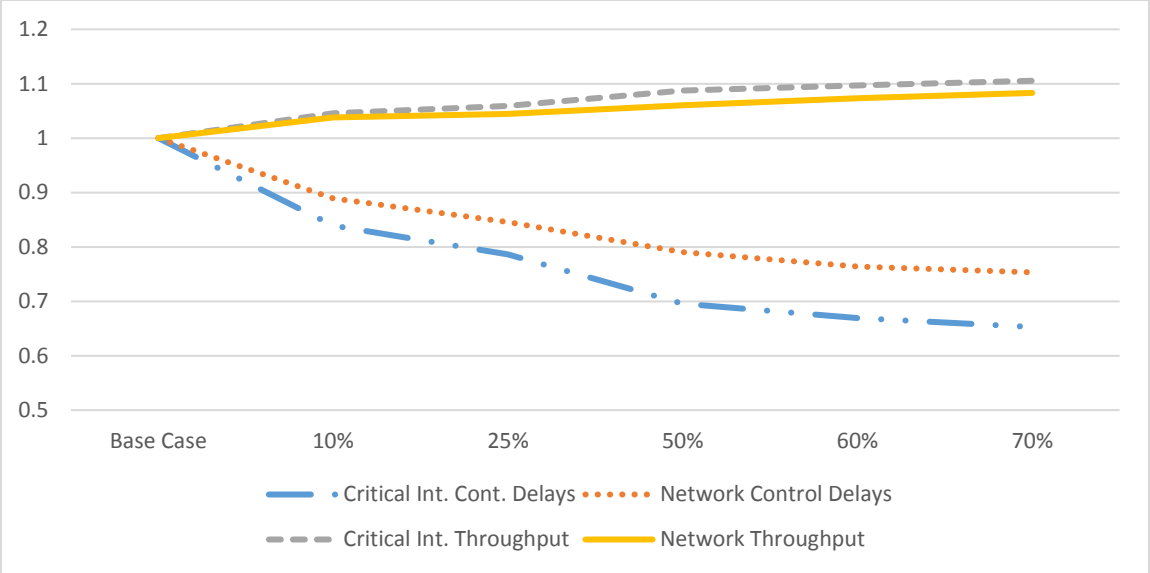

Figure 8.1 Throughput and Control Delays on Critical Intersection and Network Wide at Different Penetration Rate

The most significant finding of this case study is that with a connected vehicle penetration rate of around 50 percent, network-wide control delays could be reduced by 15 percent on minor direction and reduced by 35 percent on major direction at the critical intersection. More importantly, the throughput has increased around 9 percent at critical intersections and increased network-wide by 6 percent. Drawing on a throughput (capacity) and delay curve, the results of this dissertation illustrate a significant phenomenon that defies traditional traffic flow theory: The higher the throughput (capacity), the lower the delay, even when the critical intersection is over-saturated. Remember, this curve is achieved by no changes to algorithms, no changes in roadway conditions, and no changes in vehicle performance. The only variable is the vehicle's penetration rate. The information in this dissertation's findings about vehicles' movement enables the optimization system to improve algorithm performance. Although artificial intelligence algorithms are not used,

the consequences—in that the algorithm can improve itself through information gains—are the same. Figure 8.1, horizontal axis, illustrates the ratio of throughput at some percentage of penetration rate to the base case throughput. The vertical axis shows the ratio of delays under different penetration rate to that in the base case.

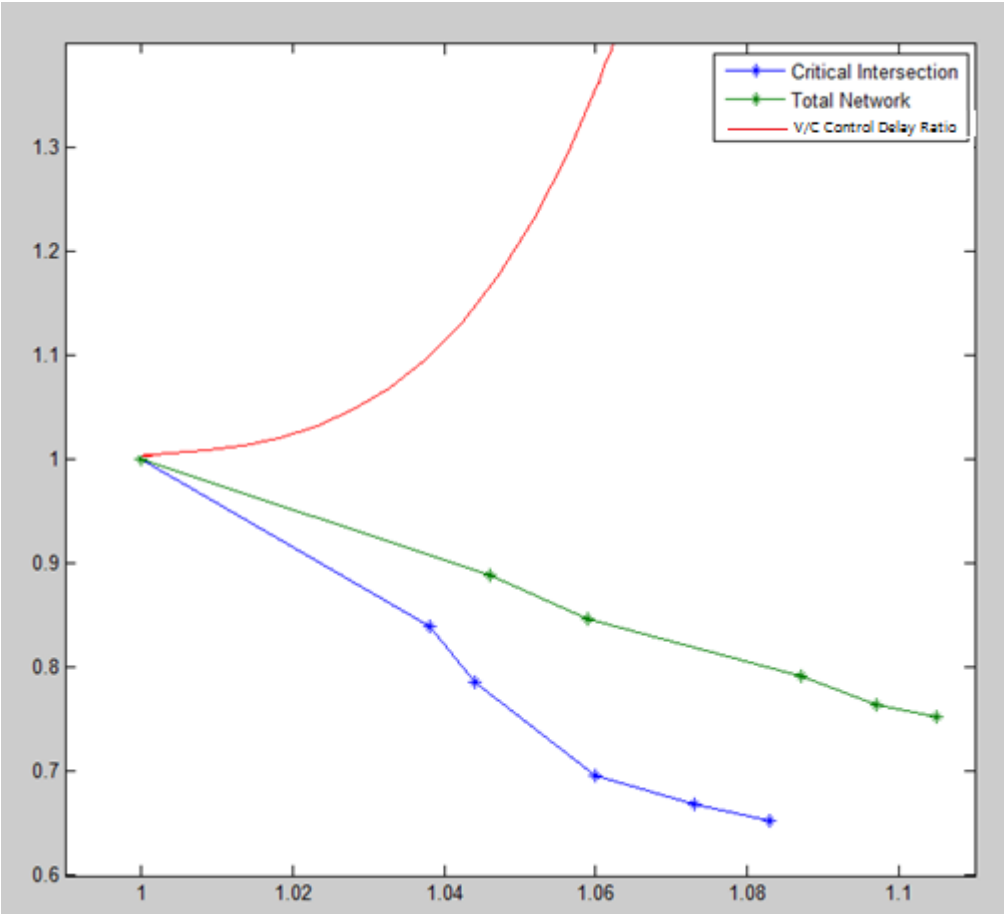

Figure 8.2 Network and Critical Intersection's Control Delays and Throughput Ratio

Table 8.3 Network and Critical Intersection's Control Delays and Throughput by Penetration Rate (CI: Critical Intersection; CD: Control Delay; TH: Throughput)

Penetration Rate	CI		Network		CI		Network	
	CD	%	Total CD	%	TH	%	Total TH	%
Base Case	102.9	1	693301	1	3110	1	12355	1
10%	86.4	0.84	616585	0.889	3253	1.046	12825	1.038
25%	80.9	0.786	586369	0.846	3294	1.059	12903	1.044
50%	71.6	0.696	548061	0.791	3382	1.087	13098	1.06
60%	68.9	0.669	529595	0.764	3411	1.097	13260	1.073
70%	67.2	0.653	522248	0.753	3438	1.105	13382	1.083

It is important to point out that the traffic signal timing plan in the base case has already been optimized by Synchro. Due to the significant traffic, the LOS at node 4 and 7 (Georgetown Pike and Dolley Madison) is calculated as "F," or oversaturated. The significant findings of this case study are that when the penetration rate reaches 50 percent, the proposed optimization strategy could effectively reduce control delay by about 38 percent. That delay reduction improves the Georgetown and Old Dominion intersections level of service by one letter grade (from "F" to "E" and from "E" to "D").

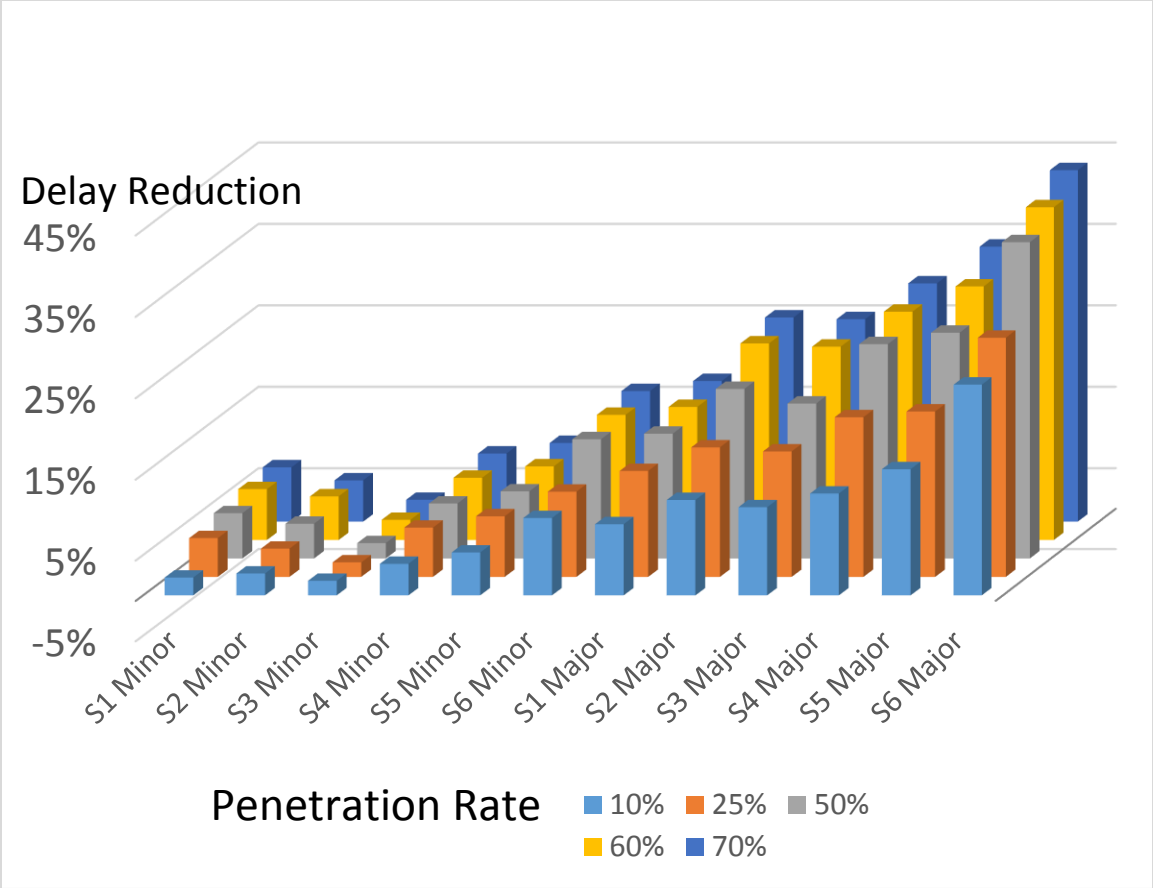

Figure 8.3 Summary of Delay Reductions by Control Strategy and Penetration Rate

Table 8.4 Major Coordinated Direction Control Delay Reduction (Percentage)

V1.0	10%	25%	50%	60%	70%
S1 Major	8.80%	13.10%	15.40%	16.40%	17.30%
S2 Major	11.80%	16.00%	20.90%	24.20%	25.10%
S3 Major	10.90%	15.50%	19.10%	23.80%	24.90%
S4 Major	12.60%	19.70%	26.40%	28.10%	29.30%
S5 Major	15.60%	20.40%	27.80%	31.20%	33.80%
S6 Major	25.98%	29.47%	38.91%	40.92%	43.19%
V1.1	10%	25%	50%	60%	70%
S1 Major	9.60%	13.00%	14.90%	16.80%	18.00%
S2 Major	11.90%	15.80%	21.20%	23.50%	25.10%
S3 Major	10.40%	14.70%	19.10%	23.70%	24.80%
S4 Major	12.50%	19.20%	25.40%	27.90%	29.00%
S5 Major	15.80%	20.70%	27.90%	31.20%	32.90%
S6 Major	26.40%	29.80%	38.40%	41.00%	43.50%
V1.2	10%	25%	50%	60%	70%
S1 Major	9.10%	12.60%	14.50%	16.20%	17.40%
S2 Major	11.20%	15.00%	20.50%	23.00%	24.70%
S3 Major	9.80%	14.20%	18.80%	23.30%	24.50%
S4 Major	11.80%	18.60%	25.00%	27.10%	28.50%
S5 Major	14.80%	19.50%	26.90%	30.40%	32.20%
S6 Major	25.90%	29.10%	37.90%	40.00%	42.50%
V0.8	10%	25%	50%	60%	70%
S1 Major	9.30%	12.70%	15.30%	16.40%	17.60%
S2 Major	11.90%	15.80%	21.20%	23.50%	25.10%
S3 Major	9.90%	14.40%	18.80%	23.60%	24.50%
S4 Major	11.80%	18.70%	25.30%	26.80%	28.60%
S5 Major	15.40%	19.90%	27.30%	31.00%	32.90%
S6 Major	25.60%	29.50%	38.40%	40.30%	42.70%
V0.9	10%	25%	50%	60%	70%
S1 Major	9.80%	13.30%	15.20%	16.90%	18.30%
S2 Major	11.20%	15.00%	20.50%	23.00%	24.70%
S3 Major	10.70%	15.00%	19.40%	23.90%	25.00%
S4 Major	13.10%	19.60%	26.00%	28.00%	29.50%
S5 Major	16.10%	20.50%	28.10%	31.30%	33.30%
S6 Major	26.30%	30.00%	38.00%	40.50%	42.70%

Table 8.5 Minor Direction Control Delay Reduction (percent)

V1.0	10%	25%	50%	60%	70%
S1 Minor	2.20%	4.80%	5.60%	6.30%	6.70%
S2 Minor	2.70%	3.50%	4.30%	5.40%	5.10%
S3 Minor	1.80%	1.80%	1.90%	2.50%	2.70%
S4 Minor	3.90%	6.10%	6.80%	7.70%	8.40%
S5 Minor	5.30%	7.50%	8.30%	9.10%	9.70%
S6 Minor	9.57%	10.54%	14.71%	15.43%	16.07%
V1.1	10%	25%	50%	60%	70%
S1 Minor	2.50%	4.80%	5.70%	7.10%	6.40%
S2 Minor	3.00%	3.50%	4.40%	6.20%	4.80%
S3 Minor	2.10%	1.80%	2.00%	3.30%	2.40%
S4 Minor	4.20%	6.10%	6.90%	8.50%	8.10%
S5 Minor	5.60%	7.50%	8.40%	9.90%	9.40%
S6 Minor	9.70%	11.00%	14.60%	15.90%	17.40%
V1.2	10%	25%	50%	60%	70%
S1 Minor	2.10%	5.10%	5.80%	5.80%	6.50%
S2 Minor	2.60%	3.80%	4.50%	4.90%	4.90%
S3 Minor	1.70%	2.10%	2.10%	2.00%	2.50%
S4 Minor	3.80%	6.40%	7.00%	7.20%	8.20%
S5 Minor	5.20%	7.80%	8.50%	8.60%	9.50%
S6 Minor	9.30%	11.50%	14.30%	15.30%	16.70%
V0.8	10%	25%	50%	60%	70%
S1 Minor	2.00%	4.90%	5.40%	5.70%	7.10%
S2 Minor	2.50%	3.60%	4.10%	4.80%	5.50%
S3 Minor	1.60%	1.90%	1.70%	1.90%	3.10%
S4 Minor	3.70%	6.20%	6.60%	7.10%	8.80%
S5 Minor	5.10%	7.60%	8.10%	8.50%	10.10%
S6 Minor	8.90%	10.80%	14.20%	14.80%	16.90%
V0.9	10%	25%	50%	60%	70%
S1 Minor	2.30%	4.70%	5.90%	6.90%	7.50%
S2 Minor	2.80%	3.40%	4.60%	6.00%	5.90%
S3 Minor	1.90%	1.70%	2.20%	3.10%	3.50%
S4 Minor	4.00%	6.00%	7.10%	8.30%	9.20%
S5 Minor	5.40%	7.40%	8.60%	9.70%	10.50%
S6 Minor	9.50%	11.00%	14.20%	15.00%	17.00%

Tables 8.4 and 8.5 list the detail mobility benefits and performance under different control strategies in this case study. The case study indicates that the proposed models significantly reduce congestion in the arterials even when one intersection (node 4, Georgetown Pike and Dolly Madison Boulevard) is oversaturated. With a penetration rate as little as 10 percent, the delay reduction benefits on the major street are more than 8-17 percent, depending on strategies, while the delays on the minor street are reduced. The delay reduction percentages are increased nicely as the penetration rates increase. When the penetration rates reach around 60 percent, the delay reduction percentage cease to grow. When the penetration rate is around 60 percent, the delay on the major street can be reduced by 16-40 percent, depending on the strategies listed in Table 8.5, while that on the minor street is reduced by around 6-15 percent.

Figure 8.3 shows how the traffic signal timing strategies and penetration rates could affect delay reduction. Similar to the previous case study in Mississippi [48], the present study found offset to be the most significant variable that affects the control delay on arterials across all penetration rates. Optimizing offset itself (S1) generates only 2-3 percent less control delay than that provided by strategies which adjust cycle length and split simultaneously. For major streets, strategies that do not include the offset adjustments (S3) are not as effective as strategies with offset adjustment, as shown in Figure 8.3. For minor streets, strategy 4 mimics the critical intersection method to adjust the cycle length; this does not reduce the minor street delays as much as other strategies do. Critical intersections increase cycle length unnecessarily for non-critical intersections and results in the performance if the proposed models are not at the optimal level. The most important

discovery in this report is that by adjusting splits and optimizing offset and cycle length, delays on major roads can be reduced by 28 percent and delays on minor roads can be reduced by 8 percent, when the connected vehicle penetration rate is around 60 percent.

Optimizing offset and adjusting split (not including common cycle length) can reduce the control delay by 12-25 percent when the penetration rate changes from 10-60 percent. This can reduce the minor street control delay by 3-6 percent. At isolated intersections, adjustment of split and optimization of cycle can almost match the performance of that in coordinated arterials. The delay reduction on major roads can be 15-33 percent and 5-9 percent on minor roads. The best performance of the optimization model is offset, split, and cycle length optimization. The major streets could reach 41 percent control delay reduction at 70% penetration. In addition, minor streets could experience 15 percent control delay reduction.

8.1.2.2 Distributed System

The distributed system has a difference in optimization model. One of the differences in the distributed system is the time limitation on optimization. The centralized system has a longer optimization time because of more variables needs to be optimized. The optimization model could provide enough time to develop an optimal solution. The distributed system, especially the two-optimization distributed system, has only half the time for optimization. The time limitation function is added to the optimization program. The optimization process would be completed when the time consumption of the optimization model becomes expired. Another difference is optimization decision variables. The distributed system would optimize major direction and minor direction

separately. The decision variables are different in the distributed system, which would affect the optimal results. Table 8.6 displays the control delay reduction of the distributed system and centralized system. The computer specification is a desktop of Processor: 3.2GHz Core i5-4460; Memory 8GB DDR3; 1TB SATA.

Table 8.6 Control Delay Reduction of Distributed System and Centralized System (S6)

DS with Time Limit & Part Optimization					
Summary	10%	25%	50%	60%	70%
Major Direction	-21.82%	-25.62%	-29.54%	-32.26%	-33.30%
Minor Direction	-7.43%	-9.54%	-10.81%	-11.63%	-12.27%
DS without Time Limit & Part Optimization					
Summary	10%	25%	50%	60%	70%
Major Direction	-23.33%	-27.48%	-31.08%	-34.05%	-34.95%
Minor Direction	-8.37%	-10.61%	-11.83%	-12.68%	-13.32%
DS without Time Limit & Full Optimization					
Summary	10%	25%	50%	60%	70%
Major Direction	-26.68%	-31.25%	-39.45%	-42.80%	-44.88%
Minor Direction	-10.35%	-11.48%	-14.92%	-15.83%	-16.75%
CS without Time Limit					
Summary	10%	25%	50%	60%	70%
Major Direction	-25.98%	-29.47%	-38.91%	-40.92%	-43.19%
Minor Direction	-9.57%	-10.54%	-14.71%	-15.43%	-16.07%

The centralized system could create a 43% control delay on major directions and 16% on minor directions in 70% penetration rate and the S6 scenario. The time limit function is a program function calculates optimization CPU time in program. If the CPU time consumption of optimization program is longer than the real clock time limitation (For example, remaining green time). The optimization process is stopped and use current feasible solution as the new timing plan. The time limit function is to simulate real world

scenarios. The distributed system with time limit and part decision variable optimization could generate 33% and 12% control delay reduction in the best-case scenario. Without a time-limit function, the distributed system could generate 34% and 13% control delay reduction. The case of the distributed system without a time limit and with full optimization could generate 44% and 16% control delay reduction.

Overall, the distributed system's performance is lower than that of the centralized system. However, the best-case scenario of the distributed system has better performance than the centralized system. The reason of this status is the double optimization distributed system, which could increase the accuracy of queue length forecast and affect queue delay estimation. However, considering CPU time consumption double full optimizations, the distributed system deploys double partial optimizations, as described previously.

8.1.3 Fuel Consumption and Emission

The Physical Emission Rate Estimator (PERE) model was developed by the EPA based on CHEM and is an improved, simplified, and already implemented version of CHEM (23). The original model is modified in an FHWA project. Figure 8.4 shows the flow chart of fuel consumption and emission calculations. GPS data from BSM is converted to vehicle trajectories and the elevation of vehicle trajectories are retrieved from Google Maps. Unfortunately, some vehicle parameters are not able to be obtained from BSM. For example, engine (gas vs. diesel) and vehicle (truck vs. passenger) types aren't provided.

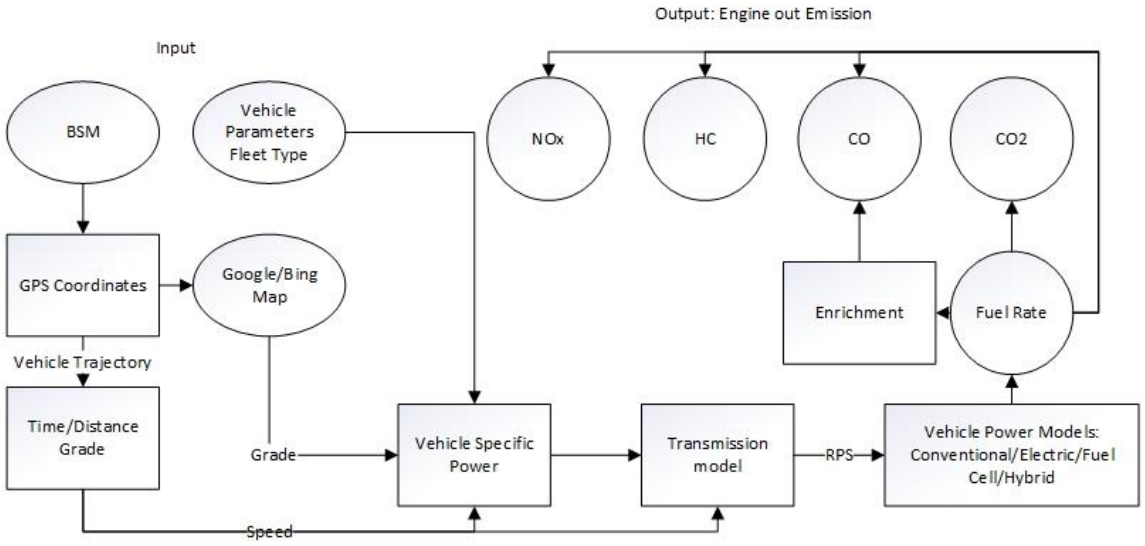

Figure 8.4 Modified PERE Model

Based on the VDOT Synchro benchmark case, fuel consumption of the total network is 743-gals. After calibration of the case study, the ETFOMM simulation fuel consumption result is 713-gals network side (the default setting is that all vehicles are conventional gas passenger vehicles). The purpose of this section is to compare different scenarios and base cases on fuel consumption and emissions (CO, CO2, HC, and NOx). This section aims to compare different scenarios and base cases on different types of gas emissions and total fuel consumption per vehicle.

The fuel consumption was generated by ETFOMM for the benchmark case. Fuel consumption is calculated by the procedures in this study, which are similar to the VDOT Synchro performance report. Table 8.7 displays a 70 percent penetration rate in different scenarios' fuel consumption and emission results. In Table 8.7, fuel consumption and emissions are calculated by the default vehicle type (passenger car) with a conventional gas engine and automatic transmission.

Table 8.7 Fuel Consumption and Emission Model Result with Different Scenarios under a 70 Percent Penetration Rate

	Fuel Consumption (Gal)	Emission CO (kg)	Emission CO2(kg)	Emission HC(kg)	Emission NOx(kg)
Scenario 0	713	33.09	32.22	24.40	43.24
Scenario 1	627.84	29.15	28.89	22.07	38.90
Percentage Difference	-11.94%	-11.90%	-10.33%	-9.53%	-10.02%
Scenario 2	624.59	28.95	28.09	21.37	38.00
Percentage Difference	-12.40%	-12.50%	-12.81%	-12.40%	-12.10%
Scenario 3	648.12	29.98	28.93	22.23	39.26
Percentage Difference	-9.10%	-9.40%	-10.20%	-8.90%	-9.20%
Scenario 4	613.89	28.26	27.71	20.74	37.23
Percentage Difference	-13.90%	-14.60%	-14.00%	-15.00%	-13.90%
Scenario 5	578.24	27.07	26.13	19.93	34.89
Percentage Difference	-18.90%	-18.20%	-18.90%	-18.30%	-19.30%
Scenario 6	538.24	24.77	24.01	17.98	32.15
Percentage Difference	-24.54%	-25.12%	-25.53%	-26.36%	-25.65%

Table 8.8 Emission Reduction in Different Scenarios and Different Penetration Rates (Percentage)

Penetration Rate	S1	S2	S3	S4	S5	S6
10 percent	5.25%	5.73%	4.45%	6.81%	8.42%	11.99%
25 percent	5.84%	7.32%	5.48%	8.19%	11.52%	14.42%
50 percent	8.10%	9.86%	7.30%	10.73%	14.60%	20.30%
60 percent	9.81%	10.47%	7.97%	11.88%	15.78%	21.78%
70 percent	10.74%	12.44%	9.36%	14.28%	18.72%	25.42%

Table 8.8 shows fuel consumption and emission reductions at all penetration rates and scenarios. The percentages are differences of total emission (summary of CO, CO2, HC, and NOx) between the base scenario and other scenarios. Table 8.8 displays that a higher penetration rate would perform better in terms of economic and emission reduction

fuel concerns. Scenarios 2 and 4 have better performance than Scenarios 1 and 3. Under different penetration rate and control strategies, fuel savings can be between 10 and 20 percent. Scenarios 5 and 6 provide the best performance in terms of fuel consumption reduction: between 20 to 25 percent That saving has an impact on future policy implications: 10 percent of fuel savings to roadway users should convince policy makers and state DOTs to implement this signal control strategy deployment of connected vehicle infrastructures.

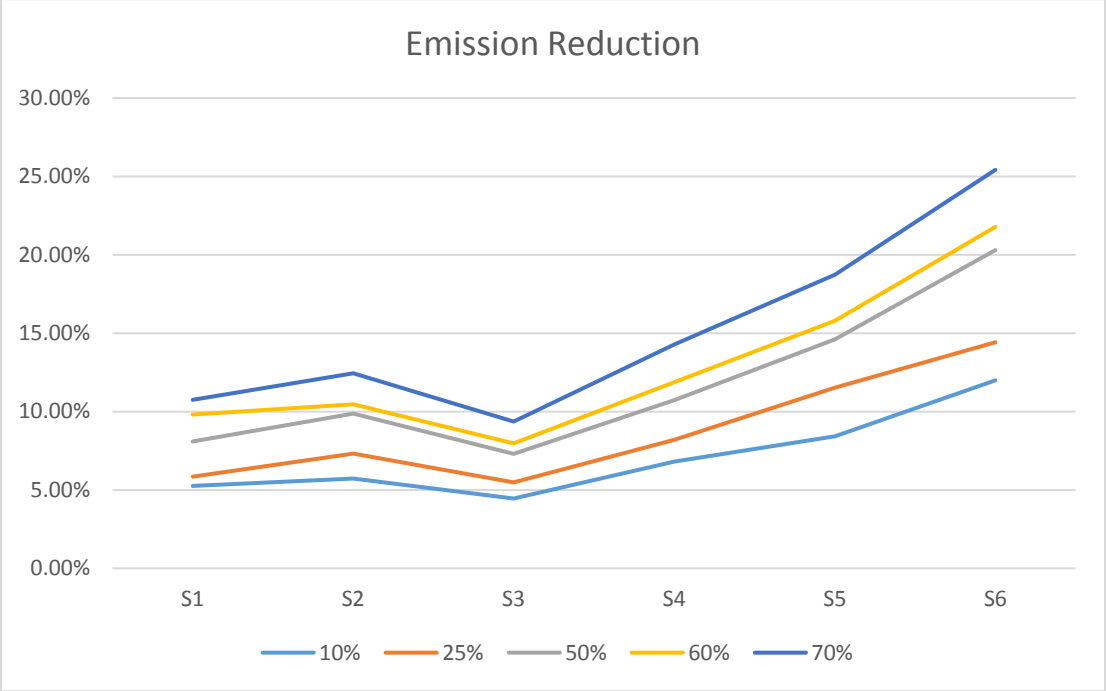

Figure 8.5 Total Emission Reduction under Different Scenarios and Different Penetration Rates

8.1.4 Surrogate Safety Performance

The purpose of this section is to use the SSAM safety analysis tool to compare different scenarios and base case on conflicts to analysis safety benefit. SSAM is a safety analysis software supported by FHWA. It uses vehicle trajectory to determine conflicts

between vehicles. Although conflicts are not real accidents in traffic, conflicts have higher opportunities of car accidents (reference). Therefore, the number of conflicts could present the safety status of a traffic network.

This dissertation applied SSAM to analyze conflicts in the base case scenario and optimization scenarios at 10%, 25%, 50% and 70% penetration rates. Figure 8.6 displays the total number of conflicts in 10 simulation runs by conflict type under different penetration rates. All runs are in the category of control strategy S5, where the common cycle length and offset are optimized against the total queue length while the split is adjusted to clear the queue.

The results indicate that about 90% of conflicts at intersections are rear end conflicts. Smooth traffic operations, even at a penetration rate of 10%, result in reductions of about 46-54% of total conflicts and rear end conflicts. 76-86% of crossing conflicts, which are more severe than other types of conflicts, can be significantly reduced. However, improved speed and smooth traffic operations encourage drivers to change lanes to seek better speeds, which can increase lane change conflicts by 8-15%. In conclusion, the SSAM indicates that, while the optimized timing plan does provide safety benefits, it is hard to evaluate its effects on accident rate and fatality reduction or monetarily quantify its benefits.

Generally speaking, conflict reduction increases as the penetration rate increases. In addition, the total number of conflicts and rear end conflicts, as shown in Figure 8.6, decrease as the penetration rate increases. For cross conflicts, it is less evident that there is a relationship between the conflict point and penetration rate, while the results of this study

do indicate a significant reduction of conflicts. However, the relationship between lane change conflicts and penetration rate is inconclusive.

Figure 8.6 Penetration Rate and Conflicts (Total, Rear End, Crossing and Lane Changes)

8.2 Optimal Signal Timing Plan Analysis

Mobility, safety, fuel consumption and the details of the optimal timing plan are important measurements of the optimization model. To measure the optimal timing plan, it is necessary to track the decision variables in the optimization model (offset, green split, and cycle length). In this section, all of the three decision variables in the optimization

model are recorded and compared with the original signal timing plan. The accuracy of queue length prediction is another target of optimal timing plan analysis.

Details of all coordinated intersection results are shown in Appendix B. The typical result of one intersection at Node 4 is discussed in this section. The other Node 5, Node 6, and Node 7 have similar status as Node 4.

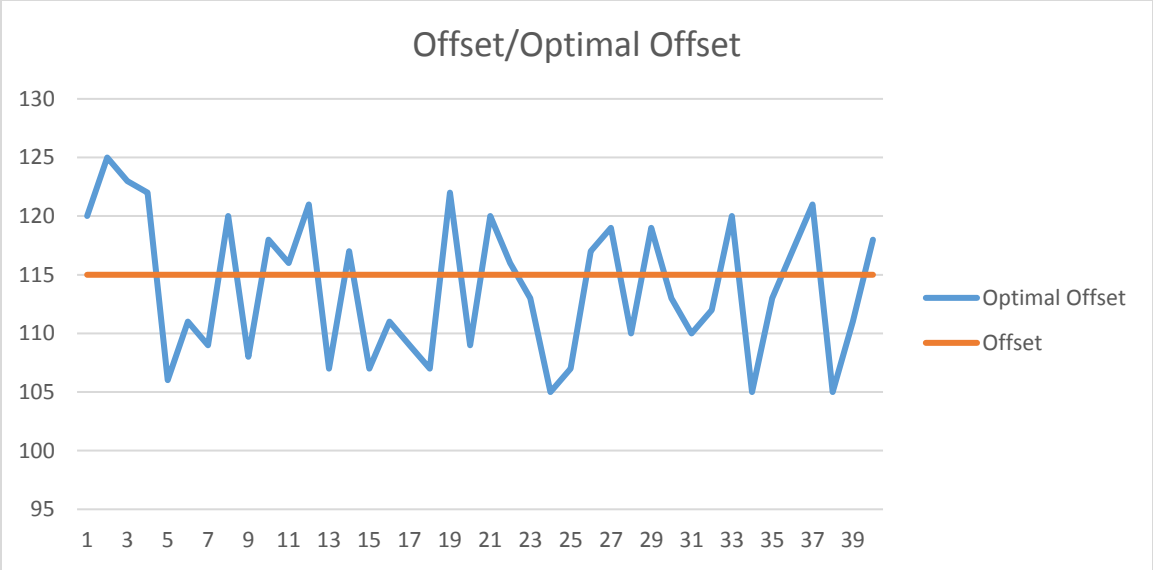

Figure 8.7 Offset and Optimal Offset Changes of Node 4 in Case Study

Figure 8.7 displays the original offset and optimal offset changes of one coordinated node 4. The optimal offsets are changed dynamically.

The original offsets are kept in one fixed value in each cycle and optimal offsets are modified by traffic status.

In addition, Figure 8.8 and Figure 8.9 display the offset difference and average travel time of previous cycle discharged vehicles. Figure 8.8 displays Node 4 to Node 5 eastbound and Figure 8.9 displays Node 7 to Node 6 westbound. Basically, average travel

times of previous cycle discharged vehicles are similar as offset differences between two coordinated intersections.

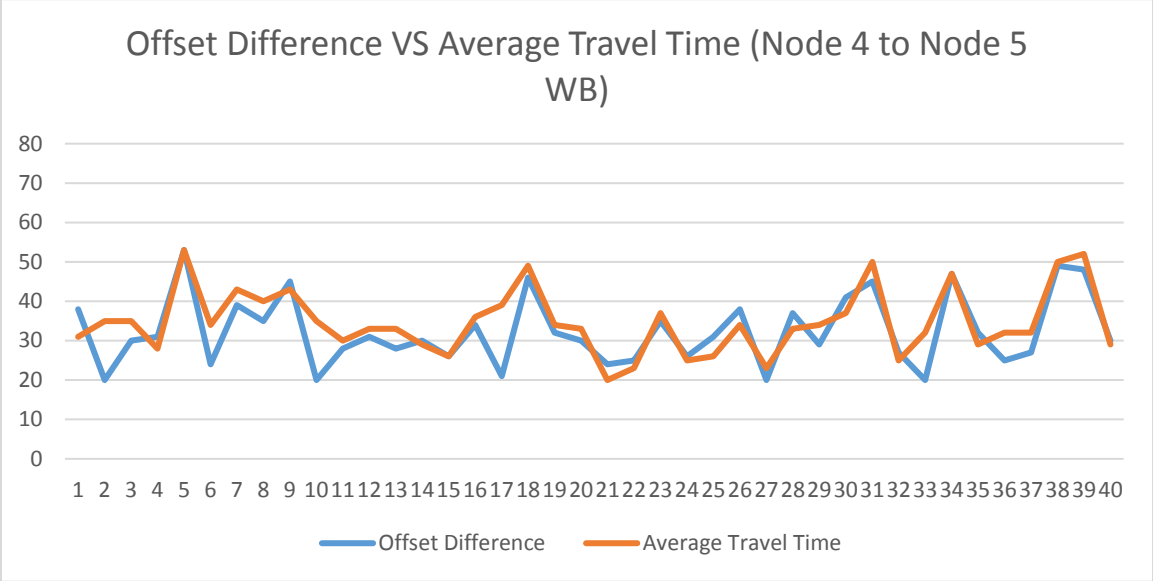

Figure 8.8 Offset Difference and Average Travel Time from Node 4 to Node 5 in Case Study (Seconds)

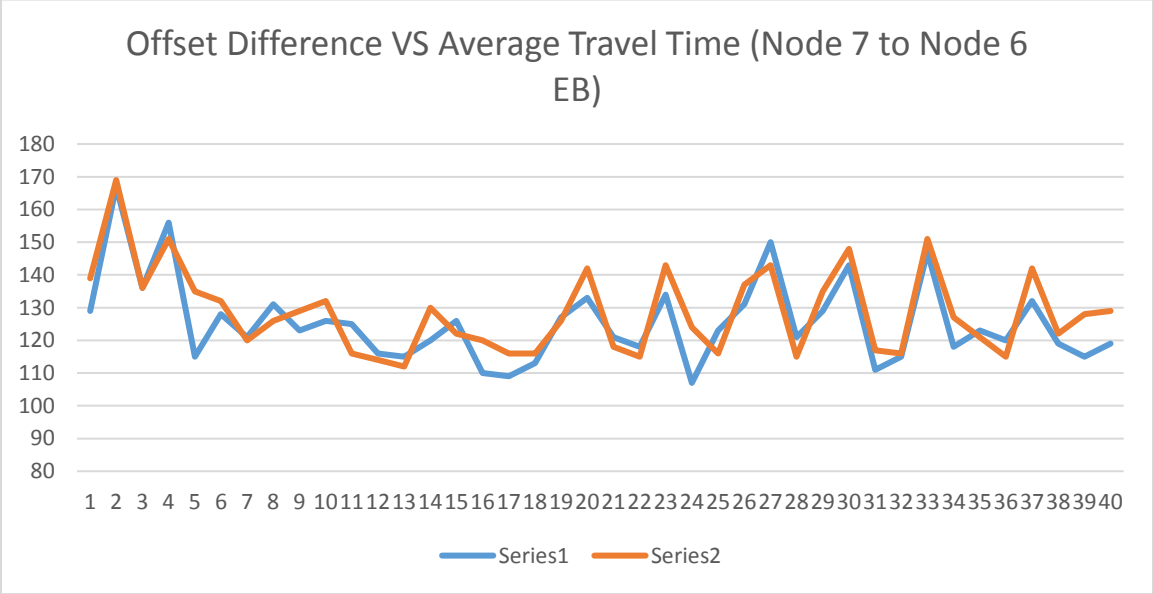

Figure 8.9 Offset Difference and Average Travel Time from Node 7 to Node 6 in Case Study (Seconds)

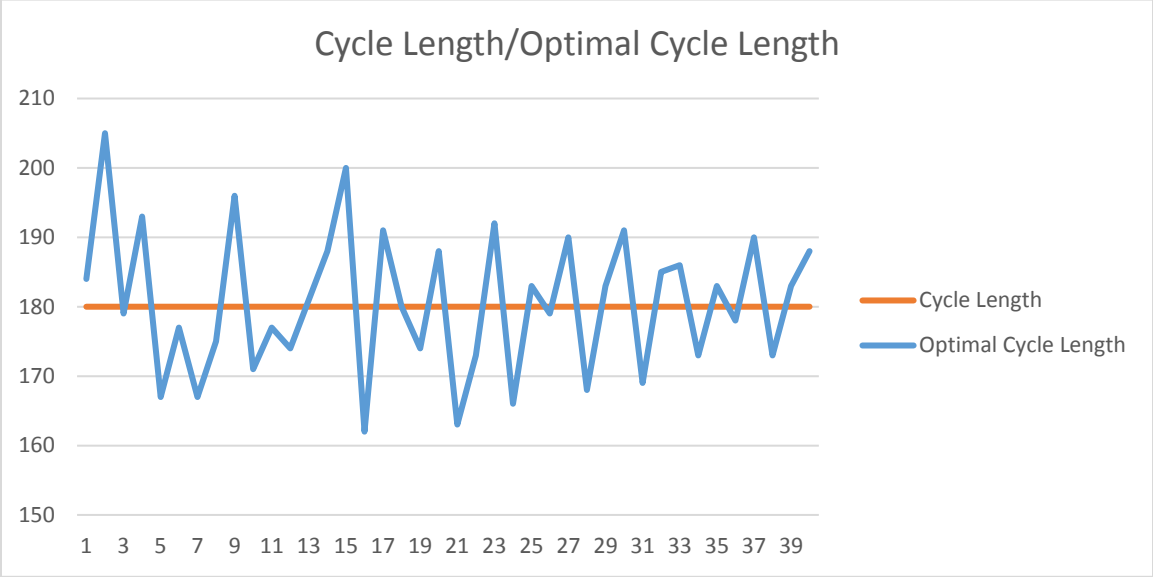

Figure 8.10 Cycle Length and Optimal Cycle Length Changes of Node 4 in Case Study

In Figure 8.10, original cycle length is similar to original offset, which is a fixed value in each cycle. The optimal cycle length of each cycle is changed by traffic volume and vehicle trajectory.

The cycle length statistical analysis summarizes the cycle length changes in the total cycles. To determine the cycle length changes, the optimal cycle lengths are divided into three groups. Each group contain 13 cycle lengths. The statistical analysis results show in Table 8.9.

Table 8.9 Statistical Analysis of Cycle Length Changes

	Group 1 (1-13)	Group 2 (14-26)	Group 3 (27-40)
Difference	38	38	22
Standard Error	3.204013	2.979785	2.05173
Standard Deviation	11.98832	11.14934	7.107401

As compared to offset and cycle length, the green split of each phase of one intersection is more complicated. Figure 8.9 displays the green splits and queue length comparison of Node 4.

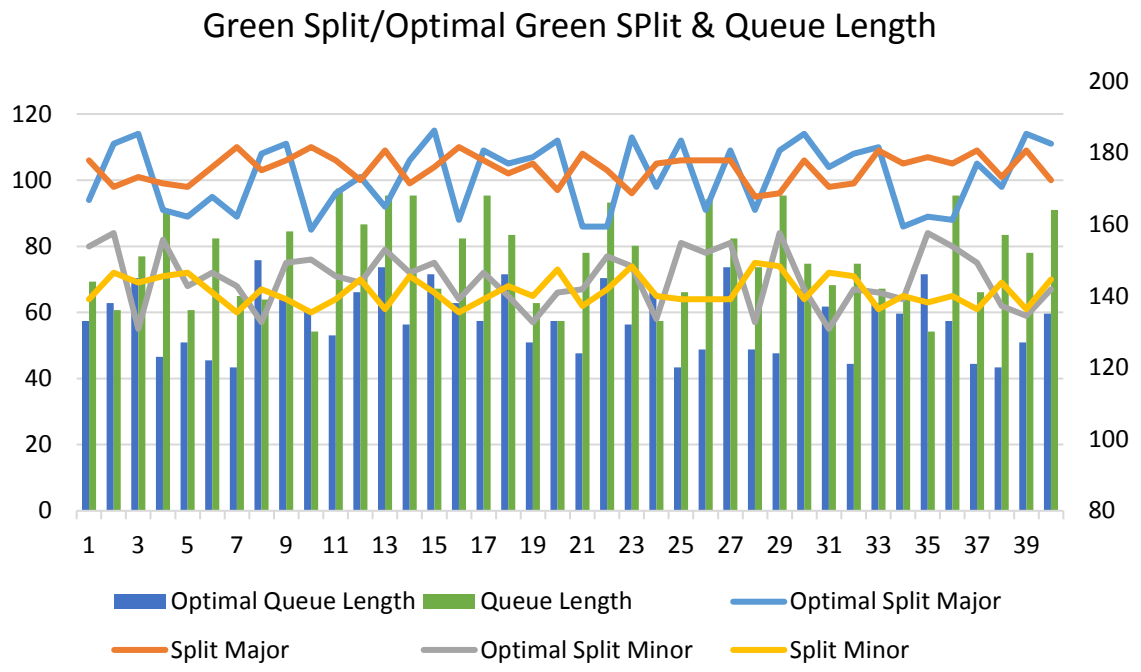

Figure 8.11 Split, Optimal Split Changes, and Queue Length of Node 4 in Case Study

Figure 8.11 shows the major and minor directions of green split changes. Most frequently, original signal timing plan green splits are different from optimal green splits in both major and minor directions. The reason for this status is that the optimization model needs to include consideration of all intersection queue lengths and queue delays, which are estimated for objective function. Therefore, the queue length of the optimal scenario is less than that of the original signal timing plan. Figure 8.12.,8.13, and 8.14 display green split and max queue length of other three coordinated intersections (Node 5, 6, 7). The status is similar as Figure 8.11.

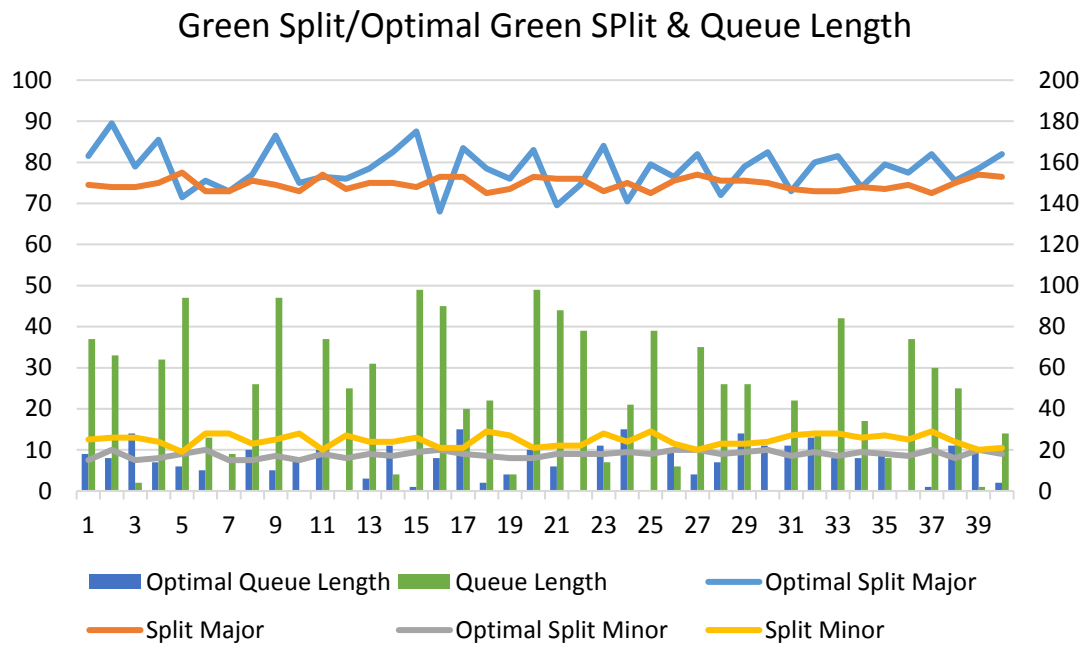

Figure 8.12 Split, Optimal Split Changes, and Queue Length of Node 5 in Case Study

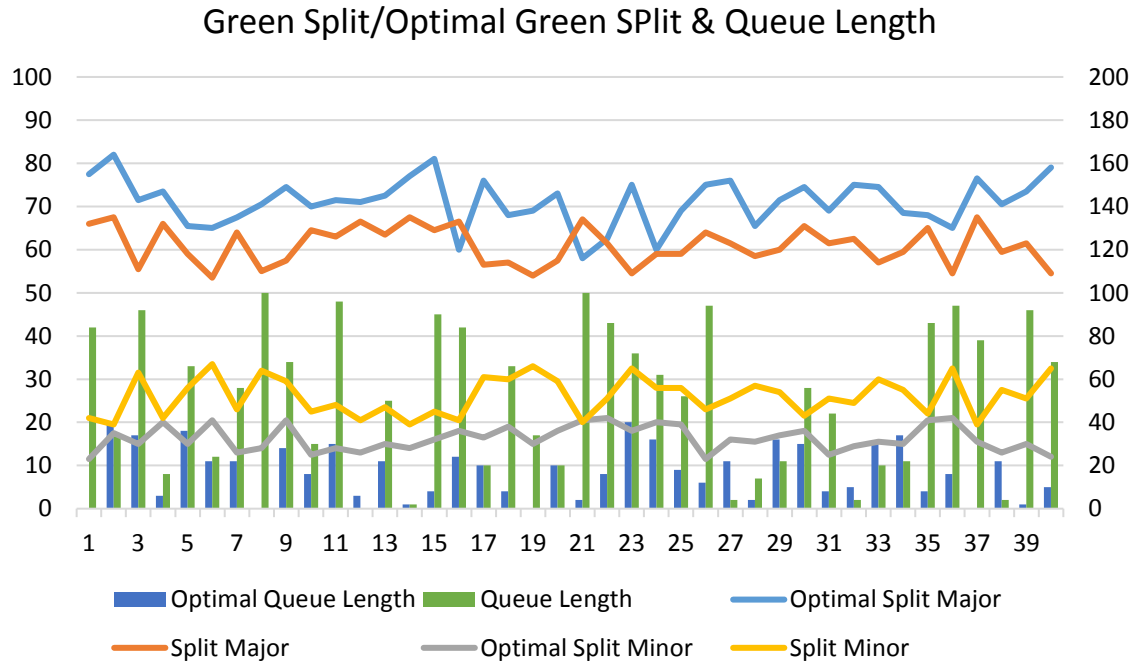

Figure 8.13 Split, Optimal Split Changes, and Queue Length of Node 6 in Case Study

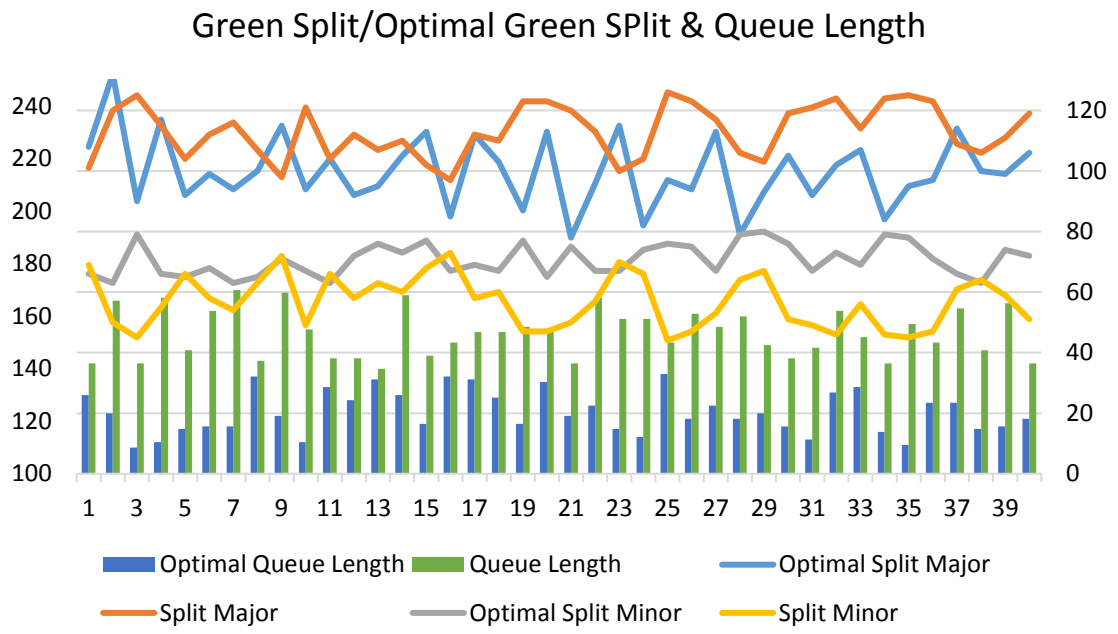

Figure 8.14 Split, Optimal Split Changes, and Queue Length of Node 7 in Case Study

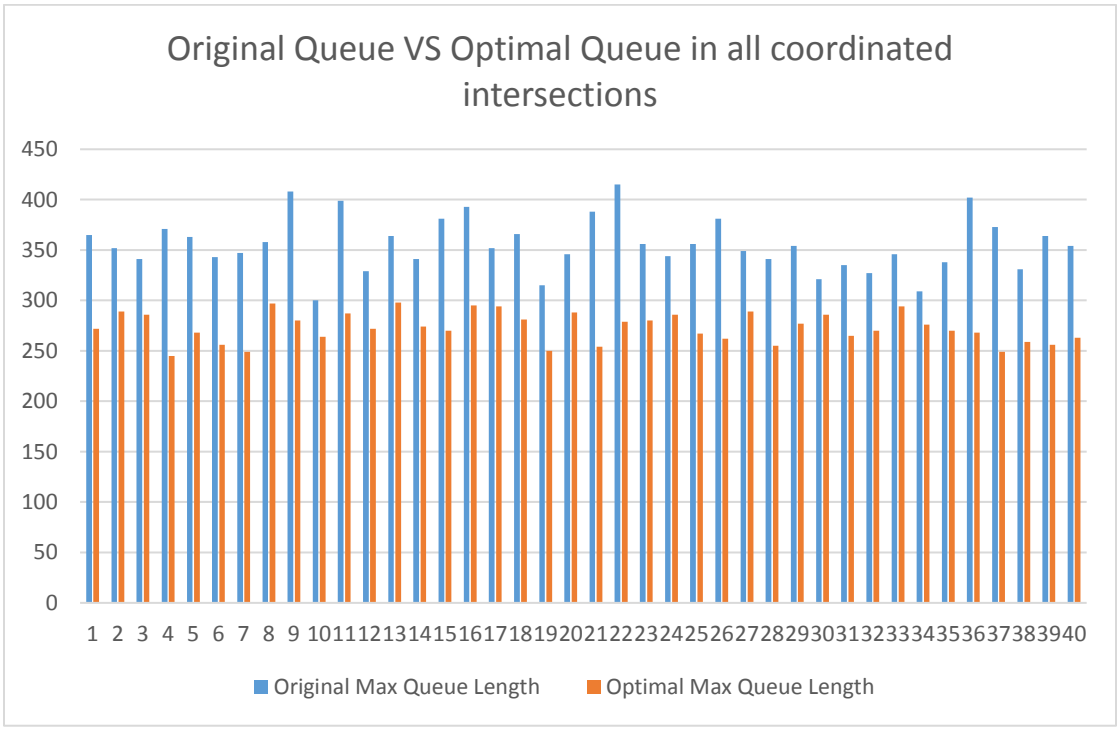

Figure 8.15 Original Queue Length and Optimal Queue Length of All Coordinated Intersections in Case Study (Vehs)

Since Figure 8.11 to Figure 8.14 displays the optimal queue length is longer than original queue in several cycles, Figure 8.15 displays the total queue length comparison in all four coordinated intersections. In Figure 8.15, all optimal max queue lengths are shorter than original max queue length in every cycle. In addition, it proves the optimization model could reduce queue delay in the network.

Overall, the optimization model could adjust the signal timing plan to be more adaptive with traffic volume and vehicle trajectory. The connected vehicle data could support this optimization model on queue delay minimization.

8.3 CPU Time Consumption on Optimizations

CPU time consumption on optimization could affect practice and future deployment of this system. This section aims to compare different scenarios and base cases on different types of optimized algorithms.

The three optimization methods are Newton's method, the steepest descent method, and the Nelder-Mead method. The three methods are comparable in terms of CPU time consumption. The timer function of optimization model records the start time and end time of optimization. The results display the optimization during analysis of the three optimization methods.

Table 8.10 shows that the results of time consumption of three different optimization methods. The steepest descent method is the fastest of the three methods. The Newton method is slightly slower than the steepest descent method. The Nelder-Mead method is ranked third in terms of speed of optimization.

Table 8.10 Results of Three Optimization Method on Time Consumption

Optimization Method	**Average Time Consumption**
Newton Method	122.123 Seconds
Steepest Descent Method	103.854 Seconds
Nelder-Mead Method	134.452 Seconds

The performance of the three methods are similar in terms of control delay reduction. The control delay reductions have only a few differences between these three optimization methods.

Table 8.11 Results of Three Optimization Method on Total Control Delay Reduction

	10%	25%	50%	60%	70%
Newton Method S5	10.48%	13.98%	18.10%	20.21%	21.81%
Newton Method S6	17.82%	20.05%	26.87%	28.24%	29.70%
Steepest Descent Method S5	9.58%	13.38%	17.10%	19.01%	20.61%
Steepest Descent Method S6	16.72%	19.25%	26.07%	27.04%	28.90%
Nelder-Mead Method S5	7.68%	10.68%	14.70%	16.11%	19.01%
Nelder-Mead Method S6	16.82%	18.15%	25.57%	27.14%	28.10%

Table 8.11 shows the results of control delay reduction of three different optimization methods. The best performance algorithm is the Newton method. The steepest descent method has similar results to the Newton method. The Nelder-Mead method has a smaller control delay reduction performance. The best scenario of 70% penetration rate in S6 still produces 28% control delay reduction. In addition, Figure 8.16 displays the comparison of these three optimization algorithms.

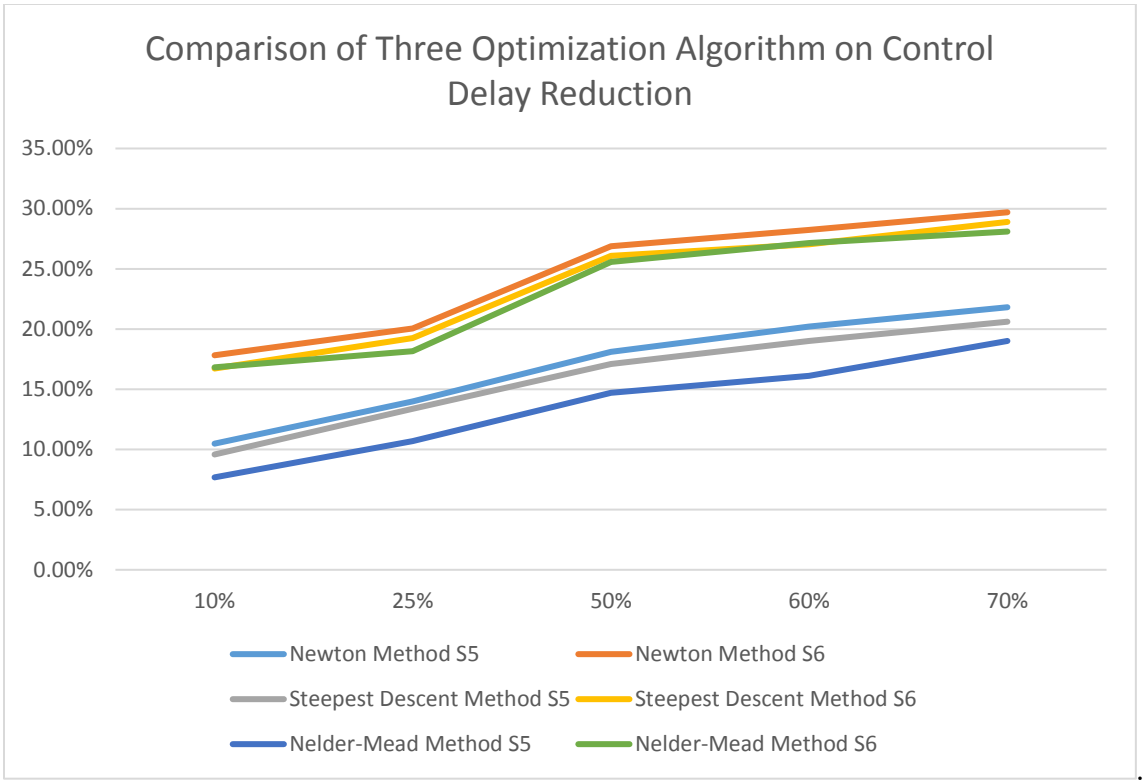

Figure 8.16 Comparison of Three Optimization Algorithms on Control Delay Reduction

CHAPTER IX

CONCLUSION AND RECOMMENDATIONS

The purpose of this dissertation is to use connected vehicle technology to solve traffic congestion in signalized arterial. This dissertation targets network wide signal control strategies base on connected vehicle technology which could generate benefits on traffic signal operation management. The solution is to develop models to adjust/optimize three key variables in signal timing plan offset, split, and cycle length. onto accommodate traffic signal operation, strategies are six combinations of offset, split, and cycle length. Some strategies optimize these all or part of three decision variables, other strategies adjust split and/or cycle length.

This dissertation formulates total queue delay for objective function. Queue lengths are forecasted within a cycle as the fundamentals of the queue delay models. In addition, this dissertation involves connected vehicle technology with BSM into queue length forecast. Different with other queue length forecast without connected vehicle technology, connected vehicle technology could increase the accuracy of queue length forecast on residual queue length check and vehicle travel status determinations. Then, to use queue length forecast, the adjustment of split and/or cycle length are based on queue length forecast function in some strategies. In the strategies contain optimization model, the

objective function is total queue delay of all directions of coordinated intersections basing on queue length forecast.

The objective function is non-linear programming problem. Three non-linear programming optimization algorithms are used in optimization. Newton's method and Steepest Descent method are gradient method. The first degree of derivative of objective function is calculated and used into gradient methods. Another optimization algorithm is Nelder-Mead method which is called MATLAB function directly be MATLAB API. The comparison of three optimization algorithms shows the time consumption of optimization program and performance on mobility benefits.

All strategies are deployed into a simulation environment for case study. The case study is a real word traffic network in Mclean Virginia provided by VDOT. The network is calibrated with VDOT performance result. The signal timing plan of base case is optimized by Synchro software. The simulation case study indicates that traffic signal control, which incorporates connected vehicle BSMs can dynamically respond to traffic changes, reduces major street delay by 25-40%. These reductions occur on a variety of traffic control strategies, even ones based on manual traffic signal timing plan development procedures. The mobility benefit on major streets does not sacrifice minor street mobility benefits. All control strategies improve both major and minor street mobility benefits simultaneously. One critical finding in case study is that with the low penetration rate of 10%, control delays are simultaneously reduced on major and minor streets, with major streets seeing at least a 10% reduction. Another critical finding is that the proposed model can easily reduce fuel consumption by 10%, according to the EPA's PERE model. Such

savings for highway users justify the cost for connected vehicle communication upgrades at intersections. Even if the penetration rate is only 10%, this produces more than 8% in terms of fuel savings. In terms of safety benefits, for a penetration rate of only 10%, 45% of total and rear end conflicts and more than 70% of crossing conflicts can be reduced with a slight increase in lane change conflicts. In addition, the higher penetration rate of connected vehicle could generate more benefits on traffic signal operation management. The strategies of this dissertation could be used from next few years to further future.

The distributed system is an architecture in signal controllers and several researches. In this dissertation, the distributed system is used to increase accuracy of queue length forecast. The distributed system has two stages optimization method to optimize major and minor directions in one cycle separately. In each stage, the shorter projection time could increase the accuracy of queue length prediction and increase communication when the transmission message is shorter and computing efficiency. The distributed system communication could transfer shorter data message between client and master computers. And the client computer could finish some tasks that could help master computer on optimization calculation. The simulation result comparison between distributed system and centralized system shows the distributed system could have similar performance as centralized system under full optimization and without time limit condition. In addition, the distributed system alleviates communication bandwidth requirement and more efficient in program computing.

In conclusion, this dissertation presents a solution of traffic signal control strategies with connected vehicle technology to relieve congestion on signalized arterial. The six

strategies could meet different requirements of coordinated signal controllers. The centralized system and distributed system could be flexibly working on different arterial situations. With the results from the proposed models and solutions to the model, the deployment of connected vehicle infrastructure will greatly benefit roadway users. The benefits roadway users enjoy will outweigh the cost of deploying connected vehicle infrastructures.

REFERENCE

[1]. Federal Highway Administration. Congestion Reduction Toolbox: Improve Service on Existing Roads. [cited 2015 Dec 5th, 2015]; Available from: https://www.fhwa.dot.gov/congestion/toolbox/service.htm.

[2]. FHWA Resource Center Operation Technical Support Team, Adaptive Control Software – Lite (ACS-Lite) Implementation Template, Sep 2006.

[3]. Research and Innovative Technology Administration. Vehicle-to-Infrastructure (V2I) Communications for Safety. Connected Vehicle Applications January 12, 2012 [cited 2012 Feb 16th, 2012]; Available from: http://www.its.dot.gov/research/v2i.htm.

[4]. Goodall, N.J., Traffic Signal Control with Connected Vehicles, in Civil Engineering. 2013, University of Virginia: Charlottesville, VA. p. 224.

[5]. Federal Highway Administration. Congestion Reduction Toolbox: Improve Service on Existing Roads. [cited 2015 Dec 5th, 2015]; Available from: https://www.fhwa.dot.gov/congestion/toolbox/service.htm.

[6]. FHWA Resource Center Operation Technical Support Team, Adaptive Control Software – Lite (ACS-Lite) Implementation Template, Sep 2006.

[7]. Research and Innovative Technology Administration. Vehicle-to-Infrastructure (V2I) Communications for Safety. Connected Vehicle Applications January 12, 2012 [cited 2012 Feb 16th, 2012]; Available from: http://www.its.dot.gov/research/v2i.htm.

[8]. Amsterdam Group., Signal Phase and Time and Map, April 2016, Available from: https://amsterdamgroup.mett.nl/downloads/handlerdownloadfiles.ashx?idnv=500795

[9]. Goodall, N.J., Traffic Signal Control with Connected Vehicles, in Civil Engineering. 2013, University of Virginia: Charlottesville, VA. p. 224.

[10]. Little John, D., M.D. Kelson, and N.H. Gartner, MAXBAND: A Versatile Program for Setting Signals on Arteries and Triangular Network. 1981, Alfred P. Sloan School of Management, Massachusetts Institute of Technology: Cambridge, MA. p. 1-30.

[11]. Little, J.D., The synchronization of traffic signals by mixed-integer linear programming. Operations Research, 1966. 14(4): p. 568-594.

[12]. Gartner, N.H., et al., A multi-band approach to arterial traffic signal optimization. Transportation Research Part B: Methodological, 1991. 25(1): p. 55-74.

[13]. Wallace, C.E. and K.G. Courage, Arterail progression--new design approach. Transportation Research Record, 1982. 881(HS-034 940): p. 53-59.

[14]. Lieberman, E.B., J. Chang, and E.S. Prassas, Formulation of real-time control policy for oversaturated arterials. Transportation Research Record: Journal of the Transportation Research Board, 2000. 1727(1): p. 77-88.

[15]. Cesme, B. and P.G. Furth. Self-Organizing Control Logic for Oversaturated Arterials. in Transportation Research Board 92nd Annual Meeting. 2013. Washington D.C.: Transportation Research Board.

[16]. Messer, C.J., et al., A variable-sequence multiphase progression optimization program. Highway Research Record, 1973(445): p. 10.

[17]. Mirchandani, P. and L. Head, A real-time traffic signal control system: architecture, algorithms, and analysis. Transportation Research Part C: Emerging Technologies, 2001. 9(6): p. 415-432.

[18]. Luyanda, F., et al., ACS-lite algorithmic architecture: Applying adaptive control system technology to closed-loop traffic signal control systems. Transportation Research Record: Journal of the Transportation Research Board, 2003. 1856(-1): p. 175-184.

[19]. Robertson, D.I. and R.D. Bretherton, Optimizing networks of traffic signals in real time: The SCOOT method. IEEE Transactions on Vehicular Technology. , 1991. 40 (1): p. 11-15.

[20]. Wilson, C., G. Millar, and R. Tudge. Microsimulation Evaluation of the Benefits of SCATS Coordinated Traffic Control Signals. in TRB 2006 Annual Meeting. 2006. Washington D.C.: Transportation Research Board.

[21]. Gartner, N.H., F.J. Pooran, and C.M. Andrews, Optimized policies for adaptive control strategy in real-time traffic adaptive control systems: Implementation and field testing. Transportation Research Record: Journal of the Transportation Research Board, 2002(1811): p. 148-156.

[22]. Chandra, R. and C. Gregory, InSync Adaptive Traffic Signal Technology: Real-Time Artificial Intelligence Delivering Real-World Results. 2012: Lenexa, Kansas.

[23]. Park, B., Messer, C., Urbanik, T., "Traffic Signal Optimization Program for Oversaturated Condistions: Genetic Algorithm Approach", Journal of the Transportation Research Board, Volume 1683, DOI: 10.3141/1683-17, 1999

[24]. Lertworawanich, P., "A Traffic Signal Split Optimization Using Time-space Diagrams", 12th WCTR, July 11-15, 2010, Lisbon, Portugal.

[25]. Park, B.B., Schneeberger, J.D., "Evaluation of traffic signal timing optimization methods using a stochastic and microscopic simulation program", Virginia Transportation Research Council, Charlottesville, Virginia, Jan 2003, VTRC 03-CR12.

[26]. Gartner, N., Pooran, F., Andrews, C., "Optimized Policies for Adaptive Control Strategy in Real-Time Traffic Adaptive Control Systems: Implantation and Field Testing", Journal of the Transportation Research Board, Volume 1811, DOI: 10.3141/1811-18, 2004

[27]. Park, B.B., Santra, P., Yun, I., Lee, D., "Optimization of Time-of-Day Breakpoints for Better Traffic Signal Control.", Journal of the Transportation Research Board, Volume 1867, DOI: 10.3141/1867-25, 2004.

[28]. An, C., Xia, J., Lu, Z., Huang, W., Nie, Q., "A New One-Way Bandwidth-Based Traffic Signal Coordination Approach Based On Travel Speed Variations", 94th Annual Meeting of Transportation Research Board, Jan, 2015, Washington D.C., USA.

[29]. Lee, J., Assessing the Potential Benefits of IntelliDrive-based Intersection Control Algorithms, in Civil and Environmental Engineering. 2010, University of Virginia: Charlottesville, VA.

[30]. SAE International, SAE J2735 Dedicated Short Range Communications (DSRC) Message Set Dictionary (Apr 2015). 2015, SAE International: Warrendale, PA. p. 402.

[31]. He, Q., K.L. Head, and J. Ding, PAMSCOD: Platoon-based arterial multi-modal signal control with online data. Transportation Research Part C: Emerging Technologies, 2012. 20(1): p. 164-184.

[32]. He, Q., K.L. Head, and J. Ding, Multi-modal traffic signal control with priority, signal actuation and coordination. Transportation Research Part C: Emerging Technologies, 2014. 46: p. 65-82.

[33]. Priemer, C. and B. Friedrich. A decentralized adaptive traffic signal control using V2I communication data. in 12th International IEEE Conference on Intelligent Transportation Systems. 2009. St. Louis, MO, USA: IEEE.

[34]. Feng, Y., et al. A Real-time Adaptive Signal Phase Allocation Algorithm in a Connected Vehicle Environment. in Transportation Research Board 94th Annual Meeting. 2015. Washington D.C.: Transportation Research Board.

[35]. Florida Department of Transportation TSM&O Program, Advanced Signal Control Technology, May 2016, Tallahassee, Florida, USA

[36]. Douglas Gettman, Overview of the Kadence Real-Time Adaptive Control System, Kimley-Horn & Associates, Mar 2012

[37]. T. Wongpiromsarn, T. Uthaicharoenpong, Y. Wang, E. Frazzoli and D. Wang, Distributed traffic signal control for maximum network throughput, 2012 15th International IEEE Conference on Intelligent Transportation Systems, Anchorage, AK, 2012, pp. 588-595.

[38]. Andy H.F. Chow and Rui Sha, Performance analysis of centralised and distributed systems for urban traffic control, in Transportation Research Board 95th Annual Meeting. 2016. Washington D.C.: Transportation Research Board.

[39]. Faisal Ahmed and Said M. Easa, Novel real-time distributed signal control system for urban traffic networks, in Transportation Research Board 96th Annual Meeting. 2017. Washington D.C.: Transportation Research Board.

[40]. S. Timotheou, C. G. Panayiotou and M. M. Polycarpou, Online distributed network traffic signal control using the cell transmission model, 17th International IEEE Conference on Intelligent Transportation Systems (ITSC), Qingdao, 2014, pp. 2523-2528

[41]. S. Timotheou, C. G. Panayiotou and M. M. Polycarpou, Distributed Traffic Signal Control Using the Cell Transmission Model via the Alternating Direction Method for Multipliers, IEEE Transaction on Intelligent Transportation System, VOL. 16, NO. 2, APRIL 2015

[42]. K. Yuan, V. L. Knoop and S. P. Hoogendoorn, "Optimal dynamic green time for distributed signal control," 2016 IEEE 19th International Conference on Intelligent Transportation Systems (ITSC), Rio de Janeiro, 2016, pp. 447-451.

[43]. A. Zaidi, B. Kulcsár and H. Wymeersch, "Traffic-adaptive signal control and vehicle routing using a decentralized back-pressure method," 2015 European Control Conference (ECC), Linz, 2015, pp. 3029-3034.

[44]. Lagarias, J. C., J. A. Reeds, M. H. Wright, and P. E. Wright. "Convergence Properties of the Nelder-Mead Simplex Method in Low Dimensions." SIAM Journal of Optimization, Vol. 9, Number 1, 1998, pp. 112–147.

[45]. Deurbrouck, T., et al. (2015). "Trajectory Conversion Algorithm Software User Manual." Version 2.3. Washington, DC p. 31.

[46]. Federal Highway Administration. (2008). "Surrogate Safety Assessment Model." Available from: https://www.fhwa.dot.gov/publications/research/safety/08049/

[47]. Smith, S.F., Barlow, G.J., Xie, X., and Rubinstein, Z.B.. (2013). "Surtrac: Scalable Urban Traffic Control." Transportation Research Board 92nd Annual Meeting.Washington D.C.

[48]. Federal Highway Administration. "Safety and Mobility Benefits of Connected Vehicles_Vol I."McLean, VA. Publication No. FHWA-JPO-18-613

[49]. Federal Highway Administration. "Safety and Mobility Benefits of Connected Vehicles_Vol II."McLean, VA. Publication No. FHWA-JPO-18-613

[50]. Huang, ZT., et al., Arterial-Level Traffic Progression Optimization Model Within Connected Vehicle Environment. Transportation Research Board 97th Annual Meeting.Washington D.C.

[51]. Zhang, L., et al., Benefits of Early Deployment of Connected Vehicles at Signalized Intersections. Transportation Research Board 97th Annual Meeting.Washington D.C.

APPENDIX A

TABLES OF OPTIMAL TIMING PLAN

Table A.1 Optimal Timing Plan of Node 4 in S6

Cycle	Queue Length	Optimal Queue Length	Green Split (Major)	Green Split (Minor)	Offset	Cycle Length	Optimal Green Split (Major)	Optimal Green Split (Minor)	Optimal Offset	Optimal Cycle Length
1	144	133	106	64	115	180	94	80	120	184
2	136	138	98	72	115	180	111	84	125	205
3	151	145	101	69	115	180	114	55	123	179
4	164	123	99	71	115	180	91	82	122	183
5	136	127	98	72	115	180	89	68	106	167
6	156	122	104	66	115	180	95	72	111	177
7	140	120	110	60	115	180	89	68	109	167
8	139	150	103	67	115	180	108	57	120	175
9	158	139	106	64	115	180	111	75	108	196
10	130	136	110	60	115	180	85	76	118	171
11	170	129	106	64	115	180	96	71	116	177
12	160	141	100	70	115	180	101	69	121	180
13	168	148	109	61	115	180	92	79	107	181
14	168	132	99	71	115	180	106	72	117	188
15	142	146	104	66	115	180	115	75	107	200
16	156	138	110	60	115	180	88	64	111	162
17	168	133	106	64	115	180	109	72	109	191
18	157	146	102	68	115	180	105	65	107	180
19	138	127	105	65	115	180	107	57	122	174
20	133	133	97	73	115	180	112	66	109	188
21	152	124	108	62	115	180	86	67	120	163
22	166	145	103	67	115	180	86	77	116	173
23	154	132	96	74	115	180	113	74	113	197
24	133	141	105	65	115	180	98	58	105	166
25	141	120	106	64	115	180	112	81	107	203
26	167	125	106	64	115	180	91	78	117	179
27	156	148	106	64	115	180	109	81	119	200
28	148	125	95	75	115	180	91	57	110	158
29	168	124	96	74	115	180	109	84	119	203
30	149	142	106	64	115	180	114	67	113	191
31	143	137	98	72	115	180	104	55	110	169
32	149	121	99	71	115	180	108	67	112	185
33	142	138	109	61	115	180	110	66	120	186
34	139	135	105	65	115	180	86	64	105	160
35	130	146	107	63	115	180	89	84	113	183

Table A.1 Optimal Timing Plan of Node 4 in S6 (Continued)

36	168	133	105	65	115	180	88	80	117	178
37	141	121	109	61	115	180	105	75	121	190
38	157	120	101	69	115	180	98	62	105	170
39	152	127	109	61	115	180	114	59	111	183
40	164	135	100	70	115	180	111	67	118	188

Table A.2 Optimal Timing Plan of Node 5 in S6

Cycle	Queue Length	Optimal Queue Length	Green Split (Major)	Green Split (Minor)	Offset	Cycle Length	Optimal Green Split (Major)	Optimal Green Split (Minor)	Optimal Offset	Optimal Cycle Length
1	37	9	149	25	154	180	163	15	158	184
2	33	8	148	26	154	180	179	20	145	205
3	2	14	148	26	154	180	158	15	153	179
4	32	7	150	24	154	180	161	16	133	183
5	47	6	155	19	154	180	143	18	159	167
6	13	5	146	28	154	180	151	20	135	177
7	9	0	146	28	154	180	146	15	148	167
8	26	10	151	23	154	180	154	15	155	175
9	47	5	149	25	154	180	173	17	153	196
10	0	8	146	28	154	180	150	15	138	171
11	37	10	154	20	154	180	153	18	144	177
12	25	0	147	27	154	180	158	16	152	180
13	31	3	150	24	154	180	157	18	135	181
14	4	11	150	24	154	180	165	17	147	188
15	49	1	148	26	154	180	175	19	133	200
16	45	8	153	21	154	180	136	20	145	162
17	20	15	153	21	154	180	167	18	130	191
18	22	2	145	29	154	180	157	17	153	180
19	4	4	147	27	154	180	152	16	154	174
20	49	10	153	21	154	180	166	16	139	188
21	44	6	152	22	154	180	139	18	144	163
22	39	0	152	22	154	180	149	18	141	173
23	7	11	146	28	154	180	173	18	148	197
24	21	15	150	24	154	180	141	19	131	166
25	39	0	145	29	154	180	179	18	138	203
26	6	10	151	23	154	180	153	20	155	179
27	35	4	154	20	154	180	174	20	139	200
28	26	7	151	23	154	180	134	18	147	158

Table A.2 Optimal Timing Plan of Node 5 in S6 (Continued)

29	26	14	151	23	154	180	178	19	138	203
30	0	11	150	24	154	180	165	20	154	191
31	22	11	147	27	154	180	146	17	155	169
32	14	13	146	28	154	180	160	19	139	185
33	42	8	146	28	154	180	163	17	130	186
34	17	8	148	26	154	180	135	19	152	160
35	8	9	147	27	154	180	159	18	145	183
36	37	0	149	25	154	180	155	17	132	178
37	30	1	145	29	154	180	164	20	138	190
38	25	11	150	24	154	180	148	16	154	170
39	1	10	154	20	154	180	157	20	159	183
40	14	2	153	21	154	180	164	18	148	188

Table A.3 Optimal Timing Plan of Node 6 in S6

Cycle	Queue Length	Optimal Queue Length	Green Split (Major)	Green Split (Minor)	Offset	Cycle Length	Optimal Green Split (Major)	Optimal Green Split (Minor)	Optimal Offset	Optimal Cycle Length
1	42	0	132	42	179	180	155	23	175	184
2	17	20	135	39	179	180	164	35	163	205
3	46	17	111	63	179	180	143	30	166	179
4	8	3	132	42	179	180	137	40	159	183
5	33	18	118	56	179	180	131	30	158	167
6	12	11	107	67	179	180	130	41	160	177
7	28	11	128	46	179	180	135	26	155	167
8	50	0	110	64	179	180	141	28	164	175
9	34	14	115	59	179	180	149	41	181	196
10	15	8	129	45	179	180	140	25	163	171
11	48	15	126	48	179	180	143	28	168	177
12	0	3	133	41	179	180	148	26	179	180
13	25	11	127	47	179	180	145	30	173	181
14	1	1	135	39	179	180	154	28	185	188
15	45	4	129	45	179	180	162	32	181	200
16	42	12	133	41	179	180	120	36	163	162
17	10	10	113	61	179	180	152	33	191	191
18	33	4	114	60	179	180	136	38	174	180
19	17	0	108	66	179	180	138	30	169	174
20	10	10	115	59	179	180	146	36	164	188
21	50	2	134	40	179	180	116	41	162	163

Table A.3 Optimal Timing Plan of Node 6 in S6 (Continued)

22	43	8	123	51	179	180	125	42	171	173
23	36	20	109	65	179	180	155	36	171	197
24	31	16	118	56	179	180	120	40	164	166
25	26	9	118	56	179	180	158	39	167	203
26	47	6	128	46	179	180	150	23	165	179
27	2	11	123	51	179	180	162	32	159	200
28	7	2	117	57	179	180	121	31	157	158
29	11	16	120	54	179	180	163	34	173	203
30	28	15	131	43	179	180	149	36	161	191
31	22	4	123	51	179	180	138	25	168	169
32	2	5	125	49	179	180	150	29	182	185
33	10	15	114	60	179	180	149	31	159	186
34	11	17	119	55	179	180	124	30	160	160
35	43	4	130	44	179	180	136	41	173	183
36	47	8	109	65	179	180	130	42	175	178
37	39	0	135	39	179	180	153	31	179	190
38	2	11	119	55	179	180	138	26	159	170
39	46	1	123	51	179	180	147	30	209	183
40	34	5	109	65	179	180	158	24	187	188

Table A.4 Optimal Timing Plan of Node 7 in S6

Cycle	Queue Length	Optimal Queue Length	Green Split (Major)	Green Split (Minor)	Offset	Cycle Length	Optimal Green Split (Major)	Optimal Green Split (Minor)	Optimal Offset	Optimal Cycle Length
1	142	130	101	69	106	180	108	66	120	184
2	166	123	120	50	106	180	132	63	125	205
3	142	110	125	45	106	180	90	79	123	179
4	167	112	115	55	106	180	107	66	122	183
5	147	117	104	66	106	180	92	65	106	167
6	162	118	112	58	106	180	99	68	111	177
7	170	118	116	54	106	180	94	63	109	167
8	143	137	107	63	106	180	100	65	120	175
9	169	122	98	72	106	180	115	71	108	196
10	155	112	121	49	106	180	94	67	118	171
11	144	133	104	66	106	180	104	63	116	177
12	144	128	112	58	106	180	98	72	121	180
13	140	136	107	63	106	180	95	76	107	181
14	168	130	110	60	106	180	105	73	117	188

Table A.4 Optimal Timing Plan of Node 7 S6 (Continued)

15	145	119	102	68	106	180	113	77	107	200
16	150	137	97	73	106	180	85	67	111	162
17	154	136	112	58	106	180	112	69	109	191
18	154	129	110	60	106	180	103	67	107	180
19	156	119	123	47	106	180	87	77	122	174
20	154	135	123	47	106	180	113	65	109	188
21	142	122	120	50	106	180	78	75	120	163
22	167	126	113	57	106	180	96	67	116	173
23	159	117	100	70	106	180	120	67	113	197
24	159	114	104	66	106	180	82	74	105	166
25	150	138	126	44	106	180	117	76	107	203
26	161	121	123	47	106	180	94	75	117	179
27	156	126	117	53	106	180	123	67	119	200
28	160	121	106	64	106	180	69	79	110	158
29	149	123	103	67	106	180	113	80	119	203
30	144	118	119	51	106	180	105	76	113	191
31	148	113	121	49	106	180	92	67	110	169
32	162	131	124	46	106	180	102	73	112	185
33	152	133	114	56	106	180	107	69	120	186
34	142	116	124	46	106	180	71	79	105	160
35	157	111	125	45	106	180	95	78	113	183
36	150	127	123	47	106	180	97	71	117	178
37	163	127	109	61	106	180	114	66	121	190
38	147	117	106	64	106	180	97	63	105	170
39	165	118	111	59	106	180	99	74	111	183
40	142	121	119	51	106	180	106	72	118	188

APPENDIX B

TABLES OF CASE STUDY RESULTS

Table B.1 Control Delay of S1 in Base Scenario (Volume Ratio 1.0)

Node 4	Control Delay Per Vehicle			
	EB	WB	NB	SB
Base Case	114.7683	62.13333	89.6375	126.58
10% Penetration Rate	104.4356	56.27416	87.84475	124.213
Differences	-9.0%	-9.4%	-2.0%	-1.9%
25% Penetration Rate	98.09249	52.54616	86.75745	122.6307
Differences	-14.5%	-15.4%	-3.2%	-3.1%
50% Penetration Rate	95.79713	51.37557	86.1627	121.1219
Differences	-16.5%	-17.3%	-3.9%	-4.3%
60% Penetration Rate	95.14295	50.94126	86.02511	119.732
Differences	-17.1%	-18.0%	-4.0%	-5.4%
70% Penetration Rate	94.85603	50.48333	85.7553	118.4662
Differences	-17.4%	-18.8%	-4.3%	-6.4%
Node 5	Control Delay Per Vehicle			
	EB	WB	NB	SB
Base Case	11.8675	13.63333	90.615	32.5425
10% Penetration Rate	10.86529	12.66073	88.79364	31.89816
Differences	-8.4%	-7.1%	-2.0%	-2.0%
25% Penetration Rate	10.69974	12.47973	88.3084	31.85911
Differences	-9.8%	-8.5%	-2.5%	-2.1%
50% Penetration Rate	10.27132	11.89236	87.68814	31.79077
Differences	-13.5%	-12.8%	-3.2%	-2.3%
60% Penetration Rate	10.15739	11.79965	87.1082	31.60853
Differences	-14.4%	-13.5%	-3.9%	-2.9%
70% Penetration Rate	9.904616	11.56925	87.00852	31.45753
Differences	-16.5%	-15.1%	-4.0%	-3.3%
Node 6	Control Delay Per Vehicle			
	EB	WB	NB	SB
Base Case	14.485	25.71	67.16	78.91
10% Penetration Rate	13.55318	23.91544	65.74292	77.3247
Differences	-6.4%	-7.0%	-2.1%	-2.0%
25% Penetration Rate	13.26681	23.47066	65.526	77.22133
Differences	-8.4%	-8.7%	-2.4%	-2.1%
50% Penetration Rate	13.05388	28.3967	65.23251	76.55217
Differences	-9.9%	-10.5%	-2.9%	-3.0%

Table B.1 Control Delay of S1 in Base Scenario (Volume Ratio 1.0) (Continued)

60% Penetration Rate	12.82936	21.73626	65.06461	76.1955
Differences	-11.4%	-15.5%	-3.1%	-3.4%
70% Penetration Rate	12.68162	21.437	64.91686	75.95877
Differences	-12.5%	-16.6%	-3.3%	-3.7%
Node 7	Control Delay Per Vehicle			
	EB	WB	NB	SB
Base Case	37.79167	49.3725	75.7575	83.43
10% Penetration Rate	33.5401	41.14704	73.83326	81.4779
Differences	-11.3%	-16.7%	-2.5%	-2.3%
25% Penetration Rate	31.7261	38.77716	73.83326	80.94379
Differences	-16.1%	-21.5%	-2.5%	-3.0%
50% Penetration Rate	31.15923	38.03657	73.37871	80.52664
Differences	-17.6%	-23.0%	-3.1%	-3.5%
60% Penetration Rate	30.78131	37.54285	73.2272	80.35978
Differences	-18.6%	-24.0%	-3.3%	-3.7%
70% Penetration Rate	30.4034	36.8072	73.07568	80.10949
Differences	-19.6%	-25.5%	-3.5%	-4.0%

Table B.2 Control Delay of S2 in Base Scenario (Volume Ratio 1.0)

Node 4	Control Delay Per Vehicle			
	EB	WB	NB	SB
Base Case	114.7683	62.13333	89.6375	126.58
10% Penetration Rate	101.0535	54.52821	87.45035	121.8333
Differences	-12.0%	-12.2%	-2.4%	-3.8%
25% Penetration Rate	96.54542	51.63094	86.3747	120.5675
Differences	-15.9%	-16.9%	-3.6%	-4.8%
50% Penetration Rate	90.13905	47.38226	85.38868	118.7953
Differences	-21.5%	-23.7%	-4.7%	-6.2%
60% Penetration Rate	86.31726	45.13365	84.31303	118.3143
Differences	-24.8%	-27.4%	-5.9%	-6.5%
70% Penetration Rate	85.55979	46.2272	83.86485	118.0359
Differences	-25.5%	-25.6%	-6.4%	-6.8%
Node 5	Control Delay Per Vehicle			
	EB	WB	NB	SB
Base Case	11.8675	13.63333	90.615	32.5425

Table B.2 Control Delay of S2 in Base Scenario (Volume Ratio 1.0) (Continued)

10% Penetration Rate	10.61429	11.87641	88.44024	31.83633
Differences	-10.6%	-12.9%	-2.4%	-2.2%
25% Penetration Rate	10.47366	11.60565	87.30755	31.60853
Differences	-11.7%	-14.9%	-3.7%	-2.9%
50% Penetration Rate	9.637953	10.95111	86.68231	31.54345
Differences	-18.8%	-19.7%	-4.3%	-3.1%
60% Penetration Rate	9.282402	10.70898	86.54639	31.5109
Differences	-21.8%	-21.5%	-4.5%	-3.2%
70% Penetration Rate	8.897065	10.26454	85.72179	31.28311
Differences	-25.0%	-24.7%	-5.4%	-3.9%
Node 6	Control Delay Per Vehicle			
	EB	WB	NB	SB
Base Case	14.485	25.71	67.16	78.91
10% Penetration Rate	12.92352	22.85876	65.83023	77.07929
Differences	-10.8%	-11.1%	-2.0%	-2.3%
25% Penetration Rate	12.46	21.97177	65.05118	75.4932
Differences	-14.0%	-14.5%	-3.1%	-4.3%
50% Penetration Rate	11.62566	20.2855	63.91617	74.96213
Differences	-19.7%	-21.1%	-4.8%	-5.0%
60% Penetration Rate	11.56627	20.01958	63.45948	74.62519
Differences	-20.2%	-22.1%	-5.5%	-5.4%
70% Penetration Rate	11.09116	19.50618	63.8423	74.19118
Differences	-23.4%	-24.1%	-4.9%	-6.0%
Node 7	Control Delay Per Vehicle			
	EB	WB	NB	SB
Base Case	37.79167	49.3725	75.7575	83.43
10% Penetration Rate	33.30202	43.71935	74.36356	81.75306
Differences	-12.0%	-12.2%	-1.8%	-2.0%
25% Penetration Rate	31.45023	40.49532	73.99235	80.72687
Differences	-16.8%	-18.0%	-2.3%	-3.2%
50% Penetration Rate	29.81838	38.96305	73.39387	79.84251
Differences	-21.1%	-21.1%	-3.1%	-4.3%
60% Penetration Rate	28.60451	37.35958	73.31508	78.92478
Differences	-24.3%	-24.3%	-3.2%	-5.4%
70% Penetration Rate	28.09055	36.81214	72.81053	79.17507
Differences	-25.7%	-25.4%	-3.9%	-5.1%

Table B.3 Control Delay of S3 in different intersections in Base Scenario (Volume Ratio 1.0)

Node 4	Control Delay Per Vehicle			
	EB	WB	NB	SB
Base Case	114.7683	62.13333	89.6375	126.58
10% Penetration Rate	102.5713	55.01655	86.99391	123.2231
Differences	-10.6%	-11.5%	-2.9%	-2.7%
25% Penetration Rate	97.31565	52.43432	86.25458	123.1922
Differences	-15.2%	-15.6%	-3.8%	-2.7%
50% Penetration Rate	92.41259	49.17853	85.51179	122.1522
Differences	-19.5%	-20.9%	-4.6%	-3.5%
60% Penetration Rate	87.09086	47.06869	85.36592	120.072
Differences	-24.1%	-24.2%	-4.8%	-5.1%
70% Penetration Rate	85.93625	45.39703	84.55431	119.6815
Differences	-25.1%	-26.9%	-5.7%	-5.4%
Node 5	Control Delay Per Vehicle			
	EB	WB	NB	SB
Base Case	11.8675	13.63333	90.615	32.5425
10% Penetration Rate	10.82648	12.2107	87.10349	31.5825
Differences	-8.8%	-10.4%	-3.9%	-3.0%
25% Penetration Rate	10.184	11.85649	85.22449	31.49789
Differences	-14.2%	-13.0%	-5.9%	-3.2%
50% Penetration Rate	9.763727	11.13639	85.62808	31.13341
Differences	-17.7%	-18.3%	-5.5%	-4.3%
60% Penetration Rate	9.174729	10.5264	85.34896	30.96419
Differences	-22.7%	-22.8%	-5.8%	-4.9%
70% Penetration Rate	9.201698	10.42411	85.35631	30.81319
Differences	-22.5%	-23.5%	-5.8%	-5.3%
Node 6	Control Delay Per Vehicle			
	EB	WB	NB	SB
Base Case	14.485	25.71	67.16	78.91
10% Penetration Rate	13.0707	23.35574	64.83159	76.23398
Differences	-9.8%	-9.2%	-3.5%	-3.4%
25% Penetration Rate	12.52098	22.44894	63.70488	74.51702
Differences	-13.6%	-12.7%	-5.1%	-5.6%
50% Penetration Rate	11.8355	20.95109	63.50057	74.39974
Differences	-18.3%	-18.5%	-5.4%	-5.7%
60% Penetration Rate	11.21666	19.79784	63.19586	74.2874
Differences	-22.6%	-23.0%	-5.9%	-5.9%

Table B.3 Control Delay of S3 in different intersections in Base Scenario (Volume Ratio 1.0) (Continued)

70% Penetration Rate	10.99447	19.42147	62.08606	72.75468
Differences	-24.1%	-24.5%	-7.6%	-7.8%
Node 7	Control Delay Per Vehicle			
	EB	WB	NB	SB
Base Case	37.79167	49.3725	75.7575	83.43
10% Penetration Rate	33.59982	44.42933	70.1466	78.65213
Differences	-11.1%	-10.0%	-7.4%	-5.7%
25% Penetration Rate	31.70683	41.26254	69.02412	77.98976
Differences	-16.1%	-16.4%	-8.9%	-6.5%
50% Penetration Rate	30.4312	39.85496	68.87283	76.72431
Differences	-19.5%	-19.3%	-9.1%	-8.0%
60% Penetration Rate	28.66542	37.26143	68.85405	76.03227
Differences	-24.1%	-24.5%	-9.1%	-8.9%
70% Penetration Rate	28.15718	36.94364	68.74928	75.54117
Differences	-25.5%	-25.2%	-9.3%	-9.5%

Table B.4 Control Delay of S4 in different intersections in Base Scenario (Volume Ratio 1.0)

Node 4	Control Delay Per Vehicle			
	EB	WB	NB	SB
Base Case	114.7683	62.13333	89.6375	126.58
10% Penetration Rate	100.4314	53.8743	86.98136	123.2231
Differences	-12.5%	-13.3%	-3.0%	-2.7%
25% Penetration Rate	92.25331	49.94899	85.35821	121.8803
Differences	-19.6%	-19.6%	-4.8%	-3.7%
50% Penetration Rate	84.36046	46.05633	84.51597	120.8864
Differences	-26.5%	-25.9%	-5.7%	-4.5%
60% Penetration Rate	82.20473	44.4697	82.6768	118.6774
Differences	-28.4%	-28.4%	-7.8%	-6.2%
70% Penetration Rate	81.11327	43.73727	81.80598	115.724
Differences	-29.3%	-29.6%	-8.7%	-8.6%
Node 5	Control Delay Per Vehicle			
	EB	WB	NB	SB
Base Case	11.8675	13.63333	90.615	32.5425
10% Penetration Rate	10.37765	11.91799	86.9991	31.61628
Differences	-12.6%	-12.6%	-4.0%	-2.8%

Table B.4 Control Delay of S4 in different intersections in Base Scenario (Volume Ratio 1.0) (Continued)

25% Penetration Rate	9.725035	11.06169	86.84977	31.42467
Differences	-18.1%	-18.9%	-4.2%	-3.4%
50% Penetration Rate	8.814327	10.23637	85.99054	30.99902
Differences	-25.7%	-24.9%	-5.1%	-4.7%
60% Penetration Rate	8.652043	9.815955	84.34856	30.73329
Differences	-27.1%	-28.0%	-6.9%	-5.6%
70% Penetration Rate	8.477925	9.740508	83.60505	30.48522
Differences	-28.6%	-28.6%	-7.7%	-6.3%
Node 6	Control Delay Per Vehicle			
	EB	WB	NB	SB
Base Case	14.485	25.71	67.16	78.91
10% Penetration Rate	12.66771	22.62326	64.77219	76.13106
Differences	-12.5%	-12.0%	-3.6%	-3.5%
25% Penetration Rate	11.7179	20.95082	64.48388	75.24758
Differences	-19.1%	-18.5%	-4.0%	-4.6%
50% Penetration Rate	10.88505	19.4716	63.45769	74.84355
Differences	-24.9%	-24.3%	-5.5%	-5.2%
60% Penetration Rate	10.46019	18.90749	62.89954	74.2266
Differences	-27.8%	-26.5%	-6.3%	-5.9%
70% Penetration Rate	10.31085	18.36357	62.62689	73.54378
Differences	-28.8%	-28.6%	-6.7%	-6.8%
Node 7	Control Delay Per Vehicle			
	EB	WB	NB	SB
Base Case	37.79167	49.3725	75.7575	83.43
10% Penetration Rate	33.01291	42.94815	70.87144	78.535
Differences	-12.6%	-13.0%	-6.4%	-5.9%
25% Penetration Rate	30.35535	39.59577	70.49511	77.98976
Differences	-19.7%	-19.8%	-6.9%	-6.5%
50% Penetration Rate	27.70054	36.13178	69.69584	77.28509
Differences	-26.7%	-26.8%	-8.0%	-7.4%
60% Penetration Rate	27.15033	35.63213	68.77069	76.03227
Differences	-28.2%	-27.8%	-9.2%	-8.9%
70% Penetration Rate	26.50809	34.87667	68.74928	77.02237
Differences	-29.9%	-29.4%	-9.3%	-7.7%

Table B.5 Control Delay of S5 in different intersection in Base Scenario (Volume Ratio 1.0)

Node 4	Control Delay Per Vehicle			
	EB	WB	NB	SB
Base Case	114.7683	62.13333	89.6375	126.58
10% Penetration Rate	96.92875	52.09187	84.33096	119.4915
Differences	-15.5%	-16.2%	-5.9%	-5.6%
25% Penetration Rate	91.08474	49.396	83.63179	119.4409
Differences	-20.6%	-20.5%	-6.7%	-5.6%
50% Penetration Rate	82.11674	44.79813	81.97602	117.2006
Differences	-28.5%	-27.9%	-8.5%	-7.4%
60% Penetration Rate	78.56939	41.64409	81.34393	115.0733
Differences	-31.5%	-33.0%	-9.3%	-9.1%
70% Penetration Rate	76.39202	40.49791	80.13164	113.5126
Differences	-33.4%	-34.8%	-10.6%	-10.3%
Node 5	Control Delay Per Vehicle			
	EB	WB	NB	SB
Base Case	11.8675	13.63333	90.615	32.5425
10% Penetration Rate	10.09924	11.4929	85.39558	34.47336
Differences	-14.9%	-15.7%	-5.8%	5.9%
25% Penetration Rate	9.582087	10.90499	84.38069	30.46636
Differences	-19.3%	-20.0%	-6.9%	-6.4%
50% Penetration Rate	8.611459	9.963165	84.30445	30.24202
Differences	-27.4%	-26.9%	-7.0%	-7.1%
60% Penetration Rate	8.196932	9.573588	83.02821	30.0144
Differences	-30.9%	-29.8%	-8.4%	-7.8%
70% Penetration Rate	8.026442	9.302341	82.85412	29.76481
Differences	-32.4%	-31.8%	-8.6%	-8.5%
Node 6	Control Delay Per Vehicle			
	EB	WB	NB	SB
Base Case	14.485	25.71	67.16	78.91
10% Penetration Rate	12.32782	21.82779	64.18969	75.47919
Differences	-14.9%	-15.1%	-4.4%	-4.3%
25% Penetration Rate	11.70508	20.74797	63.79897	74.63411
Differences	-19.2%	-19.3%	-5.0%	-5.4%
50% Penetration Rate	10.67653	18.62786	62.87185	73.48246
Differences	-26.3%	-27.5%	-6.4%	-6.9%
60% Penetration Rate	10.18281	18.03614	61.74603	72.51514
Differences	-29.7%	-29.8%	-8.1%	-8.1%

Table B.5 Control Delay of S5 in different intersection in Base Scenario (Volume Ratio 1.0) (Continued)

70% Penetration Rate	9.878625	17.86624	61.45804	72.08628
Differences	-31.8%	-30.5%	-8.5%	-8.6%
Node 7	Control Delay Per Vehicle			
	EB	WB	NB	SB
Base Case	37.79167	49.3725	75.7575	83.43
10% Penetration Rate	31.82058	41.52227	72.48478	79.52548
Differences	-15.8%	-15.9%	-4.3%	-4.7%
25% Penetration Rate	30.16018	38.80222	71.34101	76.46055
Differences	-20.2%	-21.4%	-5.8%	-8.4%
50% Penetration Rate	26.94546	35.89381	68.42344	75.14689
Differences	-28.7%	-27.3%	-9.7%	-9.9%
60% Penetration Rate	25.89345	33.6056	68.17982	74.54144
Differences	-31.5%	-31.9%	-10.0%	-10.7%
70% Penetration Rate	24.56554	32.41207	67.40126	74.05997
Differences	-35.0%	-34.4%	-11.0%	-11.2%

Table B.6 Control Delay of S6 in different intersections in Base Scenario (Volume Ratio 1.0)

Node 4	Control Delay Per Vehicle			
	EB	WB	NB	SB
Base Case	114.8	62.1	89.6	126.6
10% Penetration Rate	85.0	46.1	80.4	113.5
Differences	-25.9%	-25.7%	-10.3%	-10.4%
25% Penetration Rate	80.3	44.1	79.7	111.8
Differences	-30.0%	-29.1%	-11.1%	-11.7%
50% Penetration Rate	68.9	37.7	76.4	106.8
Differences	-40.0%	-39.4%	-14.8%	-15.6%
60% Penetration Rate	67.4	36.7	76.2	106.1
Differences	-41.3%	-40.9%	-15.0%	-16.2%
70% Penetration Rate	66.9	36.0	73.5	104.9
Differences	-41.7%	-42.0%	-18.0%	-17.1%
Node 5	Control Delay Per Vehicle			
	EB	WB	NB	SB
Base Case	11.9	13.6	90.6	32.5
10% Penetration Rate	8.9	9.9	82.7	29.9
Differences	-25.0%	-27.4%	-8.8%	-8.0%

Table B.6 Control Delay of S6 in different intersections in Base Scenario (Volume Ratio 1.0) (Continued)

25% Penetration Rate	8.4	9.7	81.7	29.4
Differences	-29.3%	-28.7%	-9.9%	-9.6%
50% Penetration Rate	7.4	8.7	78.9	28.4
Differences	-37.5%	-36.5%	-13.0%	-12.9%
60% Penetration Rate	7.2	8.3	78.6	28.1
Differences	-39.2%	-39.1%	-13.3%	-13.5%
70% Penetration Rate	6.7	7.8	78.3	27.9
Differences	-43.6%	-42.5%	-13.6%	-14.4%
Node 6	Control Delay Per Vehicle			
	EB	WB	NB	SB
Base Case	14.5	25.7	67.2	78.9
10% Penetration Rate	10.7	19.1	61.7	71.9
Differences	-25.9%	-25.6%	-8.1%	-8.9%
25% Penetration Rate	10.2	18.1	60.5	71.4
Differences	-29.7%	-29.7%	-10.0%	-9.6%
50% Penetration Rate	9.1	15.9	58.0	68.3
Differences	-37.3%	-38.3%	-13.7%	-13.5%
60% Penetration Rate	8.7	15.5	57.4	67.6
Differences	-40.2%	-39.9%	-14.6%	-14.3%
70% Penetration Rate	8.4	15.0	56.6	66.7
Differences	-42.3%	-41.8%	-15.7%	-15.4%
Node 7	Control Delay Per Vehicle			
	EB	WB	NB	SB
Base Case	37.8	49.4	75.8	83.4
10% Penetration Rate	27.9	36.6	68.2	74.8
Differences	-26.1%	-25.9%	-10.0%	-10.4%
25% Penetration Rate	27.2	34.3	67.3	73.9
Differences	-28.0%	-30.4%	-11.2%	-11.4%
50% Penetration Rate	23.1	30.3	64.7	70.5
Differences	-39.0%	-38.6%	-14.5%	-15.5%
60% Penetration Rate	22.4	29.1	63.7	69.8
Differences	-40.9%	-41.1%	-15.9%	-16.3%
70% Penetration Rate	21.3	27.3	62.8	68.5
Differences	-43.6%	-44.8%	-17.1%	-17.9%

Table B.7 Control Delay of S1 in different intersections in Base Scenario (Volume Ratio 1.1)

Node 4	Control Delay Per Vehicle			
	EB	WB	NB	SB
Base Case	125.1	69.0	98.6	140.5
10% Penetration Rate	114.7	62.0	97.1	136.4
Differences	-8.3%	-10.2%	-1.6%	-2.9%
25% Penetration Rate	108.2	58.0	95.1	135.4
Differences	-13.5%	-15.9%	-3.6%	-3.6%
50% Penetration Rate	105.9	56.8	95.2	133.2
Differences	-15.4%	-17.7%	-3.4%	-5.2%
60% Penetration Rate	104.7	56.2	95.0	131.9
Differences	-16.3%	-18.5%	-3.7%	-6.1%
70% Penetration Rate	104.2	55.6	94.2	130.1
Differences	-16.7%	-19.4%	-4.4%	-7.4%
Node 5	Control Delay Per Vehicle			
	EB	WB	NB	SB
Base Case	13.3	15.1	101.5	36.4
10% Penetration Rate	11.9	14.0	98.1	35.1
Differences	-10.2%	-7.6%	-3.3%	-3.7%
25% Penetration Rate	11.8	13.7	97.6	35.1
Differences	-11.0%	-9.5%	-3.9%	-3.7%
50% Penetration Rate	11.3	13.0	96.5	34.9
Differences	-14.8%	-13.9%	-5.0%	-4.3%
60% Penetration Rate	11.2	13.0	96.3	34.6
Differences	-15.7%	-14.1%	-5.2%	-5.0%
70% Penetration Rate	10.9	12.7	95.9	34.8
Differences	-17.7%	-16.2%	-5.5%	-4.6%
Node 6	Control Delay Per Vehicle			
	EB	WB	NB	SB
Base Case	15.6	28.8	74.5	85.2
10% Penetration Rate	15.0	26.3	72.0	85.4
Differences	-4.4%	-8.8%	-3.4%	0.3%
25% Penetration Rate	14.6	25.8	72.0	85.1
Differences	-6.5%	-10.4%	-3.4%	-0.1%
50% Penetration Rate	14.3	31.4	71.4	84.3
Differences	-8.4%	-9.0%	-4.2%	-1.1%
60% Penetration Rate	14.1	23.8	71.6	83.7
Differences	-10.0%	-17.3%	-4.0%	-1.7%

Table B.7 Control Delay of S1 in different intersections in Base Scenario (Volume Ratio 1.1) (Continued)

70% Penetration Rate	14.0	23.5	71.6	83.3
Differences	-10.7%	-18.4%	-3.9%	-2.2%
Node 7	Control Delay Per Vehicle			
	EB	WB	NB	SB
Base Case	41.9	53.8	83.3	91.8
10% Penetration Rate	36.9	45.4	81.4	89.5
Differences	-12.0%	-15.7%	-2.4%	-2.5%
25% Penetration Rate	34.8	42.8	80.8	89.4
Differences	-17.0%	-20.5%	-3.0%	-2.6%
50% Penetration Rate	34.3	42.0	80.6	89.0
Differences	-18.2%	-22.0%	-3.3%	-3.0%
60% Penetration Rate	33.7	41.4	80.2	88.3
Differences	-19.7%	-23.1%	-3.8%	-3.8%
70% Penetration Rate	33.5	40.5	80.5	87.9
Differences	-20.1%	-24.8%	-3.5%	-4.2%

Table B.8 Control Delay of S2 in different intersections in Base Scenario (Volume Ratio 1.1)

Node 4	Control Delay Per Vehicle			
	EB	WB	NB	SB
Base Case	125.1	69.0	98.6	140.5
10% Penetration Rate	111.0	59.9	95.8	133.4
Differences	-11.3%	-13.2%	-2.8%	-5.1%
25% Penetration Rate	105.8	56.7	95.4	132.3
Differences	-15.4%	-17.8%	-3.3%	-5.9%
50% Penetration Rate	99.3	52.3	94.3	130.9
Differences	-20.6%	-24.2%	-4.4%	-6.8%
60% Penetration Rate	94.9	49.8	92.8	129.7
Differences	-24.1%	-27.8%	-5.9%	-7.7%
70% Penetration Rate	93.8	51.0	92.0	129.8
Differences	-25.0%	-26.1%	-6.7%	-7.6%
Node 5	Control Delay Per Vehicle			
	EB	WB	NB	SB
Base Case	13.3	15.1	101.5	36.4
10% Penetration Rate	11.7	13.1	97.7	35.0
Differences	-12.1%	-13.7%	-3.7%	-3.9%

Table B.8 Control Delay of S2 in different intersections in Base Scenario (Volume Ratio 1.1) (Continued)

25% Penetration Rate	11.5	12.8	95.9	34.8
Differences	-13.5%	-15.6%	-5.5%	-4.5%
50% Penetration Rate	10.6	12.0	94.9	34.7
Differences	-20.5%	-20.8%	-6.5%	-4.9%
60% Penetration Rate	10.2	11.8	95.5	34.6
Differences	-22.9%	-21.9%	-5.9%	-5.1%
70% Penetration Rate	9.8	11.3	94.6	34.4
Differences	-26.2%	-25.0%	-6.8%	-5.5%
Node 6	Control Delay Per Vehicle			
	EB	WB	NB	SB
Base Case	15.6	28.8	74.5	85.2
10% Penetration Rate	14.2	25.3	72.6	84.5
Differences	-9.3%	-12.3%	-2.6%	-0.9%
25% Penetration Rate	13.7	24.1	71.3	83.1
Differences	-12.6%	-16.3%	-4.4%	-2.5%
50% Penetration Rate	12.8	22.3	70.1	82.5
Differences	-18.5%	-22.5%	-5.9%	-3.2%
60% Penetration Rate	12.7	21.9	69.7	81.7
Differences	-18.5%	-23.8%	-6.5%	-4.1%
70% Penetration Rate	12.2	21.5	70.0	81.5
Differences	-22.3%	-25.3%	-6.1%	-4.4%
Node 7	Control Delay Per Vehicle			
	EB	WB	NB	SB
Base Case	41.9	53.8	83.3	91.8
10% Penetration Rate	36.7	47.9	81.6	89.7
Differences	-12.4%	-11.0%	-2.1%	-2.3%
25% Penetration Rate	34.6	44.4	81.2	88.4
Differences	-17.5%	-17.5%	-2.5%	-3.7%
50% Penetration Rate	32.7	42.8	80.9	88.2
Differences	-22.1%	-20.4%	-2.9%	-3.9%
60% Penetration Rate	31.5	41.0	80.3	86.9
Differences	-24.9%	-23.8%	-3.7%	-5.3%
70% Penetration Rate	31.0	40.6	80.4	87.3
Differences	-26.2%	-24.5%	-3.5%	-4.8%

Table B.9 Control Delay of S3 in different intersections in Base Scenario (Volume Ratio 1.1)

Node 4	Control Delay Per Vehicle			
	EB	WB	NB	SB
Base Case	125.1	69.0	98.6	140.5
10% Penetration Rate	113.3	60.4	95.3	135.2
Differences	-9.4%	-12.5%	-3.3%	-3.8%
25% Penetration Rate	106.9	57.9	94.6	136.1
Differences	-14.5%	-16.0%	-4.0%	-3.1%
50% Penetration Rate	102.1	54.1	94.4	134.7
Differences	-18.4%	-21.5%	-4.3%	-4.1%
60% Penetration Rate	95.7	52.0	93.5	131.7
Differences	-23.5%	-24.7%	-5.2%	-6.3%
70% Penetration Rate	95.0	50.0	93.1	131.4
Differences	-24.1%	-27.5%	-5.6%	-6.5%
Node 5	Control Delay Per Vehicle			
	EB	WB	NB	SB
Base Case	13.3	15.1	101.5	36.4
10% Penetration Rate	11.9	13.4	96.1	34.8
Differences	-10.3%	-11.2%	-5.3%	-4.6%
25% Penetration Rate	11.2	13.1	93.3	34.7
Differences	-15.9%	-13.4%	-8.0%	-4.7%
50% Penetration Rate	10.7	12.3	94.0	34.1
Differences	-19.5%	-18.8%	-7.4%	-6.5%
60% Penetration Rate	10.1	11.6	93.9	34.0
Differences	-23.8%	-23.5%	-7.5%	-6.6%
70% Penetration Rate	10.1	11.5	94.3	34.0
Differences	-23.8%	-24.3%	-7.1%	-6.8%
Node 6	Control Delay Per Vehicle			
	EB	WB	NB	SB
Base Case	15.6	28.8	74.5	85.2
10% Penetration Rate	14.4	25.6	71.6	83.9
Differences	-7.7%	-11.2%	-3.9%	-1.6%
25% Penetration Rate	13.8	24.8	69.8	82.3
Differences	-11.6%	-13.9%	-6.3%	-3.5%
50% Penetration Rate	13.1	23.0	70.2	81.8
Differences	-16.4%	-20.0%	-5.9%	-4.0%
60% Penetration Rate	12.4	21.7	69.8	80.8
Differences	-20.8%	-24.7%	-6.4%	-5.2%

Table B.9 Control Delay of S3 in different intersections in Base Scenario (Volume Ratio 1.1) (Continued)

70% Penetration Rate	12.1	21.3	68.0	79.7
Differences	-22.4%	-26.1%	-8.7%	-6.4%
Node 7	Control Delay Per Vehicle			
	EB	WB	NB	SB
Base Case	41.9	53.8	83.3	91.8
10% Penetration Rate	37.0	48.9	77.2	86.4
Differences	-11.9%	-9.1%	-7.3%	-5.8%
25% Penetration Rate	34.9	45.4	75.7	85.7
Differences	-16.8%	-15.7%	-9.2%	-6.6%
50% Penetration Rate	33.4	44.0	75.8	84.4
Differences	-20.3%	-18.3%	-9.0%	-8.0%
60% Penetration Rate	31.6	41.0	75.7	84.0
Differences	-24.6%	-23.8%	-9.1%	-8.5%
70% Penetration Rate	30.9	40.8	75.6	83.0
Differences	-26.2%	-24.2%	-9.3%	-9.5%

Table B.10 Control Delay of S4 in different intersections in Base Scenario (Volume Ratio 1.1)

Node 4	Control Delay Per Vehicle			
	EB	WB	NB	SB
Base Case	125.1	69.0	98.6	140.5
10% Penetration Rate	110.4	60.1	96.6	136.8
Differences	-11.8%	-12.9%	-2.0%	-2.7%
25% Penetration Rate	101.1	55.2	94.5	134.9
Differences	-19.2%	-19.9%	-4.2%	-4.0%
50% Penetration Rate	93.6	51.0	93.1	133.9
Differences	-25.1%	-26.1%	-5.6%	-4.7%
60% Penetration Rate	90.0	49.0	90.9	132.3
Differences	-28.0%	-29.0%	-7.8%	-5.8%
70% Penetration Rate	90.0	48.5	91.1	126.8
Differences	-28.1%	-29.7%	-7.6%	-9.7%
Node 5	Control Delay Per Vehicle			
	EB	WB	NB	SB
Base Case	13.3	15.1	101.5	36.4
10% Penetration Rate	11.5	13.2	96.2	34.7
Differences	-13.2%	-13.0%	-5.2%	-4.8%

Table B.10 Control Delay of S4 in different intersections in Base Scenario (Volume Ratio 1.1) (Continued)

25% Penetration Rate	10.7	12.3	96.6	34.9
Differences	-19.3%	-18.7%	-4.8%	-4.3%
50% Penetration Rate	9.7	11.2	95.4	34.5
Differences	-26.7%	-25.7%	-6.0%	-5.4%
60% Penetration Rate	9.6	10.7	92.5	34.2
Differences	-27.5%	-29.0%	-8.8%	-6.1%
70% Penetration Rate	9.4	10.7	92.0	33.9
Differences	-29.6%	-29.1%	-9.3%	-7.1%
Node 6	Control Delay Per Vehicle			
	EB	WB	NB	SB
Base Case	15.6	28.8	74.5	85.2
10% Penetration Rate	14.0	24.8	71.7	84.0
Differences	-10.3%	-14.0%	-3.8%	-1.5%
25% Penetration Rate	12.9	23.3	71.1	82.8
Differences	-17.4%	-19.2%	-4.6%	-2.9%
50% Penetration Rate	12.1	21.7	69.7	82.3
Differences	-22.6%	-24.7%	-6.5%	-3.4%
60% Penetration Rate	11.5	20.8	69.8	81.5
Differences	-26.4%	-27.8%	-6.4%	-4.4%
70% Penetration Rate	11.5	20.2	68.8	80.7
Differences	-26.5%	-30.0%	-7.8%	-5.3%
Node 7	Control Delay Per Vehicle			
	EB	WB	NB	SB
Base Case	41.9	53.8	83.3	91.8
10% Penetration Rate	36.5	47.3	77.7	87.4
Differences	-13.0%	-12.1%	-6.8%	-4.8%
25% Penetration Rate	33.3	43.4	77.8	85.8
Differences	-20.6%	-19.4%	-6.7%	-6.5%
50% Penetration Rate	30.6	40.1	76.9	84.9
Differences	-27.2%	-25.5%	-7.7%	-7.5%
60% Penetration Rate	30.0	39.3	75.6	83.9
Differences	-28.5%	-27.0%	-9.3%	-8.5%
70% Penetration Rate	29.3	38.5	75.7	83.8
Differences	-30.2%	-28.5%	-9.2%	-8.7%

Table B.11 Control Delay of S5 in different intersections in Base Scenario (Volume Ratio 1.1)

Node 4	Control Delay Per Vehicle			
	EB	WB	NB	SB
Base Case	125.1	69.0	98.6	140.5
10% Penetration Rate	106.2	57.1	92.0	131.1
Differences	-15.1%	-17.2%	-6.7%	-6.7%
25% Penetration Rate	99.3	54.1	91.6	132.2
Differences	-20.6%	-21.5%	-7.1%	-5.9%
50% Penetration Rate	90.2	49.4	90.6	129.0
Differences	-27.9%	-28.4%	-8.1%	-8.2%
60% Penetration Rate	87.1	45.8	88.7	126.5
Differences	-30.4%	-33.6%	-10.0%	-10.0%
70% Penetration Rate	84.6	45.0	88.1	124.5
Differences	-32.3%	-34.8%	-10.6%	-11.4%
Node 5	Control Delay Per Vehicle			
	EB	WB	NB	SB
Base Case	13.3	15.1	101.5	36.4
10% Penetration Rate	11.0	12.8	93.4	37.9
Differences	-16.9%	-15.7%	-7.9%	3.9%
25% Penetration Rate	10.5	11.9	92.1	34.5
Differences	-21.3%	-21.1%	-9.2%	-5.3%
50% Penetration Rate	9.6	10.9	92.2	33.6
Differences	-28.1%	-27.8%	-9.1%	-7.9%
60% Penetration Rate	9.0	10.6	92.0	33.2
Differences	-32.6%	-30.3%	-9.4%	-9.0%
70% Penetration Rate	8.9	10.3	91.1	32.5
Differences	-33.0%	-32.3%	-10.2%	-10.7%
Node 6	Control Delay Per Vehicle			
	EB	WB	NB	SB
Base Case	15.6	28.8	74.5	85.2
10% Penetration Rate	13.6	24.2	71.1	83.1
Differences	-13.2%	-16.0%	-4.6%	-2.5%
25% Penetration Rate	12.8	22.8	70.4	82.1
Differences	-18.4%	-20.8%	-5.6%	-3.7%
50% Penetration Rate	11.7	20.4	69.7	80.4
Differences	-24.9%	-29.0%	-6.5%	-5.7%
60% Penetration Rate	11.3	20.0	68.2	80.1
Differences	-28.0%	-30.5%	-8.5%	-6.1%

Table B.11 Control Delay of S5 in different intersections in Base Scenario (Volume Ratio 1.1) (Continued)

70% Penetration Rate	10.9	19.8	68.1	79.6
Differences	-30.5%	-31.1%	-8.7%	-6.6%
Node 7	Control Delay Per Vehicle			
	EB	WB	NB	SB
Base Case	41.9	53.8	83.3	91.8
10% Penetration Rate	34.9	45.4	79.2	87.3
Differences	-16.8%	-15.6%	-4.9%	-4.9%
25% Penetration Rate	33.4	42.4	78.6	84.7
Differences	-20.5%	-21.3%	-5.7%	-7.7%
50% Penetration Rate	29.5	39.1	75.1	83.4
Differences	-29.6%	-27.3%	-9.9%	-9.1%
60% Penetration Rate	28.2	36.8	74.9	81.8
Differences	-32.7%	-31.6%	-10.1%	-10.8%
70% Penetration Rate	27.2	35.5	74.7	81.3
Differences	-35.2%	-34.1%	-10.3%	-11.4%

Table B.12 Control Delay of S6 in different intersections in Base Scenario (Volume Ratio 1.1)

Node 4	Control Delay Per Vehicle			
	EB	WB	NB	SB
Base Case	125.1	69.0	98.6	140.5
10% Penetration Rate	95.2	50.8	86.9	125.9
Differences	-23.9%	-26.4%	-11.9%	-10.4%
25% Penetration Rate	89.2	49.4	87.7	123.0
Differences	-28.7%	-28.4%	-11.1%	-12.5%
50% Penetration Rate	75.1	41.1	83.3	117.5
Differences	-40.0%	-40.5%	-15.6%	-16.4%
60% Penetration Rate	73.5	39.7	82.6	116.8
Differences	-41.3%	-42.5%	-16.3%	-16.9%
70% Penetration Rate	73.0	38.7	80.1	115.4
Differences	-41.7%	-44.0%	-18.7%	-17.8%
Node 5	Control Delay Per Vehicle			
	EB	WB	NB	SB
Base Case	13.3	15.1	101.5	36.4
10% Penetration Rate	9.7	11.0	92.6	32.9
Differences	-27.0%	-27.4%	-8.8%	-9.7%

Table B.12 Control Delay of S6 in different intersections in Base Scenario (Volume Ratio 1.1) (Continued)

25% Penetration Rate	9.1	10.5	89.8	32.7
Differences	-31.2%	-30.6%	-11.5%	-10.4%
50% Penetration Rate	8.0	9.7	87.5	31.5
Differences	-39.8%	-35.9%	-13.8%	-13.7%
60% Penetration Rate	7.8	9.2	87.2	30.4
Differences	-41.3%	-39.1%	-14.1%	-16.6%
70% Penetration Rate	7.4	8.6	84.6	30.0
Differences	-44.6%	-43.0%	-16.7%	-17.6%
Node 6	Control Delay Per Vehicle			
	EB	WB	NB	SB
Base Case	15.6	28.8	74.5	85.2
10% Penetration Rate	11.6	20.7	67.9	79.8
Differences	-25.9%	-28.3%	-8.9%	-6.4%
25% Penetration Rate	11.0	20.1	65.9	79.2
Differences	-29.7%	-30.3%	-11.6%	-7.1%
50% Penetration Rate	10.2	17.8	62.6	75.7
Differences	-35.0%	-38.3%	-16.0%	-11.1%
60% Penetration Rate	9.4	16.9	62.5	75.1
Differences	-39.6%	-41.5%	-16.1%	-11.9%
70% Penetration Rate	9.0	16.2	62.1	74.7
Differences	-42.3%	-43.8%	-16.7%	-12.3%
Node 7	Control Delay Per Vehicle			
	EB	WB	NB	SB
Base Case	41.9	53.8	83.3	91.8
10% Penetration Rate	30.2	40.6	75.0	81.5
Differences	-28.1%	-24.6%	-10.0%	-11.2%
25% Penetration Rate	30.2	37.1	73.4	80.6
Differences	-28.0%	-31.1%	-12.0%	-12.2%
50% Penetration Rate	25.1	33.6	72.5	76.1
Differences	-40.1%	-37.5%	-13.0%	-17.1%
60% Penetration Rate	24.4	32.0	70.1	74.2
Differences	-41.9%	-40.5%	-15.9%	-19.1%
70% Penetration Rate	23.9	29.5	67.8	73.0
Differences	-43.1%	-45.3%	-18.7%	-20.5%

Table B.13 Control Delay of S1 in different intersections in Base Scenario (Volume Ratio 1.2)

Node 4	Control Delay Per Vehicle			
	EB	WB	NB	SB
Base Case	137.7	73.3	109.4	151.9
10% Penetration Rate	125.3	67.7	105.3	148.6
Differences	-9.0%	-7.7%	-3.7%	-2.2%
25% Penetration Rate	117.8	63.3	103.8	147.0
Differences	-14.5%	-13.6%	-5.1%	-3.2%
50% Penetration Rate	115.2	61.8	103.4	145.5
Differences	-16.3%	-15.8%	-5.5%	-4.2%
60% Penetration Rate	114.6	61.3	103.6	143.9
Differences	-16.8%	-16.4%	-5.3%	-5.3%
70% Penetration Rate	114.0	60.6	103.0	142.3
Differences	-17.2%	-17.3%	-5.8%	-6.3%
Node 5	Control Delay Per Vehicle			
	EB	WB	NB	SB
Base Case	14.4	16.4	107.8	39.4
10% Penetration Rate	13.0	15.2	106.7	38.4
Differences	-9.2%	-6.9%	-1.0%	-2.5%
25% Penetration Rate	12.8	14.9	105.8	38.4
Differences	-10.6%	-8.8%	-1.9%	-2.6%
50% Penetration Rate	12.3	14.2	105.1	38.3
Differences	-14.0%	-13.1%	-2.5%	-2.7%
60% Penetration Rate	12.2	14.1	104.8	37.9
Differences	-14.9%	-13.8%	-2.8%	-3.8%
70% Penetration Rate	11.9	13.9	104.4	37.8
Differences	-16.9%	-15.1%	-3.2%	-4.1%
Node 6	Control Delay Per Vehicle			
	EB	WB	NB	SB
Base Case	17.2	31.1	79.2	96.3
10% Penetration Rate	16.3	28.6	79.0	93.2
Differences	-5.4%	-8.1%	-0.4%	-3.2%
25% Penetration Rate	15.9	28.2	78.6	92.7
Differences	-7.6%	-9.2%	-0.9%	-3.7%
50% Penetration Rate	15.7	34.1	78.2	92.2
Differences	-8.7%	-9.5%	-1.3%	-4.3%
60% Penetration Rate	15.4	26.0	78.2	91.6
Differences	-10.9%	-16.5%	-1.3%	-4.9%

Table B.13 Control Delay of S1 in different intersections in Base Scenario (Volume Ratio 1.2) (Continued)

70% Penetration Rate	15.2	25.7	77.9	91.3
Differences	-12.1%	-17.4%	-1.7%	-5.2%
Node 7	Control Delay Per Vehicle			
	EB	WB	NB	SB
Base Case	44.6	58.8	90.9	101.8
10% Penetration Rate	40.1	49.2	88.3	97.7
Differences	-10.0%	-16.3%	-2.9%	-4.0%
25% Penetration Rate	37.9	46.3	88.9	97.3
Differences	-15.0%	-21.1%	-2.2%	-4.4%
50% Penetration Rate	37.3	45.7	88.1	96.3
Differences	-16.4%	-22.2%	-3.1%	-5.4%
60% Penetration Rate	36.8	45.2	87.9	96.8
Differences	-17.4%	-23.0%	-3.3%	-4.9%
70% Penetration Rate	36.4	44.3	87.4	95.7
Differences	-18.3%	-24.6%	-3.9%	-5.9%

Table B.14 Control Delay of S2 in different intersections in Base Scenario (Volume Ratio 1.2)

Node 4	Control Delay Per Vehicle			
	EB	WB	NB	SB
Base Case	137.7	73.3	109.4	151.9
10% Penetration Rate	121.8	65.7	105.0	146.0
Differences	-11.6%	-10.4%	-4.0%	-3.9%
25% Penetration Rate	115.6	61.7	103.4	144.1
Differences	-16.1%	-15.8%	-5.5%	-5.1%
50% Penetration Rate	108.2	57.0	102.2	143.1
Differences	-21.5%	-22.3%	-6.5%	-5.8%
60% Penetration Rate	103.8	54.3	100.8	142.1
Differences	-24.7%	-25.9%	-7.8%	-6.5%
70% Penetration Rate	103.0	55.4	100.8	142.0
Differences	-25.2%	-24.4%	-7.8%	-6.5%
Node 5	Control Delay Per Vehicle			
	EB	WB	NB	SB
Base Case	14.4	16.4	107.8	39.4
10% Penetration Rate	12.7	14.2	106.3	38.3
Differences	-11.4%	-13.0%	-1.4%	-2.7%

Table B.14 Control Delay of S2 in different intersections in Base Scenario (Volume Ratio 1.2) (Continued)

25% Penetration Rate	12.6	14.0	104.3	38.0
Differences	-12.5%	-14.5%	-3.2%	-3.6%
50% Penetration Rate	11.5	13.1	104.1	37.8
Differences	-19.7%	-19.9%	-3.5%	-4.0%
60% Penetration Rate	11.1	12.9	103.6	37.8
Differences	-22.8%	-21.3%	-3.9%	-3.9%
70% Penetration Rate	10.6	12.3	102.9	37.5
Differences	-26.0%	-24.8%	-4.6%	-4.7%
Node 6	Control Delay Per Vehicle			
	EB	WB	NB	SB
Base Case	17.2	31.1	79.2	96.3
10% Penetration Rate	15.5	27.3	79.0	92.5
Differences	-10.3%	-12.2%	-0.3%	-3.9%
25% Penetration Rate	14.9	26.3	78.1	90.3
Differences	-13.3%	-15.5%	-1.4%	-6.2%
50% Penetration Rate	14.0	24.3	76.6	89.9
Differences	-19.1%	-21.9%	-3.4%	-6.6%
60% Penetration Rate	13.9	24.1	76.2	89.3
Differences	-19.5%	-22.6%	-3.9%	-7.3%
70% Penetration Rate	13.3	23.3	76.8	88.8
Differences	-22.6%	-25.0%	-3.1%	-7.8%
Node 7	Control Delay Per Vehicle			
	EB	WB	NB	SB
Base Case	44.6	58.8	90.9	101.8
10% Penetration Rate	39.8	52.7	89.2	98.3
Differences	-10.7%	-10.3%	-1.8%	-3.4%
25% Penetration Rate	37.7	48.8	88.7	96.5
Differences	-15.5%	-17.0%	-2.4%	-5.1%
50% Penetration Rate	35.9	46.9	88.0	95.9
Differences	-19.6%	-20.2%	-3.2%	-5.8%
60% Penetration Rate	34.2	44.6	87.8	94.6
Differences	-23.2%	-24.0%	-3.5%	-7.1%
70% Penetration Rate	33.8	44.1	87.5	95.2
Differences	-24.3%	-25.0%	-3.7%	-6.5%

Table B.15 Control Delay of S3 in different intersections in Base Scenario (Volume Ratio 1.2)

Node 4	Control Delay Per Vehicle			
	EB	WB	NB	SB
Base Case	137.7	73.3	109.4	151.9
10% Penetration Rate	122.6	66.2	104.4	147.9
Differences	-11.0%	-9.7%	-4.5%	-2.7%
25% Penetration Rate	116.4	62.9	103.2	148.3
Differences	-15.5%	-14.2%	-5.6%	-2.4%
50% Penetration Rate	110.5	58.8	103.0	146.8
Differences	-19.7%	-19.8%	-5.9%	-3.3%
60% Penetration Rate	104.1	56.2	102.2	143.6
Differences	-24.4%	-23.3%	-6.6%	-5.5%
70% Penetration Rate	103.0	54.2	101.5	143.5
Differences	-25.2%	-26.0%	-7.2%	-5.5%
Node 5	Control Delay Per Vehicle			
	EB	WB	NB	SB
Base Case	14.4	16.4	107.8	39.4
10% Penetration Rate	13.0	14.7	104.3	37.7
Differences	-9.6%	-10.2%	-3.2%	-4.2%
25% Penetration Rate	12.2	14.3	102.2	37.9
Differences	-15.0%	-12.7%	-5.2%	-3.8%
50% Penetration Rate	11.7	13.3	102.6	37.5
Differences	-18.5%	-18.7%	-4.9%	-4.8%
60% Penetration Rate	11.0	12.6	102.4	37.2
Differences	-23.5%	-22.7%	-5.0%	-5.5%
70% Penetration Rate	11.1	12.5	102.3	37.1
Differences	-23.0%	-23.6%	-5.1%	-5.7%
Node 6	Control Delay Per Vehicle			
	EB	WB	NB	SB
Base Case	17.2	31.1	79.2	96.3
10% Penetration Rate	15.6	28.1	78.0	91.6
Differences	-9.3%	-9.6%	-1.6%	-4.9%
25% Penetration Rate	15.0	27.1	76.4	89.0
Differences	-13.0%	-13.0%	-3.6%	-7.5%
50% Penetration Rate	14.2	25.1	75.9	88.9
Differences	-17.3%	-19.4%	-4.2%	-7.6%
60% Penetration Rate	13.5	23.7	75.8	89.0
Differences	-21.8%	-24.0%	-4.3%	-7.6%

Table B.15 Control Delay of S3 in different intersections in Base Scenario (Volume Ratio 1.2) (Continued)

70% Penetration Rate	13.2	23.2	74.8	87.5
Differences	-23.3%	-25.4%	-5.7%	-9.2%
Node 7	Control Delay Per Vehicle			
	EB	WB	NB	SB
Base Case	44.6	58.8	90.9	101.8
10% Penetration Rate	40.2	53.3	84.3	94.4
Differences	-9.9%	-9.3%	-7.3%	-7.3%
25% Penetration Rate	38.2	49.6	83.2	93.2
Differences	-14.4%	-15.5%	-8.5%	-8.4%
50% Penetration Rate	36.5	47.7	82.7	92.1
Differences	-18.2%	-18.8%	-9.0%	-9.5%
60% Penetration Rate	34.3	44.7	82.3	91.5
Differences	-23.2%	-23.9%	-9.4%	-10.1%
70% Penetration Rate	33.6	44.2	82.2	90.3
Differences	-24.5%	-24.8%	-9.6%	-11.3%

Table B.16 Control Delay of S4 in different intersections in Base Scenario (Volume Ratio 1.2)

Node 4	Control Delay Per Vehicle			
	EB	WB	NB	SB
Base Case	137.7	73.3	109.4	151.9
10% Penetration Rate	121.8	64.6	105.6	148.0
Differences	-11.5%	-11.9%	-3.4%	-2.6%
25% Penetration Rate	110.3	60.0	103.4	148.0
Differences	-19.9%	-18.1%	-5.5%	-2.6%
50% Penetration Rate	101.5	55.6	101.8	145.5
Differences	-26.3%	-24.1%	-6.9%	-4.2%
60% Penetration Rate	98.9	54.0	100.4	143.7
Differences	-28.2%	-26.3%	-8.2%	-5.4%
70% Penetration Rate	97.2	53.1	99.1	139.0
Differences	-29.4%	-27.6%	-9.3%	-8.5%
Node 5	Control Delay Per Vehicle			
	EB	WB	NB	SB
Base Case	14.4	16.4	107.8	39.4
10% Penetration Rate	12.6	14.4	105.4	38.0
Differences	-12.3%	-12.1%	-2.3%	-3.6%

Table B.16 Control Delay of S4 in different intersections in Base Scenario (Volume Ratio 1.2) (Continued)

25% Penetration Rate	11.6	13.4	104.7	37.8
Differences	-19.1%	-17.8%	-2.9%	-4.0%
50% Penetration Rate	10.5	12.4	102.8	37.3
Differences	-26.6%	-24.1%	-4.6%	-5.2%
60% Penetration Rate	10.4	11.8	101.6	36.9
Differences	-27.5%	-28.1%	-5.7%	-6.3%
70% Penetration Rate	10.3	11.6	101.4	36.5
Differences	-28.3%	-28.8%	-6.0%	-7.4%
Node 6	Control Delay Per Vehicle			
	EB	WB	NB	SB
Base Case	17.2	31.1	79.2	96.3
10% Penetration Rate	15.2	27.5	78.2	92.3
Differences	-11.7%	-11.6%	-1.3%	-4.2%
25% Penetration Rate	14.1	25.3	77.8	90.2
Differences	-18.2%	-18.7%	-1.8%	-6.3%
50% Penetration Rate	13.1	23.6	76.0	89.6
Differences	-24.1%	-24.1%	-4.2%	-6.9%
60% Penetration Rate	12.6	22.8	76.4	90.2
Differences	-27.0%	-26.6%	-3.6%	-6.3%
70% Penetration Rate	12.4	22.1	75.4	88.9
Differences	-27.9%	-29.1%	-4.9%	-7.6%
Node 7	Control Delay Per Vehicle			
	EB	WB	NB	SB
Base Case	44.6	58.8	90.9	101.8
10% Penetration Rate	39.5	51.8	85.8	95.4
Differences	-11.5%	-11.8%	-5.6%	-6.3%
25% Penetration Rate	36.3	48.0	85.7	93.7
Differences	-18.5%	-18.3%	-5.8%	-7.9%
50% Penetration Rate	33.6	43.6	84.1	93.8
Differences	-24.6%	-25.8%	-7.5%	-7.8%
60% Penetration Rate	32.7	43.3	82.2	91.9
Differences	-26.7%	-26.4%	-9.5%	-9.7%
70% Penetration Rate	32.1	42.0	82.6	91.6
Differences	-28.1%	-28.5%	-9.2%	-10.0%

Table B.17 Control Delay of S5 in different intersections in Base Scenario (Volume Ratio 1.2)

Node 4	Control Delay Per Vehicle			
	EB	WB	NB	SB
Base Case	137.7	73.3	109.4	151.9
10% Penetration Rate	116.0	62.8	102.3	142.9
Differences	-15.8%	-14.3%	-6.5%	-5.9%
25% Penetration Rate	110.4	59.4	101.1	145.1
Differences	-19.8%	-19.0%	-7.5%	-4.5%
50% Penetration Rate	98.6	53.9	99.4	141.5
Differences	-28.4%	-26.4%	-9.1%	-6.9%
60% Penetration Rate	94.3	50.3	97.6	138.9
Differences	-31.5%	-31.4%	-10.7%	-8.6%
70% Penetration Rate	92.3	49.2	96.5	136.2
Differences	-33.0%	-32.9%	-11.8%	-10.3%
Node 5	Control Delay Per Vehicle			
	EB	WB	NB	SB
Base Case	14.4	16.4	107.8	39.4
10% Penetration Rate	12.2	13.9	103.0	41.5
Differences	-15.2%	-15.0%	-4.5%	5.5%
25% Penetration Rate	11.6	13.0	102.2	36.8
Differences	-19.5%	-20.3%	-5.2%	-6.5%
50% Penetration Rate	10.4	12.0	101.1	36.5
Differences	-27.7%	-26.9%	-6.3%	-7.2%
60% Penetration Rate	9.9	11.6	100.0	36.2
Differences	-31.2%	-29.1%	-7.2%	-8.0%
70% Penetration Rate	9.7	11.2	100.3	36.0
Differences	-32.1%	-31.5%	-7.0%	-8.5%
Node 6	Control Delay Per Vehicle			
	EB	WB	NB	SB
Base Case	17.2	31.1	79.2	96.3
10% Penetration Rate	14.9	26.3	76.8	91.1
Differences	-13.5%	-15.3%	-3.1%	-5.4%
25% Penetration Rate	14.1	25.0	77.5	89.3
Differences	-18.2%	-19.7%	-2.3%	-7.3%
50% Penetration Rate	13.0	22.6	76.1	88.8
Differences	-24.9%	-27.5%	-3.9%	-7.8%
60% Penetration Rate	12.3	21.8	74.0	86.9
Differences	-28.5%	-29.8%	-6.7%	-9.7%

Table B.17 Control Delay of S5 in different intersections in Base Scenario (Volume Ratio 1.2) (Continued)

70% Penetration Rate	11.9	21.7	73.5	87.2
Differences	-31.0%	-30.2%	-7.2%	-9.4%
Node 7	Control Delay Per Vehicle			
	EB	WB	NB	SB
Base Case	44.6	58.8	90.9	101.8
10% Penetration Rate	38.4	49.9	88.0	95.0
Differences	-13.9%	-15.1%	-3.2%	-6.6%
25% Penetration Rate	36.4	46.4	85.9	92.1
Differences	-18.4%	-21.1%	-5.5%	-9.6%
50% Penetration Rate	32.7	42.9	82.1	90.3
Differences	-26.6%	-26.9%	-9.7%	-11.3%
60% Penetration Rate	31.1	40.3	82.7	90.0
Differences	-30.2%	-31.5%	-9.0%	-11.5%
70% Penetration Rate	29.5	39.3	80.8	89.6
Differences	-33.9%	-33.2%	-11.1%	-12.0%

Table B.18 Control Delay of S6 in different intersections in Base Scenario (Volume Ratio 1.2)

Node 4	Control Delay Per Vehicle			
	EB	WB	NB	SB
Base Case	137.7	73.3	109.4	151.9
10% Penetration Rate	100.3	55.4	95.7	138.4
Differences	-27.1%	-24.5%	-12.5%	-8.9%
25% Penetration Rate	97.2	53.3	94.1	135.3
Differences	-29.4%	-27.3%	-14.0%	-10.9%
50% Penetration Rate	84.0	46.0	92.4	128.2
Differences	-39.0%	-37.3%	-15.5%	-15.6%
60% Penetration Rate	81.5	44.1	91.4	129.4
Differences	-40.8%	-39.9%	-16.4%	-14.8%
70% Penetration Rate	81.7	43.3	89.0	123.8
Differences	-40.7%	-41.0%	-18.6%	-18.5%
Node 5	Control Delay Per Vehicle			
	EB	WB	NB	SB
Base Case	14.4	16.4	107.8	39.4
10% Penetration Rate	10.7	11.9	99.2	35.3
Differences	-25.6%	-27.4%	-8.0%	-10.3%

Table B.18 Control Delay of S6 in different intersections in Base Scenario (Volume Ratio 1.2) (Continued)

25% Penetration Rate	9.9	11.5	98.0	35.0
Differences	-31.1%	-29.8%	-9.1%	-11.1%
50% Penetration Rate	8.7	10.6	95.4	34.3
Differences	-39.1%	-35.4%	-11.5%	-12.9%
60% Penetration Rate	8.8	9.8	92.7	33.5
Differences	-38.7%	-40.1%	-14.0%	-14.9%
70% Penetration Rate	7.9	9.4	92.4	33.4
Differences	-45.0%	-42.5%	-14.3%	-15.1%
Node 6	Control Delay Per Vehicle			
	EB	WB	NB	SB
Base Case	17.2	31.1	79.2	96.3
10% Penetration Rate	12.7	23.3	75.3	87.7
Differences	-26.5%	-25.0%	-5.0%	-8.9%
25% Penetration Rate	12.4	21.3	71.9	84.9
Differences	-27.9%	-31.4%	-9.2%	-11.8%
50% Penetration Rate	10.7	19.4	70.1	80.6
Differences	-37.8%	-37.8%	-11.5%	-16.3%
60% Penetration Rate	10.2	18.2	68.9	80.5
Differences	-40.7%	-41.3%	-13.1%	-16.4%
70% Penetration Rate	10.1	18.0	68.5	78.7
Differences	-41.3%	-42.2%	-13.5%	-18.2%
Node 7	Control Delay Per Vehicle			
	EB	WB	NB	SB
Base Case	44.6	58.8	90.9	101.8
10% Penetration Rate	33.5	43.1	82.5	90.5
Differences	-24.8%	-26.6%	-9.3%	-11.1%
25% Penetration Rate	32.9	41.6	80.1	87.9
Differences	-26.2%	-29.3%	-11.9%	-13.6%
50% Penetration Rate	27.9	35.7	78.3	84.5
Differences	-37.4%	-39.2%	-13.8%	-16.9%
60% Penetration Rate	27.3	35.5	77.8	83.2
Differences	-38.9%	-39.6%	-14.5%	-18.3%
70% Penetration Rate	25.1	33.3	75.9	82.9
Differences	-43.6%	-43.4%	-16.5%	-18.6%

Table B.19 Control Delay of S1 in different intersections in Base Scenario (Volume Ratio 0.8)

Node 4	Control Delay Per Vehicle			
	EB	WB	NB	SB
Base Case	92.96235	49.08533	72.60638	101.264
10% Penetration Rate	83.02632	45.18815	70.53933	99.24615
Differences	-10.7%	-7.9%	-2.8%	-2.0%
25% Penetration Rate	78.67018	41.98438	68.97217	97.61404
Differences	-15.4%	-14.5%	-5.0%	-3.6%
50% Penetration Rate	76.8293	40.89495	68.75784	97.26086
Differences	-17.4%	-16.7%	-5.3%	-4.0%
60% Penetration Rate	76.39979	40.90583	68.64804	96.38428
Differences	-17.8%	-16.7%	-5.5%	-4.8%
70% Penetration Rate	76.07453	40.18473	68.26122	95.00991
Differences	-18.2%	-18.1%	-6.0%	-6.2%
Node 5	Control Delay Per Vehicle			
	EB	WB	NB	SB
Base Case	9.494	11.043	73.39815	26.35943
10% Penetration Rate	8.735693	10.17923	71.03491	25.39093
Differences	-8.0%	-7.8%	-3.2%	-3.7%
25% Penetration Rate	8.59189	9.933865	70.20517	25.58286
Differences	-9.5%	-10.0%	-4.4%	-2.9%
50% Penetration Rate	8.247871	9.549562	70.41357	25.46441
Differences	-13.1%	-13.5%	-4.1%	-3.4%
60% Penetration Rate	8.075128	9.42792	69.86078	25.25522
Differences	-14.9%	-14.6%	-4.8%	-4.2%
70% Penetration Rate	7.903883	9.22069	69.4328	25.13457
Differences	-16.7%	-16.5%	-5.4%	-4.6%
Node 6	Control Delay Per Vehicle			
	EB	WB	NB	SB
Base Case	11.44315	20.8251	53.728	63.9171
10% Penetration Rate	10.8832	19.06061	52.5286	61.93708
Differences	-4.9%	-8.5%	-2.2%	-3.1%
25% Penetration Rate	10.57365	18.72959	52.55185	61.85428
Differences	-7.6%	-10.1%	-2.2%	-3.2%
50% Penetration Rate	10.49532	22.77415	52.12077	61.08863
Differences	-8.3%	-9.4%	-3.0%	-4.4%
60% Penetration Rate	10.27632	17.47595	51.85649	60.57542
Differences	-10.2%	-16.1%	-3.5%	-5.2%

Table B.19 Control Delay of S1 in different intersections in Base Scenario (Volume Ratio 0.8) (Continued)

70% Penetration Rate	10.11993	17.10672	52.25807	60.69105
Differences	-11.6%	-17.9%	-2.7%	-5.0%
Node 7	Control Delay Per Vehicle			
	EB	WB	NB	SB
Base Case	30.61125	39.99173	59.84843	65.9097
10% Penetration Rate	26.83208	32.83534	58.69744	65.50824
Differences	-12.3%	-17.9%	-1.9%	-0.6%
25% Penetration Rate	25.38088	31.02173	59.06661	64.83597
Differences	-17.1%	-22.4%	-1.3%	-1.6%
50% Penetration Rate	24.89622	30.27711	58.84973	64.74342
Differences	-18.7%	-24.3%	-1.7%	-1.8%
60% Penetration Rate	24.47114	29.92165	58.21562	64.44854
Differences	-20.1%	-25.2%	-2.7%	-2.2%
70% Penetration Rate	24.1707	29.37214	58.09517	63.84726
Differences	-21.0%	-26.6%	-2.9%	-3.1%

Table B.20 Control Delay of S2 in different intersections in Base Scenario (Volume Ratio 0.8)

Node 4	Control Delay Per Vehicle			
	EB	WB	NB	SB
Base Case	92.96235	49.08533	72.60638	101.264
10% Penetration Rate	82.53965	43.34993	70.39753	97.22293
Differences	-11.2%	-11.7%	-3.0%	-4.0%
25% Penetration Rate	77.13979	41.25312	68.92701	96.21283
Differences	-17.0%	-16.0%	-5.1%	-5.0%
50% Penetration Rate	72.38166	37.6689	68.48172	95.15506
Differences	-22.1%	-23.3%	-5.7%	-6.0%
60% Penetration Rate	69.14013	36.24232	67.70337	94.1782
Differences	-25.6%	-26.2%	-6.8%	-7.0%
70% Penetration Rate	68.70451	37.2129	67.5112	94.78279
Differences	-26.1%	-24.2%	-7.0%	-6.4%
Node 5	Control Delay Per Vehicle			
	EB	WB	NB	SB
Base Case	9.494	11.043	73.39815	26.35943
10% Penetration Rate	8.512662	9.513001	70.48687	25.37355
Differences	-10.3%	-13.9%	-4.0%	-3.7%

Table B.20 Control Delay of S2 in different intersections in Base Scenario (Volume Ratio 0.8) (Continued)

25% Penetration Rate	8.399877	9.238096	69.4095	25.44487
Differences	-11.5%	-16.3%	-5.4%	-3.5%
50% Penetration Rate	7.739276	8.738987	69.77926	25.36093
Differences	-18.5%	-20.9%	-4.9%	-3.8%
60% Penetration Rate	7.453769	8.567187	68.80438	25.20872
Differences	-21.5%	-22.4%	-6.3%	-4.4%
70% Penetration Rate	7.126549	8.170571	68.66315	24.96392
Differences	-24.9%	-26.0%	-6.5%	-5.3%
Node 6	Control Delay Per Vehicle			
	EB	WB	NB	SB
Base Case	11.44315	20.8251	53.728	63.9171
10% Penetration Rate	10.35174	18.26415	52.66419	61.81759
Differences	-9.5%	-12.3%	-2.0%	-3.3%
25% Penetration Rate	9.943078	17.57741	51.78074	60.31906
Differences	-13.1%	-15.6%	-3.6%	-5.6%
50% Penetration Rate	9.312154	16.20811	50.94119	60.26955
Differences	-18.6%	-22.2%	-5.2%	-5.7%
60% Penetration Rate	9.229885	15.97562	50.45029	59.62552
Differences	-19.3%	-23.3%	-6.1%	-6.7%
70% Penetration Rate	8.906205	15.54642	51.13768	59.05618
Differences	-22.2%	-25.3%	-4.8%	-7.6%
Node 7	Control Delay Per Vehicle			
	EB	WB	NB	SB
Base Case	30.61125	39.99173	59.84843	65.9097
10% Penetration Rate	27.00831	34.93176	59.86267	65.6477
Differences	-11.8%	-12.7%	0.0%	-0.4%
25% Penetration Rate	25.16018	32.55824	58.82392	64.50077
Differences	-17.8%	-18.6%	-1.7%	-2.1%
50% Penetration Rate	23.82489	31.13148	58.6417	63.55464
Differences	-22.2%	-22.2%	-2.0%	-3.6%
60% Penetration Rate	22.96942	29.81294	58.3588	63.29767
Differences	-25.0%	-25.5%	-2.5%	-4.0%
70% Penetration Rate	22.38817	29.44971	57.95718	63.57758
Differences	-26.9%	-26.4%	-3.2%	-3.5%

Table B.21 Control Delay of S3 in different intersections in Base Scenario (Volume Ratio 0.8)

Node 4	Control Delay Per Vehicle			
	EB	WB	NB	SB
Base Case	92.96235	49.08533	72.60638	101.264
10% Penetration Rate	81.74934	44.28832	69.76912	98.45526
Differences	-12.1%	-9.8%	-3.9%	-2.8%
25% Penetration Rate	78.24179	41.99989	69.08992	98.80015
Differences	-15.8%	-14.4%	-4.8%	-2.4%
50% Penetration Rate	74.1149	39.19529	68.1529	98.0882
Differences	-20.3%	-20.1%	-6.1%	-3.1%
60% Penetration Rate	69.23724	37.51375	68.54884	96.53792
Differences	-25.5%	-23.6%	-5.6%	-4.7%
70% Penetration Rate	68.749	36.49921	67.47434	95.1468
Differences	-26.0%	-25.6%	-7.1%	-6.0%
Node 5	Control Delay Per Vehicle			
	EB	WB	NB	SB
Base Case	9.494	11.043	73.39815	26.35943
10% Penetration Rate	8.672013	9.707503	69.857	25.32916
Differences	-8.7%	-12.1%	-4.8%	-3.9%
25% Penetration Rate	8.167569	9.520763	68.60572	25.19831
Differences	-14.0%	-13.8%	-6.5%	-4.4%
50% Penetration Rate	7.830509	8.964794	68.67372	25.00013
Differences	-17.5%	-18.8%	-6.4%	-5.2%
60% Penetration Rate	7.339783	8.431646	68.19382	24.92617
Differences	-22.7%	-23.6%	-7.1%	-5.4%
70% Penetration Rate	7.31535	8.328865	67.85827	24.5273
Differences	-22.9%	-24.6%	-7.5%	-7.0%
Node 6	Control Delay Per Vehicle			
	EB	WB	NB	SB
Base Case	11.44315	20.8251	53.728	63.9171
10% Penetration Rate	10.41735	18.7313	51.54112	61.06342
Differences	-9.0%	-10.1%	-4.1%	-4.5%
25% Penetration Rate	9.991742	17.93671	51.15502	59.9862
Differences	-12.7%	-13.9%	-4.8%	-6.1%
50% Penetration Rate	9.409226	16.82373	50.67346	59.22219
Differences	-17.8%	-19.2%	-5.7%	-7.3%
60% Penetration Rate	8.939681	15.91746	50.24071	59.42992
Differences	-21.9%	-23.6%	-6.5%	-7.0%

Table B.21 Control Delay of S3 in different intersections in Base Scenario (Volume Ratio 0.8) (Continued)

70% Penetration Rate	8.817562	15.53718	49.66884	58.13099
Differences	-22.9%	-25.4%	-7.6%	-9.1%
Node 7	Control Delay Per Vehicle			
	EB	WB	NB	SB
Base Case	30.61125	39.99173	59.84843	65.9097
10% Penetration Rate	26.74545	35.49903	56.25757	63.15766
Differences	-12.6%	-11.2%	-6.0%	-4.2%
25% Penetration Rate	25.33376	32.80372	55.28832	62.54778
Differences	-17.2%	-18.0%	-7.6%	-5.1%
50% Penetration Rate	24.19281	31.76441	55.30488	61.60962
Differences	-21.0%	-20.6%	-7.6%	-6.5%
60% Penetration Rate	22.93234	29.95819	54.80782	61.12994
Differences	-25.1%	-25.1%	-8.4%	-7.3%
70% Penetration Rate	22.66653	29.40713	54.65568	60.65956
Differences	-26.0%	-26.5%	-8.7%	-8.0%

Table B.22 Control Delay of S4 in different intersections in Base Scenario (Volume Ratio 0.8)

Node 4	Control Delay Per Vehicle			
	EB	WB	NB	SB
Base Case	92.96235	49.08533	72.60638	101.264
10% Penetration Rate	79.84296	42.83007	69.15018	98.7017
Differences	-14.1%	-12.7%	-4.8%	-2.5%
25% Penetration Rate	73.7104	40.10904	68.28656	97.38239
Differences	-20.7%	-18.3%	-5.9%	-3.8%
50% Penetration Rate	67.57273	36.79901	67.69729	96.22556
Differences	-27.3%	-25.0%	-6.8%	-5.0%
60% Penetration Rate	65.59937	35.75364	66.14144	94.46718
Differences	-29.4%	-27.2%	-8.9%	-6.7%
70% Penetration Rate	65.29618	34.77113	65.44479	92.4635
Differences	-29.8%	-29.2%	-9.9%	-8.7%
Node 5	Control Delay Per Vehicle			
	EB	WB	NB	SB
Base Case	9.494	11.043	73.39815	26.35943
10% Penetration Rate	8.302123	9.498636	69.68628	25.4511
Differences	-12.6%	-14.0%	-5.1%	-3.4%

Table B.22 Control Delay of S4 in different intersections in Base Scenario (Volume Ratio 0.8) (Continued)

25% Penetration Rate	7.741128	8.805101	69.13241	25.04546
Differences	-18.5%	-20.3%	-5.8%	-5.0%
50% Penetration Rate	7.042647	8.178862	68.53446	24.83021
Differences	-25.8%	-25.9%	-6.6%	-5.8%
60% Penetration Rate	6.912982	7.901844	67.5632	24.5559
Differences	-27.2%	-28.4%	-7.9%	-6.8%
70% Penetration Rate	6.765384	7.782666	66.71683	24.44915
Differences	-28.7%	-29.5%	-9.1%	-7.2%
Node 6	Control Delay Per Vehicle			
	EB	WB	NB	SB
Base Case	11.44315	20.8251	53.728	63.9171
10% Penetration Rate	10.18484	18.1891	51.88252	60.52419
Differences	-11.0%	-12.7%	-3.4%	-5.3%
25% Penetration Rate	9.397752	16.76066	51.45814	60.34856
Differences	-17.9%	-19.5%	-4.2%	-5.6%
50% Penetration Rate	8.664498	15.59675	50.95653	60.09937
Differences	-24.3%	-25.1%	-5.2%	-6.0%
60% Penetration Rate	8.420453	15.18272	50.00513	59.23283
Differences	-26.4%	-27.1%	-6.9%	-7.3%
70% Penetration Rate	8.217745	14.6174	50.10151	58.90857
Differences	-28.2%	-29.8%	-6.7%	-7.8%
Node 7	Control Delay Per Vehicle			
	EB	WB	NB	SB
Base Case	30.61125	39.99173	59.84843	65.9097
10% Penetration Rate	26.54238	34.35852	56.62628	62.98507
Differences	-13.3%	-14.1%	-5.4%	-4.4%
25% Penetration Rate	24.4057	31.51823	56.46658	62.78175
Differences	-20.3%	-21.2%	-5.7%	-4.7%
50% Penetration Rate	22.29893	29.01382	56.03546	61.44165
Differences	-27.2%	-27.5%	-6.4%	-6.8%
60% Penetration Rate	21.58451	28.43444	54.74147	61.57788
Differences	-29.5%	-28.9%	-8.5%	-6.6%
70% Penetration Rate	21.17996	27.90133	54.86193	61.3098
Differences	-30.8%	-30.2%	-8.3%	-7.0%

Table B.23 Control Delay of S5 in different intersections in Base Scenario (Volume Ratio 0.8)

Node 4	Control Delay Per Vehicle			
	EB	WB	NB	SB
Base Case	92.96	49.09	72.61	101.26
10% Penetration Rate	77.25	41.41	67.46	95.12
Differences	-16.9%	-15.6%	-7.1%	-6.1%
25% Penetration Rate	72.41	39.42	66.82	95.07
Differences	-22.1%	-19.7%	-8.0%	-6.1%
50% Penetration Rate	65.28	35.70	65.33	93.88
Differences	-29.8%	-27.3%	-10.0%	-7.3%
60% Penetration Rate	62.86	33.52	65.40	92.06
Differences	-32.4%	-31.7%	-9.9%	-9.1%
70% Penetration Rate	61.19	32.36	63.95	90.70
Differences	-34.2%	-34.1%	-11.9%	-10.4%
Node 5	Control Delay Per Vehicle			
	EB	WB	NB	SB
Base Case	9.49	11.04	73.40	26.36
10% Penetration Rate	8.08	9.17	67.89	27.41
Differences	-14.9%	-16.9%	-7.5%	4.0%
25% Penetration Rate	7.69	8.68	67.50	24.53
Differences	-19.0%	-21.4%	-8.0%	-7.0%
50% Penetration Rate	6.92	7.96	67.19	24.04
Differences	-27.1%	-27.9%	-8.5%	-8.8%
60% Penetration Rate	6.59	7.66	66.59	23.86
Differences	-30.6%	-30.6%	-9.3%	-9.5%
70% Penetration Rate	6.43	7.40	65.95	23.87
Differences	-32.3%	-33.0%	-10.1%	-9.4%
Node 6	Control Delay Per Vehicle			
	EB	WB	NB	SB
Base Case	11.44	20.83	53.73	63.92
10% Penetration Rate	9.90	17.35	51.29	60.01
Differences	-13.5%	-16.7%	-4.5%	-6.1%
25% Penetration Rate	9.36	16.66	50.91	59.48
Differences	-18.2%	-20.0%	-5.2%	-6.9%
50% Penetration Rate	8.49	14.88	50.30	58.57
Differences	-25.8%	-28.5%	-6.4%	-8.4%
60% Penetration Rate	8.11	14.43	49.58	58.30
Differences	-29.2%	-30.7%	-7.7%	-8.8%

Table B.23 Control Delay of S5 in different intersections in Base Scenario (Volume Ratio 0.8) (Continued)

70% Penetration Rate	7.92	14.33	49.23	57.89
Differences	-30.8%	-31.2%	-8.4%	-9.4%
Node 7	Control Delay Per Vehicle			
	EB	WB	NB	SB
Base Case	30.61	39.99	59.85	65.91
10% Penetration Rate	25.33	33.34	57.77	63.22
Differences	-17.3%	-16.6%	-3.5%	-4.1%
25% Penetration Rate	24.22	30.85	57.14	61.32
Differences	-20.9%	-22.9%	-4.5%	-7.0%
50% Penetration Rate	21.61	28.54	54.88	59.82
Differences	-29.4%	-28.6%	-8.3%	-9.2%
60% Penetration Rate	20.82	26.72	54.61	59.56
Differences	-32.0%	-33.2%	-8.7%	-9.6%
70% Penetration Rate	19.65	26.06	53.58	59.40
Differences	-35.8%	-34.8%	-10.5%	-9.9%

Table B.24 Control Delay of S6 in different intersections in Base Scenario (Volume Ratio 0.8)

Node 4	Control Delay Per Vehicle			
	EB	WB	NB	SB
Base Case	92.96	49.09	72.61	101.26
10% Penetration Rate	67.18	37.37	64.33	89.63
Differences	-27.7%	-23.9%	-11.4%	-11.5%
25% Penetration Rate	63.47	34.81	64.57	89.46
Differences	-31.7%	-29.1%	-11.1%	-11.7%
50% Penetration Rate	56.43	30.52	61.87	87.48
Differences	-39.3%	-37.8%	-14.8%	-13.6%
60% Penetration Rate	54.59	29.74	61.70	85.93
Differences	-41.3%	-39.4%	-15.0%	-15.1%
70% Penetration Rate	54.22	29.20	58.09	82.91
Differences	-41.7%	-40.5%	-20.0%	-18.1%
Node 5	Control Delay Per Vehicle			
	EB	WB	NB	SB
Base Case	9.49	11.04	73.40	26.36
10% Penetration Rate	7.21	7.91	66.14	23.94
Differences	-24.0%	-28.3%	-9.9%	-9.2%

Table B.24 Control Delay of S6 in different intersections in Base Scenario (Volume Ratio 0.8) (Continued)

25% Penetration Rate	6.79	7.68	65.32	23.24
Differences	-28.5%	-30.4%	-11.0%	-11.8%
50% Penetration Rate	5.93	7.01	63.87	22.68
Differences	-37.5%	-36.5%	-13.0%	-14.0%
60% Penetration Rate	5.70	6.56	62.87	22.52
Differences	-39.9%	-40.6%	-14.3%	-14.6%
70% Penetration Rate	5.36	6.35	63.44	22.06
Differences	-43.6%	-42.5%	-13.6%	-16.3%
Node 6	Control Delay Per Vehicle			
	EB	WB	NB	SB
Base Case	11.44	20.83	53.73	63.92
10% Penetration Rate	8.59	15.30	49.39	57.48
Differences	-25.0%	-26.5%	-8.1%	-10.1%
25% Penetration Rate	8.04	14.46	48.36	57.10
Differences	-29.7%	-30.6%	-10.0%	-10.7%
50% Penetration Rate	7.36	12.85	45.79	53.94
Differences	-35.7%	-38.3%	-14.8%	-15.6%
60% Penetration Rate	6.93	12.37	45.90	53.42
Differences	-39.4%	-40.6%	-14.6%	-16.4%
70% Penetration Rate	6.77	11.83	45.31	52.71
Differences	-40.8%	-43.2%	-15.7%	-17.5%
Node 7	Control Delay Per Vehicle			
	EB	WB	NB	SB
Base Case	30.61	39.99	59.85	65.91
10% Penetration Rate	22.07	29.25	55.20	60.55
Differences	-27.9%	-26.9%	-7.8%	-8.1%
25% Penetration Rate	22.04	27.13	53.16	59.12
Differences	-28.0%	-32.2%	-11.2%	-10.3%
50% Penetration Rate	18.21	24.54	51.14	57.07
Differences	-40.5%	-38.6%	-14.5%	-13.4%
60% Penetration Rate	17.88	23.57	50.99	55.86
Differences	-41.6%	-41.1%	-14.8%	-15.2%
70% Penetration Rate	17.25	21.82	49.59	54.12
Differences	-43.6%	-45.4%	-17.1%	-17.9%

Table B.25 Control Delay of S1 in different intersections in Base Scenario (Volume Ratio 0.9)

Node 4	Control Delay Per Vehicle			
	EB	WB	NB	SB
Base Case	104.4392	55.92	80.67375	112.6562
10% Penetration Rate	94.51424	50.36537	79.23596	111.1706
Differences	-9.5%	-9.9%	-1.8%	-1.3%
25% Penetration Rate	88.67562	47.39664	78.34197	110.3676
Differences	-15.1%	-15.2%	-2.9%	-2.0%
50% Penetration Rate	86.40901	46.13526	77.80492	108.7674
Differences	-17.3%	-17.5%	-3.6%	-3.5%
60% Penetration Rate	85.24808	45.84713	77.85272	107.2799
Differences	-18.4%	-18.0%	-3.5%	-4.8%
70% Penetration Rate	85.56014	45.63693	77.26553	106.5011
Differences	-18.1%	-18.4%	-4.2%	-5.5%
Node 5	Control Delay Per Vehicle			
	EB	WB	NB	SB
Base Case	10.56208	12.13367	80.64735	29.28825
10% Penetration Rate	9.7353	11.40732	80.18066	28.67644
Differences	-7.8%	-6.0%	-0.6%	-2.1%
25% Penetration Rate	9.576266	11.21928	79.9191	28.57762
Differences	-9.3%	-7.5%	-0.9%	-2.4%
50% Penetration Rate	9.275003	10.72691	78.91932	28.61169
Differences	-12.2%	-11.6%	-2.1%	-2.3%
60% Penetration Rate	9.192441	10.58429	78.83292	28.41607
Differences	-13.0%	-12.8%	-2.2%	-3.0%
70% Penetration Rate	8.874535	10.36605	77.95964	28.37469
Differences	-16.0%	-14.6%	-3.3%	-3.1%
Node 6	Control Delay Per Vehicle			
	EB	WB	NB	SB
Base Case	13.18135	22.8819	59.7724	71.019
10% Penetration Rate	12.18431	21.64348	59.16863	69.43758
Differences	-7.6%	-5.4%	-1.0%	-2.2%
25% Penetration Rate	12.00646	21.02971	59.0355	68.80808
Differences	-8.9%	-8.1%	-1.2%	-3.1%
50% Penetration Rate	11.74849	25.61382	58.70926	68.59074
Differences	-10.9%	-11.9%	-1.8%	-3.4%
60% Penetration Rate	11.58492	19.5409	58.75334	68.34736
Differences	-12.1%	-14.6%	-1.7%	-3.8%

Table B.25 Control Delay of S1 in different intersections in Base Scenario (Volume Ratio 0.9) (Continued)

70% Penetration Rate	11.4515	19.40048	58.555	68.05905
Differences	-13.1%	-15.2%	-2.0%	-4.2%
Node 7	Control Delay Per Vehicle			
	EB	WB	NB	SB
Base Case	33.63458	44.92898	67.42418	74.2527
10% Penetration Rate	30.08547	37.07348	66.22843	73.49307
Differences	-10.6%	-17.5%	-1.8%	-1.0%
25% Penetration Rate	28.6804	34.82189	66.23377	72.52563
Differences	-14.7%	-22.5%	-1.8%	-2.3%
50% Penetration Rate	27.88751	34.11881	66.11422	72.79608
Differences	-17.1%	-24.1%	-1.9%	-2.0%
60% Penetration Rate	27.70318	33.71348	65.83125	72.56488
Differences	-17.6%	-25.0%	-2.4%	-2.3%
70% Penetration Rate	27.30225	33.01606	65.47581	72.09854
Differences	-18.8%	-26.5%	-2.9%	-2.9%

Table B.26 Control Delay of S2 in different intersections in Base Scenario (Volume Ratio 0.9)

Node 4	Control Delay Per Vehicle			
	EB	WB	NB	SB
Base Case	104.4392	55.92	80.67375	112.6562
10% Penetration Rate	92.74606	49.02086	78.79276	110.2591
Differences	-11.2%	-12.3%	-2.3%	-2.1%
25% Penetration Rate	87.3736	46.26132	77.4781	108.993
Differences	-16.3%	-17.3%	-4.0%	-3.3%
50% Penetration Rate	81.12514	42.40712	76.67904	107.2722
Differences	-22.3%	-24.2%	-5.0%	-4.8%
60% Penetration Rate	77.42659	40.39462	76.30329	106.8378
Differences	-25.9%	-27.8%	-5.4%	-5.2%
70% Penetration Rate	77.00381	41.41957	75.22677	106.8224
Differences	-26.3%	-25.9%	-6.8%	-5.2%
Node 5	Control Delay Per Vehicle			
	EB	WB	NB	SB
Base Case	10.56208	12.13367	80.64735	29.28825
10% Penetration Rate	9.510406	10.64126	79.86154	28.71637
Differences	-10.0%	-12.3%	-1.0%	-2.0%

Table B.26 Control Delay of S2 in different intersections in Base Scenario (Volume Ratio 0.9) (Continued)

25% Penetration Rate	9.394875	10.4799	79.01334	28.28963
Differences	-11.1%	-13.6%	-2.0%	-3.4%
50% Penetration Rate	8.66452	9.856	78.27413	28.29447
Differences	-18.0%	-18.8%	-2.9%	-3.4%
60% Penetration Rate	8.382009	9.670212	77.63211	28.35981
Differences	-20.6%	-20.3%	-3.7%	-3.2%
70% Penetration Rate	7.989564	9.289406	76.89245	28.12351
Differences	-24.4%	-23.4%	-4.7%	-4.0%
Node 6	Control Delay Per Vehicle			
	EB	WB	NB	SB
Base Case	13.18135	22.8819	59.7724	71.019
10% Penetration Rate	11.99239	20.57288	59.11555	69.44844
Differences	-9.0%	-10.1%	-1.1%	-2.2%
25% Penetration Rate	11.17662	19.73065	58.67616	67.79289
Differences	-15.2%	-13.8%	-1.8%	-4.5%
50% Penetration Rate	10.52122	18.15552	57.39672	67.54088
Differences	-20.2%	-20.7%	-4.0%	-4.9%
60% Penetration Rate	10.43278	18.11772	56.8597	67.46117
Differences	-20.9%	-20.8%	-4.9%	-5.0%
70% Penetration Rate	9.948775	17.51655	57.13885	66.54949
Differences	-24.5%	-23.4%	-4.4%	-6.3%
Node 7	Control Delay Per Vehicle			
	EB	WB	NB	SB
Base Case	33.63458	44.92898	67.42418	74.2527
10% Penetration Rate	29.8053	39.25998	67.07593	73.25074
Differences	-11.4%	-12.6%	-0.5%	-1.3%
25% Penetration Rate	28.33665	36.48629	66.88908	72.49273
Differences	-15.8%	-18.8%	-0.8%	-2.4%
50% Penetration Rate	26.86636	34.94985	65.90769	72.25747
Differences	-20.1%	-22.2%	-2.2%	-2.7%
60% Penetration Rate	25.62964	33.58626	65.76363	71.11123
Differences	-23.8%	-25.2%	-2.5%	-4.2%
70% Penetration Rate	25.19722	33.20455	65.60229	71.41591
Differences	-25.1%	-26.1%	-2.7%	-3.8%

Table B.27 Control Delay of S3 in different intersections in Base Scenario (Volume Ratio 0.9)

Node 4	Control Delay Per Vehicle			
	EB	WB	NB	SB
Base Case	104.4392	55.92	80.67375	112.6562
10% Penetration Rate	92.6219	49.73496	78.29452	110.5311
Differences	-11.3%	-11.1%	-2.9%	-1.9%
25% Penetration Rate	87.38946	47.03359	77.97414	111.2426
Differences	-16.3%	-15.9%	-3.3%	-1.3%
50% Penetration Rate	83.07892	44.30986	76.53306	109.3262
Differences	-20.5%	-20.8%	-5.1%	-3.0%
60% Penetration Rate	77.94632	42.22062	76.74396	107.4645
Differences	-25.4%	-24.5%	-4.9%	-4.6%
70% Penetration Rate	77.42856	41.03892	75.76066	108.0724
Differences	-25.9%	-26.6%	-6.1%	-4.1%
Node 5	Control Delay Per Vehicle			
	EB	WB	NB	SB
Base Case	10.56208	12.13367	80.64735	29.28825
10% Penetration Rate	9.765488	11.05068	78.13183	28.45583
Differences	-7.5%	-8.9%	-3.1%	-2.8%
25% Penetration Rate	9.196153	10.69456	76.95772	28.3796
Differences	-12.9%	-11.9%	-4.6%	-3.1%
50% Penetration Rate	8.836173	9.978206	76.80839	27.8644
Differences	-16.3%	-17.8%	-4.8%	-4.9%
60% Penetration Rate	8.30313	9.421128	76.89941	27.9297
Differences	-21.4%	-22.4%	-4.6%	-4.6%
70% Penetration Rate	8.23552	9.433821	77.07675	27.70106
Differences	-22.0%	-22.3%	-4.4%	-5.4%
Node 6	Control Delay Per Vehicle			
	EB	WB	NB	SB
Base Case	13.18135	22.8819	59.7724	71.019
10% Penetration Rate	11.7767	20.97345	58.34843	68.53435
Differences	-10.7%	-8.3%	-2.4%	-3.5%
25% Penetration Rate	11.20628	20.24895	57.46181	66.91629
Differences	-15.0%	-11.5%	-3.9%	-5.8%
50% Penetration Rate	10.6993	18.85598	57.08701	66.81096
Differences	-18.8%	-17.6%	-4.5%	-5.9%
60% Penetration Rate	10.08378	17.77846	56.5603	66.48722
Differences	-23.5%	-22.3%	-5.4%	-6.4%

Table B.27 Control Delay of S3 in different intersections in Base Scenario (Volume Ratio 0.9) (Continued)

70% Penetration Rate	9.89502	17.44048	56.00162	65.55197
Differences	-24.9%	-23.8%	-6.3%	-7.7%
Node 7	Control Delay Per Vehicle			
	EB	WB	NB	SB
Base Case	33.63458	44.92898	67.42418	74.2527
10% Penetration Rate	30.07183	40.11968	63.13194	70.94422
Differences	-10.6%	-10.7%	-6.4%	-4.5%
25% Penetration Rate	28.69468	37.13628	62.05268	69.95681
Differences	-14.7%	-17.3%	-8.0%	-5.8%
50% Penetration Rate	27.41851	35.86947	62.12329	68.74498
Differences	-18.5%	-20.2%	-7.9%	-7.4%
60% Penetration Rate	25.68422	33.4235	62.31291	68.65714
Differences	-23.6%	-25.6%	-7.6%	-7.5%
70% Penetration Rate	25.20068	33.32316	61.87435	67.91151
Differences	-25.1%	-25.8%	-8.2%	-8.5%

Table B.28 Control Delay of S4 in different intersections in Base Scenario (Volume Ratio 0.9)

Node 4	Control Delay Per Vehicle			
	EB	WB	NB	SB
Base Case	104.4392	55.92	80.67375	112.6562
10% Penetration Rate	90.28782	49.24111	77.84832	112.0098
Differences	-13.5%	-11.9%	-3.5%	-0.6%
25% Penetration Rate	83.12024	44.80424	77.33453	109.8142
Differences	-20.4%	-19.9%	-4.1%	-2.5%
50% Penetration Rate	77.18982	41.77309	76.14889	109.7648
Differences	-26.1%	-25.3%	-5.6%	-2.6%
60% Penetration Rate	75.05292	40.68978	74.49179	106.2162
Differences	-28.1%	-27.2%	-7.7%	-5.7%
70% Penetration Rate	73.73196	39.71344	74.44345	103.8045
Differences	-29.4%	-29.0%	-7.7%	-7.9%
Node 5	Control Delay Per Vehicle			
	EB	WB	NB	SB
Base Case	10.56208	12.13367	80.64735	29.28825
10% Penetration Rate	9.402155	10.71427	77.86419	28.80243
Differences	-11.0%	-11.7%	-3.5%	-1.7%

Table B.28 Control Delay of S4 in different intersections in Base Scenario (Volume Ratio 0.9) (Continued)

25% Penetration Rate	8.898407	9.922332	77.99109	28.5336
Differences	-15.8%	-18.2%	-3.3%	-2.6%
50% Penetration Rate	7.906451	9.243445	77.13351	27.83712
Differences	-25.1%	-23.8%	-4.4%	-5.0%
60% Penetration Rate	7.830099	8.912887	75.57631	28.12096
Differences	-25.9%	-26.5%	-6.3%	-4.0%
70% Penetration Rate	7.587743	8.785938	75.32815	27.34525
Differences	-28.2%	-27.6%	-6.6%	-6.6%
Node 6	Control Delay Per Vehicle			
	EB	WB	NB	SB
Base Case	13.18135	22.8819	59.7724	71.019
10% Penetration Rate	11.52761	20.45142	58.74837	69.127
Differences	-12.5%	-10.6%	-1.7%	-2.7%
25% Penetration Rate	10.71016	19.0024	58.16446	67.94857
Differences	-18.7%	-17.0%	-2.7%	-4.3%
50% Penetration Rate	9.785658	17.42708	57.04846	67.05983
Differences	-25.8%	-23.8%	-4.6%	-5.6%
60% Penetration Rate	9.560614	17.168	57.11278	66.43281
Differences	-27.5%	-25.0%	-4.4%	-6.5%
70% Penetration Rate	9.341628	16.69249	56.48946	65.82169
Differences	-29.1%	-27.0%	-5.5%	-7.3%
Node 7	Control Delay Per Vehicle			
	EB	WB	NB	SB
Base Case	33.63458	44.92898	67.42418	74.2527
10% Penetration Rate	30.04175	39.21166	64.2804	70.9171
Differences	-10.7%	-12.7%	-4.7%	-4.5%
25% Penetration Rate	27.50195	35.47781	63.65708	69.87882
Differences	-18.2%	-21.0%	-5.6%	-5.9%
50% Penetration Rate	25.26289	32.66313	63.14443	69.78844
Differences	-24.9%	-27.3%	-6.3%	-6.0%
60% Penetration Rate	24.7611	32.31835	62.71887	69.49349
Differences	-26.4%	-28.1%	-7.0%	-6.4%
70% Penetration Rate	23.85728	31.59826	61.6681	69.32142
Differences	-29.1%	-29.7%	-8.5%	-6.6%

Table B.29 Control Delay of S5 in different intersections in Base Scenario (Volume Ratio 0.9)

Node 4	Control Delay Per Vehicle			
	EB	WB	NB	SB
Base Case	104.44	55.92	80.67	112.66
10% Penetration Rate	87.33	46.73	75.64	107.66
Differences	-16.4%	-16.4%	-6.2%	-4.4%
25% Penetration Rate	82.25	44.56	75.10	107.86
Differences	-21.2%	-20.3%	-6.9%	-4.3%
50% Penetration Rate	74.23	40.23	74.02	105.36
Differences	-28.9%	-28.1%	-8.2%	-6.5%
60% Penetration Rate	71.03	37.65	73.29	103.68
Differences	-32.0%	-32.7%	-9.2%	-8.0%
70% Penetration Rate	68.37	36.45	71.96	101.93
Differences	-34.5%	-34.8%	-10.8%	-9.5%
Node 5	Control Delay Per Vehicle			
	EB	WB	NB	SB
Base Case	10.56	12.13	80.65	29.29
10% Penetration Rate	9.14	10.32	76.51	31.09
Differences	-13.5%	-14.9%	-5.1%	6.2%
25% Penetration Rate	8.64	9.81	76.03	27.42
Differences	-18.2%	-19.1%	-5.7%	-6.4%
50% Penetration Rate	7.79	8.98	76.13	27.31
Differences	-26.2%	-26.0%	-5.6%	-6.8%
60% Penetration Rate	7.34	8.58	74.81	27.01
Differences	-30.5%	-29.3%	-7.2%	-7.8%
70% Penetration Rate	7.24	8.34	74.57	26.64
Differences	-31.5%	-31.2%	-7.5%	-9.0%
Node 6	Control Delay Per Vehicle			
	EB	WB	NB	SB
Base Case	13.18	22.88	59.77	71.02
10% Penetration Rate	11.11	19.60	57.45	67.86
Differences	-15.7%	-14.3%	-3.9%	-4.5%
25% Penetration Rate	10.50	18.63	57.42	67.10
Differences	-20.3%	-18.6%	-3.9%	-5.5%
50% Penetration Rate	9.65	16.84	56.58	66.35
Differences	-26.8%	-26.4%	-5.3%	-6.6%
60% Penetration Rate	9.11	16.25	55.32	65.34
Differences	-30.9%	-29.0%	-7.4%	-8.0%

Table B.30 Table B.29 Control Delay of S5 in different intersections in Base Scenario (Volume Ratio 0.9) (Continued)

70% Penetration Rate	8.86	16.17	55.31	64.59
Differences	-32.8%	-29.3%	-7.5%	-9.1%
Node 7	Control Delay Per Vehicle			
	EB	WB	NB	SB
Base Case	33.63	44.93	67.42	74.25
10% Penetration Rate	28.61	37.37	65.60	71.33
Differences	-14.9%	-16.8%	-2.7%	-3.9%
25% Penetration Rate	27.02	35.04	64.49	69.20
Differences	-19.7%	-22.0%	-4.3%	-6.8%
50% Penetration Rate	24.30	32.30	61.85	67.48
Differences	-27.7%	-28.1%	-8.3%	-9.1%
60% Penetration Rate	23.23	30.21	61.70	67.24
Differences	-30.9%	-32.8%	-8.5%	-9.4%
70% Penetration Rate	22.08	29.27	60.66	66.51
Differences	-34.3%	-34.9%	-10.0%	-10.4%

Table B.31 Control Delay of 6 in different intersections in Base Scenario (Volume Ratio 0.9)

Node 4	Control Delay Per Vehicle			
	EB	WB	NB	SB
Base Case	104.44	55.92	80.67	112.66
10% Penetration Rate	77.39	41.52	71.57	102.12
Differences	-25.9%	-25.7%	-11.3%	-9.4%
25% Penetration Rate	72.31	40.10	72.54	101.76
Differences	-30.8%	-28.3%	-10.1%	-9.7%
50% Penetration Rate	62.69	33.53	67.98	96.16
Differences	-40.0%	-40.0%	-15.7%	-14.6%
60% Penetration Rate	60.66	32.68	69.32	94.42
Differences	-41.9%	-41.6%	-14.1%	-16.2%
70% Penetration Rate	60.02	32.80	66.18	94.45
Differences	-42.5%	-41.3%	-18.0%	-16.2%
Node 5	Control Delay Per Vehicle			
	EB	WB	NB	SB
Base Case	10.56	12.13	80.65	29.29
10% Penetration Rate	8.01	8.90	73.58	27.23
Differences	-24.1%	-26.6%	-8.8%	-7.0%

Table B.30 Control Delay of 6 in different intersections in Base Scenario (Volume Ratio 0.9) (Continued)

25% Penetration Rate	7.46	8.75	74.31	26.18
Differences	-29.3%	-27.9%	-7.9%	-10.6%
50% Penetration Rate	6.75	7.71	70.97	25.52
Differences	-36.1%	-36.5%	-12.0%	-12.9%
60% Penetration Rate	6.50	7.56	71.51	25.45
Differences	-38.5%	-37.7%	-11.3%	-13.1%
70% Penetration Rate	6.02	6.98	70.49	25.07
Differences	-43.0%	-42.5%	-12.6%	-14.4%
Node 6	Control Delay Per Vehicle			
	EB	WB	NB	SB
Base Case	13.18	22.88	59.77	71.02
10% Penetration Rate	9.55	17.21	54.94	64.67
Differences	-27.5%	-24.8%	-8.1%	-8.9%
25% Penetration Rate	9.16	16.27	55.01	64.22
Differences	-30.5%	-28.9%	-8.0%	-9.6%
50% Penetration Rate	8.08	14.12	51.59	62.13
Differences	-38.7%	-38.3%	-13.7%	-12.5%
60% Penetration Rate	7.71	13.76	52.21	61.54
Differences	-41.5%	-39.9%	-12.6%	-13.3%
70% Penetration Rate	7.52	13.48	51.55	60.72
Differences	-42.9%	-41.1%	-13.8%	-14.5%
Node 7	Control Delay Per Vehicle			
	EB	WB	NB	SB
Base Case	33.63	44.93	67.42	74.25
10% Penetration Rate	25.42	33.28	61.34	68.02
Differences	-24.4%	-25.9%	-9.0%	-8.4%
25% Penetration Rate	24.21	30.56	59.89	65.77
Differences	-28.0%	-32.0%	-11.2%	-11.4%
50% Penetration Rate	20.98	26.96	58.26	62.71
Differences	-37.6%	-40.0%	-13.6%	-15.5%
60% Penetration Rate	20.34	26.19	58.00	62.54
Differences	-39.5%	-41.7%	-14.0%	-15.8%
70% Penetration Rate	18.96	24.82	55.86	61.66
Differences	-43.6%	-44.8%	-17.1%	-17.0%